TOWARDS UNDERSTANDING THE PROOXIDATIVE MECHANISMS OF SUPEROXIDE DISMUTASE

A MATHEMATICAL APPROACH

Rui Gardner Costa de Oliveira

Instituto de Ciências Biomédicas de Abel Salazar • Universidade do Porto • Porto, 2004

Towards Understanding the Prooxidative Mechanisms of Superoxide Dismutase

A mathematical Approach

Rui Gardner Costa de Oliveira

Dissertação de Candidatura ao grau de Doutor em
Ciências Biomédicas submetida ao
Instituto de Ciências Biomédicas de Abel Salazar.

Orientador: Professor Doutor Pedro Moradas-Ferreira
Co-orientador: Doutor Armindo Salvador

- to Marta and Tiago

Preceitos Legais:

Esclarece-se ser da responsabilidade do autor a execução do trabalho que esteve na origem dos resultados apresentados nesta Dissertação, assim como a sua interpretação, discussão e redacção.

Nesta Dissertação são apresentados resultados contidos no artigo seguidamente descriminado, publicado em revista internacional indexada (ISI, PubMed):

Gardner, R., Salvador, A., Moradas-Ferreira, P. (2002) Why does SOD overexpression sometimes enhance, sometimes decrease, hydrogen peroxide production? A minimalist explanation. *Free Radic. Biol. Med.* **32**(12):1351-1357.

Acknowledgements

As I sit down to write these acknowledgements I can't help being overwhelmed by the sense that I have met so many people during these years with whom I've shared so many experiences, and that have supported me so much during this time. When I first started my PhD I figured it would be a hard road to follow. But I only thought of this in professional ways. Little did I imagine that I would gain so many friends and strengthen does I already had (actually, I would predict just the opposite). In short, I would like to thank all that contributed in any way (willingly or unwillingly!) to help me achieve my goals. Below I name but a few. Any omissions I might make are just an indicative of how lucky I am to have had so many people to remember.

I wish to begin by thanking the following institutions for financial and institutional support during my doctoral work: Fundação para a Ciência e Tecnologia (FCT) and grant PRAXIS/BD/16251/98, Instituto de Ciências Biomédicas Abel Salazar (ICBAS), Instituto de Biologia Molecular e Celular (IBMC), Instituto de Investigação Científica Bento Rocha Cabral (IICBRC), University of Michigan and the Department of Microbiology and Immunology, University of Southern California and the Department of Molecular Pharmacology and Toxicology, and the Instituto Gulbenkian de Ciência.

I thank my supervisors Armindo Salvador, and Prof. Pedro Moradas-Ferreira for all the support, friendship and having believed in me from the very first time we met in Porto. I would also like to express my gratitude to my supervising committee and their support throughout the various stages of my thesis.

To Enrique Cadenas I would like to express my gratitude for hosting me at his lab, for providing all the conditions to perform my work, and for giving me the honor and pleasure of experiencing his scientific expertise.

To Mike Savageau, I wish to express my deepest thanks. As an inspiring friend and scientist, for his dedication, for all his wonderful support, for making me feel at home, I feel largely in debt to him. Thanks!

To all the staff at Rocha Cabral (Paula, João António, D. Maria Teresa), of the department of Microbiology and Immunology at the University of Michigan (Jane Holland, Michelle Melis), of the department of Molecular Pharmacology and Toxicology at the University of Southern California (Mye Yasui) at the Instituto Gulbenkian de Ciência (Fátima Mateus, Maria Matoso), my deepest thanks for all your friendship, dedication and professionalism.

I would also like to thank my lab members at the IBMC, and specially Odília Queirós, for the sympathy and making me feel part of the group.

To Prof. Ruy Pinto, for his support and inspirational view of science!

I wish also to thank those that have helped me in many ways, by giving me support, inspiration, and friendship: Miguel Machuqueiro (Migas), Rui Alves, Maria João Moreno, Ana Margarida, Carlos Cordeiro, Francisco and Guida Pinto, Nuno Canto and my beautiful God-daughter Matilde, Ana d'Évora, Célia Romão, the Canteiro family, Lorenzo, Alessandra and Anna Romeri, Herman Gartner, Laura Mancino, all at Kolossos, Uter Dics, RadioHead, Simeone Marino, Eberhart Voit, Albert Sorribas, Ann Savageau, Derick Han, Raffaella Canali, Francesca Daneri, Isabel Gordo, Francisco Dionísio, Ana Cláudia, Kalet Léon, Isabel Abreu, Ramiro Magno, Joana Moreira and all at the EAO.

A very special thanks to my dearest friends that unfortunately had to share the bad times but fortunately also shared with me the accomplishments and good times, João Sousa, João Garcia, Ana Sofia Canto, Sergej Aksenov, Chikoo Oosawa, Tiago Paixão, Nuno Sepúlveda and Íris Caramalho.

To my parents and brothers, Diogo and Stephanie (thanks for all the time and love you've given to Tiago when we most needed. It meant a lot to me!).

I would also like to thank José Faro for all he has done for me. I would have never finished my doctoral work if it were not for his valuable support during these last years. As if this were not enough, I still have the pleasure of his friendship. Thanks, José!

My deepest thanks also go to Jorge Carneiro. I know very few people that could match his generosity, his wit, his availability, his stubbornness, and his ability to pick the finest bunch of characters for his group that have made me feel at home as well as giving me a great scientific environment (and here I must thank particularly Tiago and Nuno. Just you guys make it all worthwhile!). Jorge has helped me in every possible way. I also feel in great debt to him and I hope I'll be able to one day restitute everything he has done to me. You're the best Jorge!

It's difficult to express my gratitude to Fernando Antunes. For his invaluable scientific and personal contributions even before I started my PhD endeavour. He is an inspiring person, both as a human being and as a scientist. To him, I owe much of my work and for that and many things more I'll be eternally grateful.

Finally, to the two people in the world I cherish most. Amidst so many friends and people I love, I'm still blessed with two wonderful people that fill my life daily with love and joy, and never once hesitated giving me all their support, encouragement and belief. Many times, as I worked extra hours I couldn't help being overwhelmed by their ability to perform their daily routines and still have time and capability to give the extra support and love I needed. I can hardly consider this project as my own achievement. As ever, from me to you... Marta and Tiaguinho!

Contents

Summary

The aim of this work is to provide a contribution towards understanding the mechanisms that lead to the prooxidative effects observed in cells and other biological systems where superoxide dismutase (SOD) activity is increased above normal levels, using a mathematical approach.

The past thirty five years have produced an exponential increase in information regarding the physiological production of superoxide ($O_2^{\bullet -}$) and hydrogen peroxide (H_2O_2), their biological targets and the enzymatic systems that modulate the steady-state concentrations of these reactive species. One of the key elements in this regulation is the enzyme superoxide dismutase (SOD). Albeit the irrefutable evidences that SOD is essential for aerobic life, a growing body of evidence has shown that elevated SOD activities can lead to deleterious effects. Yet, in spite of the evidence, the mechanisms underlying these observations remain unclear. Some have suggested that the adverse effects of high SOD activities are due to an increase in the product of the reaction catalysed by SOD - H_2O_2 - whereas others have proposed that excessive $O_2^{\bullet -}$ depletion may inhibit important physiological processes in which it may be involved. Given the low physiological concentrations of $O_2^{\bullet -}$ and H_2O_2, their high reactivity and hence short half-life in biological systems, it has been hard to characterize experimentally the effects of SOD on the steady-state fluxes and concentrations of these reactive species. This has lead to apparent contradictory results. Before the present work, there was still a controversy regarding whether increasing SOD activity would produce an increase or decrease in H_2O_2 production. To overcome these limitations, we have taken advantage of quantitative and analytical mathematical tools to set up and analyse a minimal model that accounts for every possible pathway of $O_2^{\bullet -}$ consumption, including the SOD-catalysed dismutation. One of the main contributions of this work was to determine the influence that changes in SOD activity may exhert on the rate of H_2O_2 production, and clearly describe the physiological conditions in which different outcomes can be observed. The results indicate that increasing SOD activity may increase, decrease or have no effect on the rate of H_2O_2 production. At normal SOD levels, the outcome depends on the ratio between the rate of non-H_2O_2-producing processes and the rate of processes that consume superoxide with high (≥ 1) H_2O_2 yield. In cells or cellular compartments where this ratio is exceptionally low (< 1), a modest decrease in H_2O_2 production upon SOD overexpression is expected, whereas in cells or cellular compartments where the ratio

is higher than unity, H_2O_2 production should increase. Yet, the minimal model only characterizes the direct influence that changes in SOD activity may have on the rate of H_2O_2 production, and predicts that H_2O_2 production increases at most linearly with SOD. To assess whether other mechanisms may contribute to higher increases in oxidative damage than those predicted by the minimal model, a second model was setup to take into account H_2O_2-mediated oxidative damage. All possible feedforward and feedback interactions of $O_2^{\bullet-}$, H_2O_2, and oxidative damage on the rates of production and depletion of each pool were analysed. The analysis was based on well-established methods in Biochemical Systems Theory, which makes only minimal assumptions about the mechanisms of physiological processes. The results show that the mechanisms that may lead to significant exacerbation of H_2O_2-mediated damage may involve both excessive $O_2^{\bullet-}$ depletion and increases in H_2O_2, and the physiological conditions in which these mechanisms are relevant are described. It is also shown that the presence of some interactions allow amplification of oxidative damage without significant changes in H_2O_2 concentration, suggesting that changes in these two concentrations are not necessarily correlated.

In an effort to understand the mechanisms responsible for the observed biphasic response of ischemia-reperfusion-related injury to increasing SOD activities, a model of lipid peroxidation was analysed in this context using a mathematical approach. The results show that the exacerbation of oxidative damage at high SOD activities is most likely due to excessive $O_2^{\bullet-}$ depletion, and the bell-shaped response of damage to increasing levels of SOD activity may be related to the dual role of $O_2^{\bullet-}$ as a toxic product and as a physiological intermediate in cellular protection. More specifically, the decrease of $O_2^{\bullet-}$ elicited by elevation of SOD activity may decrease the rate of lipid peroxidation by lowering the rate of initiation through perhydroxyl radicals at low SOD activities, without a significant increase in chain-length. Whereas at higher SOD activities depletion of $O_2^{\bullet-}$ may dramatically exacerbate the chain-length by assuming that $O_2^{\bullet-}$ can either inhibit metal-catalyzed chain-branching reactions, induce the rate of termination or induce the rate of lipid hydroperoxide removal.

Overall, the results indicate that the different mechanisms responsible for the prooxidative effects of high SOD activities may depend ultimately on the prooxidant and antioxidant reactions of the cell, which may explain the observed discrepancies. Furthemore, the models presented here may constitute a basic framework that will help other researchers rationalize and interpret future experimental results.

Resumo

O objectivo deste trabalho é fornecer uma contribuição para a compreensão dos mecanismos que conduzem aos efeitos prooxidativos observados em células e outros sistemas biológicos onde a actividade do enzima superóxido dismutase (SOD) se encontra elevada acima dos níveis normais, usando uma abordagem matemática.

Os passados trinta e cinco anos produziram um aumento exponencial da informação respeitante à produção fisiológica do radical superóxido ($O_2^{\bullet -}$) e do peróxido de hidrogénio (H_2O_2), dos seus alvos biológicos e dos sistemas enzimáticos que modulam as concentrações de estado estacionário destas espécies reactivas. Um dos elementos chave nesta regulação é o enzima superóxido dismutase (SOD). Não obstante as evidências irrefutáveis que o SOD é essencial para a vida aeróbica, um crescente conjunto de evidências tem vindo a mostrar que actividades elevadas de SOD podem conduzir a efeitos deletérios. No entanto, apesar destas evidências, os mecanismos subjacentes a estas observações permanecem por esclarecer. Alguns sugeriram que os efeitos adversos de actividades elevadas de SOD são devido a um aumento do produto da reacção catalisada pelo próprio SOD, H_2O_2. Outros propuseram que a remoção excessiva de $O_2^{\bullet -}$ pode inibir processos fisiológicos importantes nos quais o $O_2^{\bullet -}$ pode estar envolvido. Considerando as reduzidas concentrações fisiológicas de $O_2^{\bullet -}$ e H_2O_2, as suas reactividades elevadas e tempos de meia-vida curtos em sistemas biológicos, tem sido muito difícil caracterizar experimentalmente os efeitos do SOD nos fluxos e nas concentrações de estado estacionário destas espécies reactivas. Estas limitações têm conduzido a resultados aparentemente contraditórios. Antes do presente trabalho, existia ainda uma controvérsia referente ao facto do aumento da actividade de SOD produzir uma aumento ou diminuição da produção de H_2O_2. Para superar estas limitações, um modelo mínimo que considera todas as possíveis vias de consumo de $O_2^{\bullet -}$, incluíndo a via de dismutação, foi caracterizado e analisado usando ferramentas matemáticas quantitativas e analíticas. Uma das contribuições principais deste trabalho foi determinar a influência que alterações na actividade do SOD podem exercer na velocidade de produção de H_2O_2, e descrever claramente as condições fisiológicas que resultados diferentes podem ser observados. Os resultados indicam que um aumento da actividade de SOD pode aumentar, diminuir ou não ter efeito na velocidade de produção de H_2O_2. A níveis normais de SOD, o resultado depende da razão entre a velocidade total dos processos que não produzem H_2O_2 e a velocidade total dos processos que consomem $O_2^{\bullet -}$ com rendimento elevado (≥ 1) de H_2O_2. Em

células ou em compartimentos celulares onde esta razão é excepcionalmente baixa (< 1), uma diminuição modesta na produção de H_2O_2 é esperada aquando da sobreexpressão do SOD. Pelo contrário, onde esta razão é superior a 1, espera-se que a produção de H_2O_2 aumente. No entanto, o modelo mínimo caracteriza apenas a influência directa que alterações na actividade do SOD podem ter na velocidade de produção de H_2O_2, e prevê que a produção de H_2O_2 aumente no máximo linearmente com o SOD. Para determinar a contribuição de outros mecanismos que possam levar a aumentos mais elevados do dano oxidativo do que aqueles previstos pelo modelo mínimo, um segundo modelo que tem em conta o dano oxidativo mediado pelo H_2O_2 foi analisado. Todas as interacções possíveis de *feedforward* e de *feedback* do $O_2^{\bullet -}$, H_2O_2 e dano oxidativo nas velocidades de produção e consumo de cada espécie, foram analisadas. A análise foi baseada em métodos bem estabelecidos em Teoria de Sistemas Bioquímicos, que permite fazer apenas suposições mínimas sobre os mecanismos dos processos fisiológicos envolvidos. Os resultados mostram que os mecanismos que podem conduzir a um aumento significativo do dano oxidativo dependente de H_2O_2 podem envolver não só a remoção excessiva de $O_2^{\bullet -}$ como o aumento dos níveis de H_2O_2, e as condições fisiológicas em que estes mecanismos são relevantes são descritas. Mostra-se também que a presença de algumas interacções permite que haja amplificação do dano oxidativo sem alterações significativas na concentração de H_2O_2, sugerindo que alterações nestas duas concentrações não estão necessariamente correlacionadas.

Num esforço para compreender os mecanismos responsáveis pela resposta bifásica dos danos relacionados com isquémia-reperfusão a actividades crescentes do SOD, um modelo matemático de peroxidação lipídica foi analisado neste contexto. Os resultados mostram que o aumento do dano oxidativo devido a actividades crescentes de SOD poderá estar relacionado com a remoção excessiva de $O_2^{\bullet -}$, e a resposta bifásica dos danos a níveis crescentes de actividades de SOD pode estar relacionada com o papel dicotómico do $O_2^{\bullet -}$ como produto tóxico para as células e como intermediário fisiológico na protecção celular. Mais especificamente, para níveis baixos de actividades de SOD, a diminuição de $O_2^{\bullet -}$ provocada pela elevação da actividade de SOD pode diminuir a velocidade de peroxidção lipídica através do decréscimo da velocidade de iniciação pelo radical perhidroxilo sem aumentar significativamente a amplificação da peroxidação lipídica. Pelo contrário, para actividades mais elevadas de SOD a diminuição de $O_2^{\bullet -}$ pode aumentar dramaticamente a amplificação da lipoperoxidação assumindo que o $O_2^{\bullet -}$ tem a capacidade de inibir reacções de propagação catalisadas por metais de transição, de induzir a velocidade de terminação ou a remoção de hidroperóxidos lipídicos.

De um modo geral, os resultados indicam que os mecanismos diferentes responsáveis pelos efeitos prooxidativos devido a actividades elevadas de SOD podem ser dependentes das reacções prooxidantes e antioxidantes que ocorrem nas células, o que poderá explicar as discrepâncias observadas. Adicionalmente, os modelos

matemáticos apresentados neste trabalho podem constituir uma estrutura básica teórica que permita a outros investigadores uma melhor racionalização e interpretação dos seus resultados experimentais.

Résumé

Le but de ce travail est de fournir une contribution a find de comprendre les mécanismes qui mènent aux effets prooxidatifs observés dans les cellules et d'autres systèmes biologiques où l'activité de superoxyde dismutase (SOD) est augmentée au-dessus des niveaux normaux, en utilisant une approche mathématique.

Les trente cinq dernières années ont produit une augmentation exponentielle de l'information concernant la production physiologique du superoxyde ($O_2^{\bullet -}$) et le peroxyde d'hydrogène (H_2O_2), leurs cibles biologiques et les systèmes enzymatiques qui modulent les concentrations de l'état stationaire de ces espèces réactives. Un des éléments principaux dans cette réglementation est l'enzyme superoxyde dismutase. Quoiqu'il soit irréfutable que le SOD est essentiel pendant la vie aérobie, un corps croissant d'évidence a prouvé que les activités élevées de SOD peuvent mener à des effets délétères. Cependant, malgré l'évidence, les mécanismes sous-tendants ces observations demeurent peu clairs. Certains ont suggéré que les effets nuisibles des activités élevées de SOD soient dus à une augmentation du produit de la réaction catalysée par SOD - H_2O_2 - tandis que d'autres ont proposé que l'épuisement excessif de $O_2^{\bullet -}$ puisse empêcher les processus physiologiques importants dans lesquels il peut être impliqué. Etant donné les basses concentrations physiologiques de $O_2^{\bullet -}$ et de H_2O_2, leur réactivité élevée, et par conséquent leur demi-vie courte dans les systèmes biologiques, il a été difficile de caractériser expérimentalement les effets du SOD sur les flux et les concentrations de l'état stationaire de ces espèces réactives. Ce qui nous amène à des résultats apparemment contradictoires. Avant ce travail, il y avait déjà une polémique à savoir si l'augmentation de l'activité de SOD produirait une augmentation ou une diminution de production de H_2O_2. Pour surmonter ces limitations, nous avons pris l'avantage des outils mathématiques quantitatifs et analytiques pour installer et analyser un modèle minimal qui explique chaque voie possible de consommation de $O_2^{\bullet -}$, y compris la dismutation catalysée par SOD. Une des contributions principales de ce travail était de déterminer l'influence que les changements de l'activité de SOD pouvraient exhert sur le taux de production de H_2O_2, et décrire clairement les conditions physiologiques au sein desquelles nous pouvrions observer différents résultats. Les résultats indiquent que l'activité croissante de SOD peut augmenter, diminuer ou ne pas avoir d'effet sur le taux de production de H_2O_2. À des niveaux normaux de SOD, les résultats dépendent du rapport entre le taux de processus non produit de H_2O_2 et le taux de processus qui consomment le superoxyde avec le rendement élevé

($\geq$ 1) de H_2O_2. En cellules ou compartiments cellulaires où ce rapport est exceptionnellement bas ($<$ 1), une diminution modeste de production de H_2O_2 sur l'overexpression de SOD est prévue, tandis qu'en cellules ou compartiments cellulaires où le rapport est plus haut que l'unité, la production de H_2O_2 devrait augmenter. Cependant, le modèle minimal caractérise seulement l'influence directe que les changements de l'activité de SOD peuvent avoir sur le taux de production de H_2O_2, et prévoit que la production de H_2O_2 augmente à le plus linéairement avec SOD. Pour savoir si d'autres mécanismes peuvent contribuer à des augmentations plus élevées des dommages oxydatifs que celles prévues par le modèle minimal, un deuxième modèle a été installé pour tenir compte des dommages oxydatifs de H_2O_2. Toutes les intéractions possibles de *feedforward* et de *feedback* de $O_2^{\bullet -}$, de H_2O_2, et de dommage oxydatif sur les taux de production et épuisement de chaque entité chimiquie considéré ont été analysés. L'analyse a été basée sur des méthodes déjà établies dans la Théorie de Systèmes Biochimiques, qui fait seulement des prétentions minimales au sujet des mécanismes des processus physiologiques. Les résultats prouvent que les mécanismes qui peuvent mener à l'exacerbation significative des dommages de H_2O_2 peuvent comporter à la fois l'épuisement excessif de $O_2^{\bullet -}$ et les augmentations de H_2O_2, et les conditions physiologiques en dequelles mécanismes relèvents sont décrites. Il est montré également que la présence de certaines interactions permettent l'amplification des dommages oxydatifs sans changements significatifs de la concentration de H_2O_2, suggérant que des changements de ces deux concentrations ne soient pas nécessairement corrélés.

Afin de comprendre les mécanismes responsables de la réponse biphasée observée des dommages de ischémie-réperfusion aux activités croissantes de SOD, un modèle de peroxydation lipidique a été analysé dans ce contexte en utilisant une approche mathématique. Les résultats prouvent que l'exacerbation des dommages oxydatifs dans des activités élevées de SOD est très probablement due à l'épuisement excessif de $O_2^{\bullet -}$, et la réponse biphasée des dommages aux niveaux croissants de l'activité de SOD peut être liée au rôle duel de $O_2^{\bullet -}$ comme produit toxique et comme intermédiaire physiologique dans la protection cellulaire. Plus spécifiquement, la diminution de $O_2^{\bullet -}$ obtenue par l'augmentation de l'activité de SOD peut diminuer le taux de peroxydation lipidique en abaissant le taux d'initiation par des radicaux perhydroxyle à de basses activités de SOD, sans augmentation significative de l'amplification de la peroxydation lipidique. Réciproquement, à des activités plus élevées de SOD, l'épuisement de $O_2^{\bullet -}$ peut nettement aggraver l'amplification en supposant que le $O_2^{\bullet -}$ peut inhibiter des réactions de propagation catalysées par métaux de transition, induire le taux de terminaison ou induire le taux de déplacement d'hydroxyperoxyde lipidique.

De façon générale, les résultats indiquent que les différents mécanismes responsables des effets prooxidatifs des activités élevées de SOD peuvent dépendre finalement des réactions prooxydantes et antioxydantes de la cellule, ce qui peut expli-

quer les anomalies observées. En autre, les modèles présentés ici peuvent constituer un cadre de base qui aidera d'autres chercheurs à rationaliser et interpréter de futurs résultats expérimentaux.

Part I

General Introduction

Chapter 1

SOD and Reactive Oxygen Species

Contents

1.1 Historical View

The study of oxygen free radicals in Biology and Medicine can be traced back to 1954 with the pioneering work by Rebecca Gerschman, Daniel Gilbert and their colleagues [1], where they related the toxic effects of high oxygen tension in mice to those of ionizing radiation. Based on their knowledge of the chemical processes responsible for oxygen poisoning and radiation injury they suggested a common biological mechanism involving the formation of oxidizing free radicals. Though free radicals were known by then to chemists in the context of radiation, polymer and combustion technology, they were unheard of in the context of the life sciences. They remained so for years even after Denham Harman suggested in 1956 the possibility that these species might play an important role in physiological events such as aging [2], and the proposed *free radical theory of oxygen toxicity* by Daniel Gilbert based on his 1963 paper on the role of pro and antioxidants in oxygen toxicity [3]. It was only in 1969 with the discovery of the superoxide dismutase enzymes by McCord and Fridovich [4] that the field of free radical research in Biology and Medicine literally "took off"[1]. These authors had previously observed that several proteins were able to inhibit the reduction of cytochrome *c* by the superoxide-producing enzyme xanthine oxidase. After months accumulating negative data, in a fortunate moment of inspiration, they realized that based on their kinetic data the inhibition of cytochrome *c* was due to a protein present as an impurity that was able to dismutate the superoxide radical [5]. Starting with bovine erythrocytes, the novel protein termed superoxide dismutase (SOD) was soon isolated based on its enzymatic activity. This finding strongly suggested that superoxide radicals could be normal physiological products of aerobic metabolism, and given the high reactivity and potential toxicity of superoxide it immediately ignited an intense field of research not only in the basic but also in the clinical sciences. The *free radical theory of oxygen toxicity* proposed by Gilbert soon became the *superoxide theory of oxygen toxicity* [6]. The years that followed the discovery of SOD were marked by a score of studies related to superoxide and superoxide dismutase. A few different and quite unrelated proteins were found to possess SOD activity and to be amazingly widespread in every aerobic organism investigated. In 1973, a manganese-containing SOD was reported to be present in mitochondria [7], and immediately suggested a connection between respiration and superoxide formation given that this organelle consumes 85-90% of the oxygen taken up by animals through the respiratory chain [6]. At the same time Boveris and coworkers demonstrated significant generation of hydrogen peroxide at the level of the mitochondrial respiratory chain [8], which was then found to be a consequence of the SOD-catalysed dismutation of superoxide [9, 10] produced at the bc_1-ubiquinone region of the respiratory chain [9]. Together, all the evidence seemed to support

[1] It may interest the reader that at the time this thesis was written (April 2004), there were more than 6,450 citations to this paper by McCord and Fridovich

the view that superoxide was produced intracellularly as a by-product of respiration, and in fact, it is now known that 1-5% of the oxygen taken up by mitochondria is converted to superoxide. This also strengthened the concept of superoxide as an accidental cellular waste product that had to be eliminated. It was proposed that the formation of oxygen-derived radicals was a necessary consequence and a price to pay for the utilization of oxygen, and that as organisms adapted to oxygenated environments, a battery of sophisticated enzymes such as SOD were invented to keep the toxic oxygen-derived species under control. Given the toxicity of these free radicals, it was soon realized that deficiencies in these antioxidant defenses could potentially lead to diseases. The 1980's were characterized by an intense study in the role of oxygen free radicals in aging and disease. Significant peroxidation of phospholipid membranes by free radicals was observed in almost every disease and in animals administered any toxin. This lead to the assumption that oxygen free radicals were responsible for many diseases and lipid peroxidation the main mechanism of action [11]. At the same time, evidence accumulated that free radicals could also exert damage in other cell components, being able to oxidize proteins and DNA. This again seemed to support the theory of oxygen toxicity and free radicals as causative agents of aging and disease. To further substantiate this view was the growing body of evidence of the beneficial role of SOD as a superoxide scavenger. However, at the same this evidence accumulated, it soon became evident to many researchers, based on their own work, that free radicals were not the actual cause of many of these diseases, neither were large amounts of SOD or other antioxidants going to cure them. Halliwell and Gutteridge suggested that increased radical formation was probably an inevitable consequence of most diseases in which tissue damage occurred [12]. Remarkably, Elroy-Stein and colleagues in 1986 found that increasing SOD activities lead to higher rates of lipid peroxidation [13]. In the years that followed a body of evidence accumulated reporting toxic effects in cells overexpressing SOD in a variety of organisms from bacteria to higher eukaryotes [14? –20], contrasting with the already long score of studies pertaining to the beneficial effects of high SOD activities. To fit these seemingly paradoxical effects to the current superoxide theory of oxygen toxicity it was proposed that the toxicity was due to excessive formation of hydrogen peroxide by SOD [13, 15, 18, 19, 21]. However, some did not accept this explanation, given the extremely high activity of SOD observed in biological systems indicating that it would already convert most superoxide into hydrogen peroxide. Adding more or overexpressing the enzyme should not have a significant effect on hydrogen peroxide production [22]. Others suggested that hydrogen peroxide would actually decrease as increasing dismutation would leave less superoxide available for reactions that produce hydrogen peroxide at higher stoichiometries, i.e., generate more hydrogen peroxide per molecule of superoxide [23]. Meanwhile, after the consolidation of molecular biology as a dominant discipline, powerful tools such as

DNA recombination, cloning and PCR enabled researchers to knockout, modify, or transfect and overexpress genes encoding defense enzymes and study the effects on oxidative damage, stress resistance and free radical metabolism. The discovery of the *Escherichia coli* regulons regulated by superoxide and hydrogen peroxide and similar pathways in yeast and higher eukaryotes lead to the concept that reactive oxygen species may be biologically important acting as cellular regulators, in cell proliferation, iron homeostasis, as second messengers, bactericidal agents, etc. The 1990's were marked by many studies investigating the role of ROS in these mechanisms, and increasing evidence suggests that there may be optimal levels of these ROS *in vivo*. This implies that cellular metabolism may be trying to *maintain* rather than *eliminate* reactive oxygen species [24]. The characterization of the physiological role of SOD is therefore of extreme importance not only in understanding the regulation of the physiological processes in which ROS are involved, but also due to the implications regarding its use as a therapeutical agent [25]. We enter the new century with the recurrent notion that Nature has still much more to reveal than we have uncovered so far, presenting increasingly higher and more captivating challenges.

1.2 Antioxidant or Prooxidant? A problem of definition

Free radicals or radical groups are chemical species that contain one or more unpaired electrons. The simplest example is atomic hydrogen - ${}^{1}_{1}H$ - which has only one electron and therefore must be unpaired. Molecular oxygen (O_2) is an interesting example of a biradical since it contains two unpaired electrons in two different orbitals [6]. The term reactive oxygen species (ROS) usually refers to oxygen centered radicals or non-radicals that are derivatives of O_2 (Table 1.1) [6]. "Reactive" is not a very fortunate term since some of these species, such as superoxide ($O_2^{\bullet -}$) and hydrogen peroxide (H_2O_2) are not particularly reactive in aqueous solution [6, 26]. To avoid this, other collective terms such as "active oxygen species", "oxygen-derived species", or simply "oxidants" are also commonly employed. Chemically, any compound, including oxygen, that can accept electrons is an *oxidant* or oxidizing agent, while a substance that donates electrons can be defined as a *reductant* or reducing agent [27]. However, in biological systems, donation of electrons is done usually by donating hydrogen or removal of oxygen. In this context, reductants and oxidants are defined as *antioxidants* and *prooxidants*, respectively [27]. However, these terms have been loosely employed within the scientific community and even beyond. *Prooxidant* has become a term commonly used to refer to compounds such as ROS that can cause oxidative damage and *antioxidant* to substances that exert the beneficial effect of eliminating prooxidants. Yet, ROS such as $O_2^{\bullet -}$ can play an important biological role either as a reducing or oxidizing agent. Therefore, depending on the physiological context, both a reducing or oxida-

Table 1.1: Radical and non-radical oxygen metabolites

Name	Symbol
Oxygen radicals	
Oxygen (bi-radical)	O_2
Superoxide ion	$O_2^{\bullet -}$
Perhydroxyl	$HO_2^{\bullet}$
Hydroxyl	$HO^{\bullet}$
Peroxyl	$ROO^{\bullet}$
Alkoxyl	$RO^{\bullet}$
Non-radicals	
Hydrogen peroxide	H_2O_2
Organic peroxide	ROOH

tive event may be, for instance, prooxidative in the broader sense of the definition. To avoid misinterpretations and ambiguities, the definition of *prooxidant* and *antioxidant* adopted throughout this thesis will be that of an *oxidant* and *reductant*, respectively, whereas *prooxidative* or *antioxidative* effects will refer to the inducing and inhibiting effects on oxidative damage.

1.3 Enzymatic and non-enzymatic sources of ROS

In general, ROS can originate from external sources such as ionizing (γ) and non-ionizing (UV) radiation, food (which contains significant amounts of peroxides, aldehydes, oxidized fatty acids, and transition metals), drugs (narcotics, anaesthetic gases) , pollutants (car exhaust, cigarette smoke), xenobiotics (herbicides such as paraquat), etc. However, aerobic organisms also deliberately produce endogenous ROS through enzymatic and non-enzymatic mechanisms. In particular, one of the most important sites of endogenous superoxide generation is the electron-transfer chain. Located in the cytoplasmic membrane of many bacteria, and in the inner mitochondrial membrane and endoplasmic reticulum of eukaryotes, the respiratory chain is responsible for transferring electrons from substrates such as NADH and $FADH_2$ to oxygen, a process that is coupled with ATP production. However, along the chain, a small percentage of electrons escapes and reduces directly oxygen to $O_2^{\bullet -}$. It is estimated that a small but significant amount ($\sim$1-5%) of the oxygen consumed in respiration is converted to $O_2^{\bullet -}$ as a by-product

of this process [28]. Given the high activity of SOD in biological tissues most $O_2^{\bullet -}$ is thought to be dismutated into O_2 and H_2O_2. Therefore, mitochondria are also regarded as an important source of cellular H_2O_2. The electron transfer chain of the endoplasmic reticulum present in microsomal fractions from various tissues has also been reported to generate $O_2^{\bullet -}$ (and H_2O_2) via NADPH:cytochrome P450 reductase [29] and NADH:cytochrome b_5 reductases [30]. Membranes surrounding the nucleus can also reduce O_2 to $O_2^{\bullet -}$ in the presence of NADPH through an electron transport system that resembles that of the endoplasmic reticulum. NADPH oxidases located in the cellular membrane of phagocytes convert O_2 to $O_2^{\bullet -}$ with electrons from NADPH. This process is characterized by a significant consumption of oxygen (the respiratory burst) and is thought to occur as a defense mechanism to destroy foreign cells given its presence in microbicidal phagocytic cells, such as neutrophils, monocytes, macrophages and eosinophils [30]. Non-phagocytic cells such as lymphocytes, fibroblasts, endothelial and kidney mesangial cells, also possess NADPH oxidase-like activities [30]. Significant $O_2^{\bullet -}$ generation has been observed by these cells in response to TNFα and other cytokines, and could be related to the inflammatory response in mammals. Additionally, hypoxanthine and xanthine oxidation by xanthine oxidase can also generate $O_2^{\bullet -}$ and H_2O_2. However, most of the xanthine/hypoxanthine oxidation that occurs in the cytoplasm *in vivo* is catalysed by xanthine dehydrogenase that transfers electrons from the substrates to NAD^+ rather than to O_2. Thus, $O_2^{\bullet -}$ is unlikely to be produced by this enzyme under physiological conditions. Yet, xanthine dehydrogenase can be converted to xanthine oxidase either by proteolytic attack or oxidation of thiol (-SH) groups. Conversion can occur when tissues are injured, such as under hypoxic or ischemic conditions [31]. Reoxygenation (reperfusion) following ischemia can thus lead to significant production of $O_2^{\bullet -}$ and H_2O_2 by xanthine oxidase. Overall, considering the variety of cellular sources, an upper limit of about 5% could be estimated for the fraction of total cellular O_2 reduced to $O_2^{\bullet -}$ [32].

Two-electron reduction of O_2 to H_2O_2 may also occur, a process catalysed by a variety of oxidases, the most important being located in the microsomal and peroxisomal fractions. In fact, enzymatic sources of H_2O_2 in these fractions account for approximately 80% of cellular H_2O_2 in hepatocytes, while the mitochondrial and cytoplasmic fractions can account up to 15% and 5%, respectively [33]. In general, intracellular H_2O_2-producing enzymes include glycolate, hydroxyacid and urate oxidases in peroxisomes, the already mentioned xanthine oxidase and SOD in the cytoplasm, SOD in the mitochondrial matrix, monoamine oxidase in the mitochondrial outer membrane, NADPH:cytochrome P450 reductase and diamine oxidase in the endoplasmic reticulum. The highly reactive hydroxyl radical ($HO^\bullet$) can be generated in biological systems by decomposition of H_2O_2 in the presence of suitable transition metals, such as reduced iron or copper, a mechanism known as the

Fenton reaction:

$$Metal^{n} + H_2O_2 \longrightarrow Metal^{n+1} + HO^{\bullet} + OH^{-} \quad (1.1)$$

The rate constant for reaction of ferrous iron (Fe^{2+}) with H_2O_2 in aqueous media is low (76 $M^{-1}s^{-1}$) [34]. On the other hand, reduced copper ion (Cu^{+}) is much more reactive with a reported rate constant for the reaction with H_2O_2 of 4.7×10^3 $M^{-1}s^{-1}$ [6]. Though most intracellular iron is stored in ferritin and protected from reacting with H_2O_2, a low molecular mass iron pool in the form of ATP- or citrate-ferrous iron chelates that is able to react with H_2O_2 is believed to exist. Kinetic constants for the reactions of H_2O_2 with ATP-Fe^{2+} and citrate-Fe^{2+} chelates ($\sim 10^4$ $M^{-1}s^{-1}$) are about two orders of magnitude higher than with the non-chelated free ion form [35]. Iron and copper may also catalyse the decomposition of organic hydroperoxides into alkoxyl and peroxyl radicals ($RO^{\bullet}$ and $ROO^{\bullet}$, respectively), accounting for much of the stimulation of lipid peroxidation by transition-metal ions in biological systems. The radicals $HO_2^{\bullet}$ and $HO^{\bullet}$ can also react with polyunsaturated phospholipids to produce carbon-centered radicals, which can subsequently lead to the formation of lipid peroxyl radicals by addition of oxygen.

1.4 Metabolic fate of superoxide and superoxide-derived species

1.4.1 Is superoxide toxic?

The limited reactivity of $O_2^{\bullet -}$ compared with radicals such as $HO^{\bullet}$ has lead some to believe that $O_2^{\bullet -}$ is chemically harmless. Yet, the increased oxidative damage and reduced cell viability observed in mutants lacking SOD activity (see below, section 1.5.3) does not seem to support this view. The superoxide anion radical ($O_2^{\bullet -}$) is the conjugate base of a weak acid, the perhydroxyl radical ($HO_2^{\bullet}$). With a pKa of 4.69 [36], most superoxide is present in the charged form under physiological pH. However, the protonated form of $O_2^{\bullet -}$ is somewhat more reactive in aqueous media than $O_2^{\bullet -}$ and can initiate lipid peroxidation. In fact, the more acidic environment close to the membrane may facilitate protonation of $O_2^{\bullet -}$. Any $O_2^{\bullet -}$ produced in the interior of hydrophobic membranes could also be very damaging, since $O_2^{\bullet -}$ is highly reactive in organic solvents [6]. In a hydrophilic environment both $O_2^{\bullet -}$ and $HO_2^{\bullet}$ can act as reducing agents, for instance, by reducing ferric (Fe^{3+}) compounds to the ferrous (Fe^{2+}) form, either chelated or free in solution [37] that could potentially be more potent oxidants than superoxide itself [6].

Superoxide can also produce H_2O_2 by dismutation, which in the presence of suitable transition metals could lead to $HO^{\bullet}$ generation. In protic solvents, $O_2^{\bullet -}$ is

unstable and will spontaneously dismute, a reaction where superoxide is both oxidized and reduced to yield O_2 and H_2O_2, respectively. The overall process is usually represented by:

$$O_2^{\bullet -} + O_2^{\bullet -} + 2H^+ \longrightarrow H_2O_2 + O_2 \tag{1.2}$$

However, it is highly unlikely that two molecules with the same charge would come together and react. The spontaneous dismutation under physiological conditions usually proceeds by reaction of $O_2^{\bullet -}$ and $HO_2^{\bullet}$:

$$HO_2^{\bullet} + O_2^{\bullet -} + H^+ \longrightarrow H_2O_2 + O_2 \tag{1.3}$$

The rate constant for this reaction is 9.7×10^7 $M^{-1}s^{-1}$ in aqueous solution at pH 7 [38]. Considering the equilibrium between $O_2^{\bullet -}$ and $HO_2^{\bullet}$ the overall process of spontaneous dismutation may be regarded simply as two $O_2^{\bullet -}$ molecules reacting together as in reaction 1.3 with a second-order rate constant of approximately 10^5 $M^{-1}s^{-1}$. At this rate, however, many other cellular metabolites such as ascorbate, cytochrome *c*, glutathione (GSH) or even nitric oxide, would be able to efficiently compete for $O_2^{\bullet -}$. However, most biological systems that produce $O_2^{\bullet -}$ have also present the superoxide dismutase enzyme capable of catalysing the dismutation reaction up to nine orders of magnitude faster than without the catalyst. Still, GSH, protein-thiol groups and possibly other metabolites may be sufficiently concentrated to compete for $O_2^{\bullet -}$. So far, the question concerning the relative amount of $O_2^{\bullet -}$ consumed and $O_2^{\bullet -}$-derived H_2O_2 produced by SOD under physiological conditions remains open.

In addition, $O_2^{\bullet -}$ has also the ability to reduce quinones, nitro compounds, ketones, organic halides, and proteins [reviewed in 28], to oxidize sulfite, thiols, diphenols, ascorbic acid and α-tocopherol [reviewed in 28], and to decrease the activity of enzymes such as catalase [39] and glutathione peroxidase [40]. However, the extent to which these reactions are relevant *in vivo* has not yet been established. On the other hand, several studies have shown that, *in vivo*, $O_2^{\bullet -}$ oxidizes enzymes that contain [4Fe-4S] clusters at their active centers, causing the release of Fe^{2+} from the cluster and consequently loss of enzymatic activity [41]. These enzymes belong to the group of dehydratases, which include dihydroxyacid dehydratase [42] fumarases [43, 44], 6-phosphogluconate dehydratase [45], and aconitase [46]. The rate constants for the inactivation reactions of dehydratases by $O_2^{\bullet -}$ are reported to be in the range $10^6 - 10^7$ $M^{-1}s^{-1}$ [41]. Loss of activity of aconitase or fumarase can cause the tricarboxylic acid to lose function during oxidative stress. As a result, cells can no longer rely on nonfermentable substrates leading to diminished respiratory capacity, less ATP production and reduced growth. Interestingly, this pathway may also serve as a negative feedback of $O_2^{\bullet -}$ on its own production un-

der physiological conditions, as it reduces the influx of reducing equivalents into the respiratory chain [47]. Down-regulation of $O_2^{\bullet -}$ production at the level of the respiratory chain may also involve mild proton leakage, a process that can potentially also be mediated by $O_2^{\bullet -}$ as evidenced by the recent observations that $O_2^{\bullet -}$ activates the mitochondrial uncoupling proteins UCP1, UCP2 and UCP3 [48].

1.4.2 Physiological consequences of the hydroxyl radical

Many *in vitro* studies show that exposure to $O_2^{\bullet -}$-generating systems may lead to damage of biomolecules and even cell death. Protection was observed by adding not only SOD, but also catalase and $HO^{\bullet}$ scavengers, such as mannitol, formate or dimethysulphoxide (DMSO) [34]. Based on these evidences it was suggested that $O_2^{\bullet -}$ could react with H_2O_2 through a process catalysed by transition metals to produce $HO^{\bullet}$. This reaction is known as the Haber-Weiss reaction and is described by the following reactions:

$$\begin{array}{rcl} Metal^{n+1} + O_2^{\bullet -} & \longrightarrow & Metal^{n} + O_2 \\ Metal^{n} + H_2O_2 & \longrightarrow & Metal^{n+1} + HO^{\bullet} + OH^{-} \\ \hline \text{Net Reaction: } O_2^{\bullet -} + H_2O_2 & \longrightarrow & O_2 + HO^{\bullet} + OH^{-} \end{array} \qquad (1.4)$$

The second reaction in this process is the Fenton reaction (reaction 1.1) and hence the process is also known as the superoxide-assisted Fenton reaction. However, the importance of $O_2^{\bullet -}$ in assisting Fenton reaction is questionable under physiological settings since there are potent reductants present at millimolar concentrations (e.g., GSH, NAD(P)H, ascorbic acid) that can easily compete with $O_2^{\bullet -}$ for the transition metals. Nonetheless, increased production of $O_2^{\bullet -}$ and H_2O_2 can generate conditions favorable for $HO^{\bullet}$ formation *in vivo*. For instance, $O_2^{\bullet -}$ is able to release iron ions from mammalian ferritin and from the iron-sulfur clusters of dehydratases, while H_2O_2 can displace iron from haem proteins [49].

Once formed, $HO^{\bullet}$ radicals react immediately and indiscriminately with the molecules in their vicinity. Several important cellular targets of $HO^{\bullet}$ such as DNA, proteins, and lipids, have been documented. Exposure of DNA to $HO^{\bullet}$ can cause damage to sugar bases, purine and pyrimidine oxidation and lead to DNA strand breakage and mutation. $HO^{\bullet}$ scavengers are not always very effective against this type of damage since the radicals can be formed from H_2O_2 reacting with metal ions bound directly to DNA. To cope with such damage, enzymatic systems were developed to repair DNA and assure its correct functioning [reviewed in 50]. It is interesting to note that DNA damage caused by oxidative stress does not have necessarily to involve direct attack on DNA by reactive species. Large increases in intracellular Ca^{2+} as a consequence of oxidative stress can activate nuclear Ca^{2+}-dependent endonucleases, which will fragment DNA.

$HO^{\bullet}$ may also attack proteins generating a variety of end-products. Importantly, thiol groups of cysteines are easily oxidized and may result in disulphides, which can undergo further oxidation to sulphonates [6]. Methionine can be oxidized to methionine sulphoxide or further oxidized to yield sulphone and loss of histidyl in certain enzymes can lead to inactivation. Peroxyl radicals and peroxides can also be form by attack of $HO^{\bullet}$ to tryptophan residues. Protein receptors and transporters are important early targets, since damage can alter essential ion balance between the intracellular and extracellular environment [6]. The failure to maintain these ionic gradients induce changes in cell volume that will affect many features of cell function [51]. Protein repair can involve the action of GSH and thioredoxin that re-reduce the protein disulphide bridges formed by cross-linking of the cysteine-SH groups. Proteins containing methionine sulphoxides can also be repaired by peptide methionine sulphoxide reductase, which uses reduced thioredoxin as a source of reducing power. Additionally, in the absence of a protein repair system, damaged amino-acid residues other than methionine sulphoxide or cysteine disulfides usually serve as a signal for proteolytic degradation.

Peroxidation of lipid membranes may also be an important target of $HO^{\bullet}$, though $HO_2^{\bullet}$ may be a more efficient initiator of lipid peroxidation, for instance, in mitochondria [52]. Generation of peroxyl and alkoxyl radicals, aldehydes and other products of lipid peroxidation within membranes and lipoproteins may seriously damage the proteins present in the membrane.

1.4.3 ROS as physiologic mediators of cellular function

Despite the evident deleterious effects perpetrated by ROS it seems that, as a whole, cellular metabolism of ROS has evolved to control the levels of ROS rather than eliminate them completely. *E. coli*, for instance, keep H_2O_2 levels under tight control (~200 nM) over a wide range of growth conditions, and in response to environmental changes [53]. The involvement of $O_2^{\bullet -}$ and H_2O_2 in numerous physiological processes seems to further support this view. For instance, the adaptive process of many bacteria and yeast to aerobic environments is accomplished by up-regulating the expression of various proteins involved in ROS-scavenging and cellular repair, which is triggered by excess ROS production. In bacteria, excess $O_2^{\bullet -}$ generation leads to the oxidation of a protein encoded by the *sox*R gene [54] that activates transcription of the *sox*S gene. The product of the *sox*S gene binds to the promoters and activates transcription of genes encoding proteins such as the cytoplasmic SOD, a DNA repair enzyme (endonuclease IV), glucose-6-phosphate dehydrogenase and others. When critical cysteine -SH groups within the protein encoded by the *oxy*R gene become oxidized by increasing H_2O_2 production in *E. coli*, the oxidized protein induces expression of proteins that include hydroperoxidase I, alkyl hydroperoxide reductase and glutathione reductase [reviewed in 55].

Like bacteria, the yeast *Saccharomyces cerevisiae* pre-exposed to H_2O_2 or $O_2^{\bullet -}$-generating systems adapts by becoming resistant to higher levels of these species. One of the genes involved is YAP1, which seems to control the expression of genes involved in biosynthesis and metabolism of glutathione and thioredoxin [reviewed in 56]. In addition, yeast growing anaerobically respond to the introduction of O_2 by activating the biosynthesis of haem through activation of O_2-dependent enzymes. This activates the expression of two haem activation complexes HAP1 and HAP2/3/4 which in turn increase synthesis of several proteins, such as the cytosolic catalase and mitochondrial SOD [56]. Redox changes and oxidative stress also regulate the activity of transcription factors in mammals, such as AP-1 (activator protein) and NF-κB, though in a somewhat more complex way, and much still remains to be established [57]. The physiological utility of ROS is also evidenced by involvement of ROS in phagocytic killing and chemotaxis, and the role of H_2O_2 in thyroid-hormone biosynthesis in animals and lignin synthesis in plants [6]. Exposure of different cell types in culture to low levels of H_2O_2 and superoxide-generating systems have been shown to activate protein kinases that favor cell proliferation [reviewed in 58]. Superoxide and H_2O_2 may also be involved in iron homeostasis. The interaction of $O_2^{\bullet -}$ with iron-sulfur clusters of certain proteins is important in sensing the redox status and in regulating the uptake and storage of iron. For example, the ferric uptake regulator of *E. coli*, Fur, is an iron-binding protein that is involved in the regulation of iron transport [59], though it is also a negative regulator of the MnSOD gene [60]. This dual action of Fur is a good indicative of the coupling between $O_2^{\bullet -}$ and iron homeostasis.

1.5 Superoxide Dismutase (SOD)

1.5.1 The SOD family

SODs are ubiquitously found in all oxygen-consuming organisms [61], in archaebacteria [62], in aerotolerant anaerobes [63] and even in obligate anaerobes [64]. It is though that the presence of SOD in anaerobes may be to provide protection to transient exposure of the cells to oxygen. SODs are a family of metalloenzymes that have been isolated from a wide range of organisms and are characterized based on the metal species present at the active site. These include the copper- and zinc-containing enzymes (CuZnSOD) [4], manganese-containing enzymes (MnSOD) [65], iron-containing enzymes (FeSOD) [66], and nickel-containing enzymes (NiSOD) [67].

CuZnSOD is widely distributed in eukaryotic cells localized mainly in the cytoplasm [4], but can also be found in lysosomes [68], nucleus [69], chloroplasts [70] and in the intermembrane space of mitochondria [71, 72]. CuZnSOD is a homodimeric enzyme with a molecular weight of ~32 kDa, containing one atom of Cu

and one of Zn per subunit. Though the subunits are stabilized by intrachain disulfide bonds, they are associated to each other by non-covalent forces. The enzyme requires Cu and Zn for its biological activity, though Zn seems to have only a structural role. Loss of Cu leads to complete inactivation, suggesting a close relationship between SOD activity and copper homeostasis. Human extracellular SOD (EC-SOD) is also a copper-zinc-containing SOD, but unlike its cytosolic counterpart, it is a tetrameric enzyme [73] and usually bound to the endothelium. It may have a role in protection against extracellular superoxide-derived stress, such as in the inflammatory response. Some pathogens also produce ECSOD which may confer resistance against killing by leukocytes. Some bacteria also possess periplasmic CuZnSOD, which is induced during aerobic growth [74].

The cytoplasmic MnSOD is widespread in prokaryotes, and is homodimeric protein with a total molecular weight of 40 kDa [65], whereas the mitochondrial form has four identical subunits with a molecular weight of 80 kDa and one manganese atom per subunit [7]. Nevertheless, the MnSOD found in mitochondria shows strong homology to the prokaryotic enzyme.

FeSOD is an iron-containing SOD that was first isolated in *E. coli* [66]. The Fe- and Mn-containing SODs show strong sequence and structural homology suggesting they have a common ancestor [75]. Yet, replacing Fe for Mn or vice-versa in the respective active sites of the enzyme render it inactive, showing that metal binding to both these types of SOD is quite specific [**? ?**].

NiSOD has only more recently been found in a few *Streptomyces* species, and is composed of four identical subunits of 13.4 kDa each [67].

1.5.2 Activity and mechanism

Superoxide dismutase catalyses the disproportionation of $O_2^{\bullet -}$ radicals to O_2 and H_2O_2 according to the scheme proposed by Fielden and coworkers [76]:

$$\begin{aligned} O_2^{\bullet -} + SOD^{ox} &\longrightarrow SOD^{rd} + O_2 \\ O_2^{\bullet -} + 2H^+ + SOD^{rd} &\longrightarrow SOD^{ox} + H_2O_2 \end{aligned} \tag{1.5}$$

Though the reaction is pH dependent, SODs catalyse the dismutation of $O_2^{\bullet -}$ at a rate close to the diffusion limit over the entire range of pH from 5 to 10 [4]. The second-order rate constant for both reactions has been reported to be $\sim 2 \times 10^9$ M^{-1} s^{-1} [77]. Since the value of the rate constant for both reactions is the same they will proceed at the same rate as long as $O_2^{\bullet -}$ is the main substrate of the enzyme. In this case, both reduced and oxidized forms of SOD will be equally concentrated, i.e., equal to half the total concentration of the enzyme. The rate of $O_2^{\bullet -}$ consumption can then be expressed simply by:

$$\frac{d[O_2^{\bullet -}]}{dt} = -k_{dism}[O_2^{\bullet -}][SOD^{ox}] - k_{dism}[O_2^{\bullet -}][SOD^{rd}]$$
$$= -k_{dism}[O_2^{\bullet -}][SOD]_{total} \quad (1.6)$$

1.5.3 SOD: Not too little, not too much

SOD is undoubtedly essential for aerobic life. This is evidenced by the phenotypic deficits exhibited by mutants lacking the enzyme. *E. coli* mutants, for instance, lacking both MnSOD and FeSOD were shown to require rich medium to grow (still they grew slower than with SOD), to be hypersentive to paraquat and H_2O_2, and presented high rate of spontaneous mutagenesis [78]. These effects were reversed by insertion of a functional gene expressing SOD [79] or by complementing the SOD-null mutants with enzymes capable of removing $O_2^{\bullet -}$, such as desulfoferrodoxin [80]. CuZnSOD- and ECSOD-deficient mice exhibit enhanced sensitivity to hyperoxia and increased cell death [81, 82], whereas MnSOD knockouts are lethal in mice [83, 84]. There are also numerous studies showing that transfection or overexpression of CuZnSOD and specially MnSOD protects many types of cells against oxidants and oxidant-generating compounds. MnSOD overexpression can lead to increased resistance to hyperoxia [85], paraquat [86], or cytokines such as TNFα [87] and interleukin-1 [88]. MnSOD overexpression can also inhibit apoptosis in mouse liver cells [89] and in human lung cells [90], and exhibit antiproliferative and tumor suppressor effects [91]. Overexpression of CuZnSOD has not shown to dramatically increase protection against oxidative stress [92], though simultaneous increase in CuZnSOD and H_2O_2-decomposing enzymes such as catalase appear to give better protection [93]. Protective and beneficial roles of SOD have been shown in a wide range of diseases and the therapeutical potential of SOD and SOD mimics has been extensively explored [reviewed in 25].

Paradoxically, studies with transfected cells from *E. coli* [14, 15, 17, 20], *Saccharomyces cerevisiae* [21], tobacco [19] and from several mammals [13, 16, 18, 94, 95], have also shown that overexpression of SOD can produce deleterious effects. Overexpression of SOD has been shown to increase lipid peroxidation [13, 16, 94, 95] and protein carbonylation [95], to increase sensitivity to radiation [17] and ROS-generating systems [14, 15, 18, 20], to cause mutations [18], growth inhibition [14, 15, 18, 20], and inhibition of cell proliferation [95]. These effects seem to suggest that too much SOD may be toxic and that an optimal cellular SOD activity may exist. This is further supported by the observed biphasic response of several oxidative stress-related markers to increasing SOD activities [22, 96–99].

The importance of understanding the effects of SOD on ROS metabolism and whether there is an optimal intracellular activity is further highlighted by the interest in

the biological and pharmacological manipulation of SOD as theurapeutical agent in a variety of diseases.

1.6 Scope of the work

The aim of this work is to provide a contribution towards understanding the mechanisms that lead to the prooxidative effects observed in cells and other biological systems where SOD activity is increased above normal levels.

Several mechanisms have been proposed to explain the adverse effects of high SOD activities. The proposed mechanisms involve two fundamental ways in which increasing SOD could possibly elicit toxic effects: a) by depleting the levels of $O_2^{\bullet -}$ or b) by modulating the rate of H_2O_2 production.

Excessive depletion of $O_2^{\bullet -}$ steady-state concentration could lead to inhibition of important physiological functions in which $O_2^{\bullet -}$ is involved [17, 20, 22, 98, 100]. However, despite thirty five years of intense study in the field where many potential biological targets of $O_2^{\bullet -}$ have been identified, still many doubts exist regarding their physiological relevance. Furthermore, the delicate balance between the beneficial and detrimental processes that involve $O_2^{\bullet -}$ hinders possible attempts to understand its mode of action.

The increased toxicity elicited by high SOD activities has been also attributed to exacerbated H_2O_2 concentration, which increases $HO^{\bullet}$ formation [13, 15, 17–19, 21, 101], and excessive removal of $O_2^{\bullet -}$ and consequently inhibiting possible important physiological processes mediated by this radical species [17, 20, 22, 98, 100].

Additionally, CuZnSOD is known to be inhibited slowly by elevated H_2O_2 concentrations [102], possibly due to the release of $HO^{\bullet}$ [103]. It has been suggested that this capacity of CuZnSOD to produce "free" $HO^{\bullet}$ from H_2O_2 may partially explain the adverse effects associated with high SOD activities [103]. However, this explanation cannot be applied to the prooxidative effects observed in cells overexpressing MnSOD as this enzyme lacks peroxidative activity [102].

Others have suggested that as SOD activity rises, the drop in $O_2^{\bullet -}$ concentration leaves the oxidized form of SOD more available to react with the target molecules for which it was supposed to provide protection [104]. In other words, increasing SOD will favor the superoxide reductase (SOR) activity over the superoxide dismutase activity [105].

However, despite all the observations and evidences presented in the literature, the effect of SOD on the rate of H_2O_2 is still controversial, making it difficult to assess the role of changes in H_2O_2 or $O_2^{\bullet -}$ on the adverse effects of high SOD activities. Using a mathematical approach, several models are presented in this dissertation that try to address the following questions:

1. What are the effects of increased SOD activities on H_2O_2 production? Does it increase or decrease H_2O_2 production?
2. In what conditions are the outcomes expected?
3. What is the magnitude of a possible increase in H_2O_2 production by SOD?
4. Is the toxicity of SOD limited to an increase in H_2O_2 or are there other mechanisms that can be involved in mediating SOD-induced oxidative damage?
5. Assuming that H_2O_2 increases with SOD activity, can these changes be correlated with the changes observed in oxidative damage?
6. How relevant are the effects of $O_2^{\bullet -}$ depletion when increasing SOD?
7. Can the dual role of $O_2^{\bullet -}$ as a toxic product and physiological metabolite explain the existence of an optimal SOD activity or does it have to involve H_2O_2-mediated processes?

The first three questions are addressed in Chapter 3 with a mathematical model describing all the possible processes of $O_2^{\bullet -}$ depletion that allows the assessment of the effects of SOD on the rate of H_2O_2 production. Chapter 4 is an extension of this model, and addresses the question of whether other interactions besides those considered in the minimal model presented in the previous chapter can account for higher increases in H_2O_2 and if these changes are correlated with those observed in the same conditions for oxidative damage. The last chapter of results (Chapter 5) addresses the particular phenomenon of ischemia-reperfusion injury where an optimal concentration of SOD has been observed. A model of lipid peroxidation in this context was analysed to assess the role of $O_2^{\bullet -}$ and/or H_2O_2 in the mechanisms that lead to a biphasic response of the rate of lipid peroxidation to increasing SOD activities. The final chapter (Chapter 6) presents a general discussion of the results.

Before the chapters of results, a brief introduction to some of the mathematical tools used throughout this work is presented, in particular those concerning the power-law formalism.

References

[1] Gerschman, R.; Gilbert, D.; Nye, S.; Dwyer, P. and Fenn, W. (1954) Oxygen poisoning and X-irradiation: A mechanism in common. *Science* **119**:623–6.

[2] Harman D. (1956) Aging: a theory based on free radical and radiation chemistry. *J Gerontol* **11**:298–300.

[3] Gilbert, D. (1963) The role of pro-oxidants and antioxidants in oxygen toxicity. *Radiat Res* **Suppl 3**:44–53.

[4] McCord, J. and Fridovich, I. (1969) Superoxide dismutase. an enzymic function for erythrocuprein (hemocuprein). *J Biol Chem* **244**:6049–6055.

[5] McCord, J.; Boyle, J.; Day Jr, E.; Rizzolo, L. and Salin, M. (1977) A manganese-containing superoxide dismutase from human liver. In A. M. Michelson; J. M. McCord and I. Fridovich (Editors), *Superoxide and superoxide dismutases*, 129–138. Academic Press, London.

[6] Halliwell, B. and Gutteridge, M. (Editors) (1999) *Free Radicals in Biology and Medicine*. Oxford University Press, UK.

[7] Weisiger, R. and Fridovich, I. (1973) Superoxide dismutase. organelle specificity. *J Biol Chem* **248**:3582–3592.

[8] Boveris, A.; Oshino, N. and Chance, B. (1972) The cellular production of hydrogen peroxide. *Biochem J* **128**:617–630.

[9] Forman, H. and Kennedy, J. (1974) Role of superoxide radical in mitochondrial dehydrogenase reactions. *Biochem Biophys Res Commun* **60**:1044–1050.

[10] Loschen, G.; Azzi, A.; Richter, C. and Flohé, L. (1974) Superoxide radicals as precursors of mitochondrial hydrogen peroxide. *FEBS Lett* **42**:68–72.

[11] Gutteridge, J. and Halliwell, B. (2000) Free radicals and antioxidants in the year 2000. A historical look to the future. *Ann N Y Acad Sci* **899**:136–47.

[12] Halliwell, B. and Gutteridge, J. (1984) Lipid peroxidation, oxygen radicals, cell damage, and antioxidant therapy. *Lancet* **1**:1396–7.

[13] Elroy-Stein, O.; Bernstein, Y. and Groner, Y. (1986) Overproduction of human Cu/Zn-superoxide dismutase in transfected cells: Extenuation of paraquat-mediated cytotoxicity and enhancement of lipid peroxidation. *EMBO J* **5**:615–622.

[14] Bloch, C. and Ausubel, F. (1986) Paraquat-mediated selection for mutations in the manganese-superoxide dismutase gene *sodA*. *J Bacteriol* **168**:795–8.

[15] Scott, M.; Meshnick, S. and Eaton, J. (1987) Superoxide dismutase-rich bacteria. Paradoxical increase in oxidant toxicity. *J Biol Chem* **262**:3640–5.

[16] Elroy-Stein, O. and Groner, Y. (1988) Impaired neurotransmitter uptake in PC12 cells overexpressing human Cu/Zn-superoxide dismutase–implication for gene dosage effects in down syndrome. *Cell* **52**:259–67.

[17] Scott, M.; Meshnick, S. and Eaton, J. (1989) Superoxide dismutase amplifies organismal sensitivity to ionizing radiation. *J Biol Chem* **264**:2498–501.

[18] Amstad, P.; Peskin, A.; Shah, G.; Mirault, M.; Moret, R.; Zbinden, I. and Cerutti, P. (1991) The balance between Cu,Zn-superoxide dismutase and catalase affects the sensitivity of mouse epidermal cells to oxidative stress. *Biochemistry* **30**:9305–13.

[19] Bowler, C.; Slooten, L.; Vandenbranden, S.; De Rycke, R.; Botterman, J.; Sybesma, C.; Van Montagu, M. and Inze, D. (1991) Manganese superoxide dismutase can reduce cellular damage mediated by oxygen radicals in transgenic plants. *EMBO J* **10**:1723–32.

[20] Liochev, S. and Fridovich, I. (1991) Effects of overproduction of superoxide dismutase on the toxicity of paraquat toward *Escherichia coli*. *J Biol Chem* **266**:8747–50.

[21] Costa, V.; Reis, E.; Quintanilha, A. and Moradas-Ferreira, P. (1993) Acquisition of ethanol tolerance in *Saccharomyces cerevisiae*: The key role of the mitochondrial superoxide dismutase. *Arch Biochem Biophys* **300**:608–614.

[22] Nelson, S.; Bose, S. and McCord, J. (1994) The toxicity of high-dose superoxide dismutase suggests that superoxide can both initiate and terminate lipid peroxidation in the reperfused heart. *Free Radic Biol Med* **16**:195–200.

[23] Liochev, S. and Fridovich, I. (1994) The role of $O_2^{\bullet -}$ in the production of $HO^{\bullet}$: In vitro and in vivo. *Free Radic Biol Med* **16**:29–33.

[24] Griendling, K. and Harrison, D. (1999) Dual role of reactive oxygen species in vascular growth. *Circ Res* **85**:562–3.

[25] Salvemini, D. and Cuzzocrea, S. (2003) Therapeutic potential of superoxide dismutase mimetics as therapeutic agents in critical care medicine. *Crit Care Med* **31**:S29–38.

[26] Sawyer, D. and Valentine, J. (1981) How super is superoxide? *Acc chem Res* **14**:393–400.

[27] Prior, R. and Cao, G. (1999) In vivo total antioxidant capacity: Comparison of different analytical methods. *Free Radic Biol Med* **27**:1173–81.

[28] Hassan, H. (1997) Cytotoxicity of oxyradicals and the evolution of superoxide dismutases. 27–47.

[29] Aust, S.; Roerig, D. and Pederson, T. (1972) Evidence for superoxide generation by nadph-cytochrome c reductase of rat liver microsomes. *Biochem Biophys Res Commun* **47**:1133–1137.

[30] Cross, A. and Jones, O. (1991) Enzymic mechanisms of superoxide production. *Biochim Biophys Acta* **1057**:281–98.

[31] McCord, J. and Turrens, J. (1994) Mitochondrial injury by ischemia and reperfusion. *Curr. Top. Bioenerg.* **17**:173–195.

[32] Boveris, A. and Cadenas, E. (1997) Cellular sources and steady-state levels of reactive oxygen species. In L. Clerch and D. Massaro (Editors), *Oxygen, gene expression, and cellular function*, 1–25. Marcel Dekker, New York.

[33] Chance, B.; Sies, H. and Boveris, A. (1979) Hydroperoxide metabolism in mammalian organs. *Physiol Rev* **59**:527–605.

[34] Halliwell, B. and Gutteridge, J. (1990) Role of free radicals and catalytic metal ions in human disease: an overview. *Methods Enzymol* **186**:1–85.

[35] Rush, J. and Koppenol, W. (1990) Reactions of Fe(II)-ATP and Fe(II)-citrate complexes with t-butyl hydroperoxide and cumyl hydroperoxide. *FEBS Lett* **275**:114–6.

[36] Bielski, B. (1978) Re-evaluation of spectral and kinetic-properties of $HO_2^{\bullet}$ and $O_2^{\bullet -}$ free radicals. *Photochem Photobiol* **28**:645–649.

[37] Koppenol, W.; Butler, J. and Van Leeuwen, J. (1978) The Haber-Weiss cycle. *Photochem Photobiol* **28**:655–660.

[38] Ross, A.; Mallard, W.; Helman, W.; Buxton, G.; Huie, R. and Neta, P. (1998) NDRL-NIST Solution Kinetics Database - Ver. 3. Tech. rep., Notre Dame Radiation Laboratory, Notre Dame, IN and NIST Standard Reference Data, Gaithersburg, MD.

[39] Kono, Y. and Fridovich, I. (1982) Superoxide radical inhibits catalase. *J Biol Chem* **257**:5751–4.

[40] Blum, J. and Fridovich, I. (1985) Inactivation of glutathione peroxidase by superoxide radical. *Arch Biochem Biophys* **240**:500–8.

[41] Gardner, P. (1997) Superoxide-driven aconitase Fe-S center cycling. *Biosci Rep* **17**:33–42.

[42] Kuo, C.; Mashino, T. and Fridovich, I. (1987) α,β-Dihydroxyisovalerate dehydratase. A superoxide-sensitive enzyme. *J Biol Chem* **262**:4724–7.

[43] Liochev, S. and Fridovich, I. (1992) Fumarase C, the stable fumarase of Escherichia coli, is controlled by the soxRS regulon. *Proc Natl Acad Sci U S A* **89**:5892–6.

[44] Liochev, S. and Fridovich, I. (1993) Modulation of the fumarases of Escherichia coli in response to oxidative stress. *Arch Biochem Biophys* **301**:379–84.

[45] Gardner, P. and Fridovich, I. (1991) Superoxide sensitivity of the *Escherichia coli* 6-phosphogluconate dehydratase. *J Biol Chem* **266**:1478–83.

[46] Gardner, P. and Fridovich, I. (1991) Superoxide sensitivity of the *Escherichia coli* aconitase. *J Biol Chem* **266**:19328–33.

[47] Skulachev, V. (1996) Role of uncoupled and non-coupled oxidations in maintenance of safely low levels of oxygen and its one-electron reductants. *Q Rev Biophys* **29**:169–202.

[48] Echtay, K.; Roussel, D.; St-Pierre, J.; Jekabsons, M.; Cadenas, S.; Stuart, J.; Harper, J.; Roebuck, S.; Morrison, A.; Pickering, S.; Clapham, J. and Brand, M. (2002) Superoxide activates mitochondrial uncoupling proteins. *Nature* **415**:96–9.

[49] Puppo, A. and Halliwell, B. (1988) Formation of hydroxyl radicals in biological systems. Does myoglobin stimulate hydroxyl radical formation from hydrogen peroxide? *Free Radic Res Commun* **4**:415–22.

[50] Sancar, A. (1996) DNA excision repair. *Annu Rev Biochem* **65**:43–81.

[51] Haussinger, D. (1996) The role of cellular hydration in the regulation of cell function. *Biochem J* **313 (Pt 3)**:697–710.

[52] Antunes, F.; Salvador, A.; Marinho, H.; Alves, R. and Pinto, R. (1996) Lipid peroxidation in mitochondrial inner membranes. I. An integrative kinetic model. *Free Radic Biol Med* **21**:917–43.

[53] Gonzalez-Flecha, B. and Demple, B. (1997) Homeostatic regulation of intracellular hydrogen peroxide concentration in aerobically growing *Escherichia coli*. *J Bacteriol* **179**:382–8.

[54] Hidalgo, E.; Ding, H. and Demple, B. (1997) Redox signal transduction via iron-sulfur clusters in the SoxR transcription activator. *Trends Biochem Sci* **22**:207–10.

[55] Gonzalez-Flecha, B. and Demple, B. (2000) Genetic responses to free radicals. Homeostasis and gene control. *Ann N Y Acad Sci* **899**:69–87.

[56] Moradas-Ferreira, P. and Costa, V. (2000) Adaptive response of the yeast *Saccharomyces cerevisiae* to reactive oxygen species: Defences, damage and death. *Redox Rep* **5**:277–85.

[57] Griendling, K.; Sorescu, D.; Lassegue, B. and Ushio-Fukai, M. (2000) Modulation of protein kinase activity and gene expression by reactive oxygen species and their role in vascular physiology and pathophysiology. *Arterioscler Thromb Vasc Biol* **20**:2175–83.

[58] Burdon, R. (1995) Superoxide and hydrogen peroxide in relation to mammalian cell proliferation. *Free Radic Biol Med* **18**:775–94.

[59] Bagg, A. and Neilands, J. (1987) Ferric uptake regulation protein acts as a repressor, employing iron (II) as a cofactor to bind the operator of an iron transport operon in Escherichia coli. *Biochemistry* **26**:5471–7.

[60] Tardat, B. and Touati, D. (1991) Two global regulators repress the anaerobic expression of MnSOD in *Escherichia coli*::Fur (ferric uptake regulation) and Arc (aerobic respiration control). *Mol Microbiol* **5**:455–65.

[61] McCord, J.; Keele, B., Jr and Fridovich, I. (1971) An enzyme-based theory of obligate anaerobiosis: The physiological function of superoxide dismutase. *Proc Natl Acad Sci U S A* **68**:1024–7.

[62] Takao, M.; Oikawa, A. and Yasui, A. (1990) Characterization of a superoxide dismutase gene from the archaebacterium *Methanobacterium thermoautotrophicum*. *Arch Biochem Biophys* **283**:210–6.

[63] Tally, F.; Goldin, B.; Jacobus, N. and Gorbach, S. (1977) Superoxide dismutase in anaerobic bacteria of clinical significance. *Infect Immun* **16**:20–5.

[64] Hewitt, J. and Morris, J. (1975) Superoxide dismutase in some obligately anaerobic bacteria. *FEBS Lett* **50**:315–8.

[65] Keele, B., Jr; McCord, J. and Fridovich, I. (1970) Superoxide dismutase from *Escherichia coli* B. A new manganese-containing enzyme. *J Biol Chem* **245**:6176–81.

[66] Yost, F. and Fridovich, I. (1973) An iron-containing superoxide dismutase from *Escherichia coli*. *J Biol Chem* **248**:4905–4908.

[67] Youn, H.; Kim, E.; Roe, J.; Hah, Y. and Kang, S. (1996) A novel nickel-containing superoxide dismutase from Streptomyces spp. *Biochem J* **318 (Pt 3)**:889–96.

[68] Liou, W.; Chang, L.; Geuze, H.; Strous, G.; Crapo, J. and Slot, J. (1993) Distribution of CuZn superoxide dismutase in rat liver. *Free Radic Biol Med* **14**:201–7.

[69] Chang, L.; Slot, J.; Geuze, H. and Crapo, J. (1988) Molecular immunocytochemistry of the CuZn superoxide dismutase in rat hepatocytes. *J Cell Biol* **107**:2169–79.

[70] Grace, S. (1990) Phylogenetic distribution of superoxide dismutase supports an endosymbiotic origin for chloroplasts and mitochondria. *Life Sci* **47**:1875–86.

[71] Peeters-Joris, C.; Vandevoorde, A. and Baudhuin, P. (1975) Subcellular localization of superoxide dismutase in rat liver. *Biochem J* **150**:31–9.

[72] Okado-Matsumoto, A. and Fridovich, I. (2001) Subcellular distribution of superoxide dismutases (SOD) in rat liver. Cu,Zn-SOD in mitochondria. *J Biol Chem* **276**:38388–93.

[73] Karlsson, K. and Marklund, S. (1988) Extracellular superoxide dismutase in the vascular system of mammals. *Biochem J* **255**:223–8.

[74] Fridovich, I. (1995) Superoxide radical and superoxide dismutases. *Annu Rev Biochem* **64**:97–112.

[75] Stallings, W.; Pattridge, K.; Strong, R. and Ludwig, M. (1984) Manganese and iron superoxide dismutases are structural homologs. *J Biol Chem* **259**:10695–9.

[76] Fielden, E.; Roberts, P.; Bray, R.; Lowe, D.; Mautner, G.; Rotilio, G. and Calabrese, L. (1974) Mechanism of action of superoxide dismutase from pulse radiolysis and electron paramagnetic resonance. Evidence that only half the active sites function in catalysis. *Biochem J* **139**:49–60.

[77] Forman, H. and Fridovich, I. (1973) Superoxide dismutase: A comparison of rate constants. *Arch Biochem Biophys* **158**:396–400.

[78] Carlioz, A. and Touati, D. (1986) Isolation of superoxide dismutase mutants in *Escherichia coli*: is superoxide dismutase necessary for aerobic life? *EMBO J* **5**:623–30.

[79] Natvig, D.; Imlay, K.; Touati, D. and Hallewell, R. (1987) Human copper-zinc superoxide dismutase complements superoxide dismutase-deficient *Escherichia coli* mutants. *J Biol Chem* **262**:14697–701.

[80] Liochev, S. and Fridovich, I. (1997) A mechanism for complementation of the *sodA sodB* defect in *Escherichia coli* by overproduction of the *rbo* gene product (desulfoferrodoxin) from *Desulfoarculus baarsii*. *J Biol Chem* **272**:25573–5.

[81] Carlsson, L.; Jonsson, J.; Edlund, T. and Marklund, S. (1995) Mice lacking extracellular superoxide dismutase are more sensitive to hyperoxia. *Proc Natl Acad Sci U S A* **92**:6264–8.

[82] Reaume, A.; Elliott, J.; Hoffman, E.; Kowall, N.; Ferrante, R.; Siwek, D.; Wilcox, H.; Flood, D.; Beal, M.; Brown, R., Jr; Scott, R. and Snider, W. (1996) Motor neurons in Cu/Zn superoxide dismutase-deficient mice develop normally but exhibit enhanced cell death after axonal injury. *Nat Genet* **13**:43–7.

[83] Li, Y.; Huang, T.; Carlson, E.; Melov, S.; Ursell, P.; Olson, J.; Noble, L.; Yoshimura, M.; Berger, C.; Chan, P. and et al. (1995) Dilated cardiomyopathy and neonatal lethality in mutant mice lacking manganese superoxide dismutase. *Nat Genet* **11**:376–81.

[84] Melov, S.; Coskun, P.; Patel, M.; Tuinstra, R.; Cottrell, B.; Jun, A.; Zastawny, T.; Dizdaroglu, M.; Goodman, S.; Huang, T.; Miziorko, H.; Epstein, C. and Wallace, D. (1999) Mitochondrial disease in superoxide dismutase 2 mutant mice. *Proc Natl Acad Sci U S A* **96**:846–51.

[85] Lindau-Shepard, B.; Shaffer, J. and Del Vecchio, P. (1994) Overexpression of manganous superoxide dismutase (MnSOD) in pulmonary endothelial cells confers resistance to hyperoxia. *J Cell Physiol* **161**:237–42.

[86] St Clair, D.; Oberley, T. and Ho, Y. (1991) Overproduction of human Mn-superoxide dismutase modulates paraquat-mediated toxicity in mammalian cells. *FEBS Lett* **293**:199–203.

[87] Wong, G.; Elwell, J.; Oberley, L. and Goeddel, D. (1989) Manganous superoxide dismutase is essential for cellular resistance to cytotoxicity of tumor necrosis factor. *Cell* **58**:923–31.

[88] Hohmeier, H.; Thigpen, A.; Tran, V.; Davis, R. and Newgard, C. (1998) Stable expression of manganese superoxide dismutase (MnSOD) in insulinoma cells prevents IL-1beta- induced cytotoxicity and reduces nitric oxide production. *J Clin Invest* **101**:1811–20.

[89] Kokoszka, J.; Coskun, P.; Esposito, L. and Wallace, D. (2001) Increased mitochondrial oxidative stress in the Sod2 (+/-) mouse results in the age-related decline of mitochondrial function culminating in increased apoptosis. *Proc Natl Acad Sci U S A* **98**:2278–83.

[90] Zwacka, R.; Dudus, L.; Epperly, M.; Greenberger, J. and Engelhardt, J. (1998) Redox gene therapy protects human IB-3 lung epithelial cells against ionizing radiation-induced apoptosis. *Hum Gene Ther* **9**:1381–6.

[91] Oberley, T. (2002) Oxidative damage and cancer. *Am J Pathol* **160**:403–8.

[92] Schwartz, P. and Coyle, J. (1998) Effects of overexpression of the cytoplasmic copper-zinc superoxide dismutase on the survival of neurons in vitro. *Synapse* **29**:206–12.

[93] Sohal, R.; Agarwal, A.; Agarwal, S. and Orr, W. (1995) Simultaneous overexpression of copper- and zinc-containing superoxide dismutase and catalase retards age-related oxidative damage and increases metabolic potential in drosophila melanogaster. *J Biol Chem* **270**:15671–4.

[94] Ceballos-Picot, I.; Nicole, A. and Sinet, P. (1992) Cellular clones and transgenic mice overexpressing copper-zinc superoxide dismutase: Models for the study of free radical metabolism and aging. In I. Emerit and B. Chance (Editors), *Free radicals and aging*, 89–98. Basel:Birkhauser Verlag, Switzerland.

[95] Lee, M.; Hyun, D.; Jenner, P. and Halliwell, B. (2001) Effect of overexpression of wild-type and mutant Cu/Zn-superoxide dismutases on oxidative damage and antioxidant defences: Relevance to Down's syndrome and familial amyotrophic lateral sclerosis. *J Neurochem* **76**:957–65.

[96] Bernier, M.; Manning, A. and Hearse, D. (1989) Reperfusion arrhythmias: Dose-related protection by anti-free radical interventions. *Am J Physiol* **256**:H1344–52.

[97] Omar, B.; Gad, N.; Jordan, M.; Striplin, S.; Russell, W.; Downey, J. and McCord, J. (1990) Cardioprotection by Cu,Zn-superoxide dismutase is lost at high doses in the reoxygenated heart. *Free Radic Biol Med* **9**:465–71.

[98] Omar, B. and McCord, J. (1990) The cardioprotective effect of Mn-superoxide dismutase is lost at high doses in the postischemic isolated rabbit heart. *Free Radic Biol Med* **9**:473–8.

[99] Galinanes, M.; Ferrari, R.; Qiu, Y.; Cargnoni, A.; Ezrin, A. and Hearse, D. (1992) PEG-SOD and myocardial antioxidant status during ischaemia and reperfusion: dose-response studies in the isolated blood perfused rabbit heart. *J Mol Cell Cardiol* **24**:1021–30.

[100] Michelson, A.; Puget, K. and Durosay, P. (1977) Clinical aspects of the dosage of erythrocuprein. In A. M. Michelson; J. M. McCord and I. Fridovich (Editors), *Superoxide and superoxide dismutases*, 467–499. Academic Press, London.

[101] Mao, G.; Thomas, P.; Lopaschuk, G. and Poznansky, M. (1993) Superoxide dismutase (SOD)-catalase conjugates. Role of hydrogen peroxide and the Fenton reaction in SOD toxicity. *J Biol Chem* **268**:416–20.

[102] Hodgson, E. and Fridovich, I. (1975) The interaction of bovine erythrocyte superoxide dismutase with hydrogen peroxide: Chemiluminescence and peroxidation. *Biochemistry* **14**:5299–303.

[103] Yim, M.; Chock, P. and Stadtman, E. (1990) Copper, zinc superoxide dismutase catalyzes hydroxyl radical production from hydrogen peroxide. *Proc Natl Acad Sci U S A* **87**:5006–10.

[104] Offer, T.; Russo, A. and Samuni, A. (2000) The pro-oxidative activity of SOD and nitroxide SOD mimics. *FASEB J* **14**:1215–23.

[105] Liochev, S. and Fridovich, I. (2000) Copper- and zinc-containing superoxide dismutase can act as a superoxide reductase and a superoxide oxidase. *J Biol Chem* **275**:38482–5.

Chapter 2

Mathematical Modeling

Contents

2.1 Why use mathematical modeling?

In recent years, the fields of biological sciences have been overwhelmed with computers and their power to perform from simple to extensive calculations, statistical analysis, massive data retrieval, storage and analysis, all of which is now familiar in what is known as bioinformatics. Yet, these are but tools that can be applied when using mathematical modeling. Mathematical modeling consists generically in the formalisation of any conceptual model (an idea, a sketch, a graph, a set of reactions) into mathematical form. This allows one to apply specific quantitative (numerical) or symbolical (analytical) tools to analyse the behaviour of the model, how it responds to external signals, how different details in the structure of the model govern its behaviour, to identify the key processes governing or regulating its behaviour, to describe how changes in parameters can influence or produce different behaviours, etc. It is common to associate mathematical modeling to simulations, though it is only one of many approaches. In fact, mathematical models are usually used as heuristic tools rather than simple instruments of prediction. They may serve to test different hypotheses, to identify flaws in different conceptual models, and to infer possible new mechanisms that may explain experimental results.

Biological systems are usually highly non-linear and their behaviour is hard to predict or understand. In particular, the metabolism of reactive oxygen species (ROS) is a complex biochemical network consisting of many interactions between the elemental determinants, which are themselves highly reactive and consequently short-lived. Hence, reactive species and the interactions in which they are involved are hard to determine experimentally. Given the technical difficulties in identifying and measuring these interactions, and the complexity in analysing them, different parts of the system are isolated and experiments are carried out *in vitro* or at least outside the context of the intact network, which characterizes the reductionist approach. Additionally, due to the ability of many of the reactive species to act both as reductants and oxidants the experimental results are highly dependent on the chemical and redox conditions in which the experiment is being performed. To overcome these limitations, mathematical modeling presents itself as a powerful alternative and complementary tool. One has the capability to set up and analyse the network of interactions in a more integrative perspective, which would be unfeasible otherwise. However, to do so without a detailed knowledge of the mechanisms involved and the kinetics of each interaction, can only be done using proper tools developed to make minimal assumptions about these processes. These methods are based on Biochemical Systems Theory and are described below. The following sections in this Chapter are adapted in part from Michael Savageau's course in "Cellular and molecular networks" [1], and extensively described in [2, 3].

2.2 Power-Laws and the S-system approach

Mathematical descriptions of biological and biochemical systems most often involve nonlinear rational functions, which are usually quite hard to analyse. About thirty five years ago, Michael Savageau [4–6] proposed a general nonlinear representation of biochemical systems based on their power-law approximation, i.e., their linearization in logarithmic coordinates. This mathematical representation was termed *S-system* (S stands for synergistic). Given the uniform mathematical structure of the S-system (see below) the model can be easily set up in a straightforward manner. Furthermore, the steady-state equations of the S-system are linear when represented in logarithmic coordinates allowing the steady-state solution to be obtained analytically without loosing the ability to capture the rich collection of behaviours observed in nonlinear systems. Though the power-law approximation has a wider range of accurate representation than a linear formalism, it is still only valid within the neighbourhood of a chosen operating point. When studying the steady-state behaviour, however, this may not pose a problem as the the operating point is usually chosen to be the actual steady-state.

2.2.1 S-system structure

Like most mathematical models, the S-system model is a formal representation that describes how each pool (dependent state variable) in a given biological system changes in time. Mathematically this is represented by a set of ordinary differential equations. One of the key features of this mathematical formalism is that each dependent state variable X_i is represented by the difference between two fluxes that describe the influx of material entering the X_i pool (V_i^+) and the efflux leaving the X_i pool (V_i^-). Generically, this is translated into the following mathematical form:

$$\frac{dX_i}{dt} = V_i^+(X_1, X_2, \ldots, X_{n+m}) - V_i^-(X_1, X_2, \ldots, X_{n+m}) \qquad i = 1, 2, \ldots, n. \quad (2.1)$$

where n is the number of dependent state variables and m the number of independent (external) state variables that do not change with time, and thus do not require a differential equation. The fluxes V_i^+ and V_i^- can be complicated, positive real functions whose detailed mathematical description are usually unknown due to lack of knowledge of either the biological mechanisms involved or their actual mathematical structure. Another important feature of the S-system model is the representation of V_i^+ and V_i^- by products of power-law functions that include only those variables that contribute directly to the corresponding process. For instance, if the flux V_1^+ is affected exclusively by X_1 and X_2, the power-law term

should contain just these two variables. A real number exponent g_{ij} is associated to each variable X_j that contributes to the production (increase) of X_i while a real exponent h_{ij} is associated to each variable X_j that contributes to the degradation (decrease) of X_i. If X_j has a positive effect on the flux the corresponding exponent is also positive, while a negative effect will be represented by a negative value. In a biochemical context the exponents g_{ij} or h_{ij} may be considered as the kinetic orders of the processes producing or consuming X_i, respectively, with respect to the state variable X_j. If the process is saturable with respect to X_i a value between 0 (full saturation) and 1 (non-saturable first-order kinetics) would be assigned to the exponents. On the other hand, if dealing with a regulatory process where cooperative interactions are likely to occur, then a value between 1 (no cooperativity) and 4 (high cooperativity) would be assigned. Similarly, when dealing with a particular inhibitory interaction, the assignments will involve negative exponents for the variables acting as inhibitors. For instance, a simple hyperbolic inhibition would be represented by a value of -1 while inhibitory cooperative kinetics would be represented by exponents between -1 (no cooperativity) and -4 (high cooperativity). Thus, positive exponents for most biological processes are usually between 0 and 4 while inhibitory interactions are usually represented by exponents between -4 and 0.

Each flux term in the differential equations also includes a non-negative multiplier that determines the rate of production or degradation processes and thus can be interpreted as the rate constant. The non-negative multiplier of the influx and efflux terms are called α_i and β_i, respectively, and carry the index of the flux function V_i^+ or V_i^-. As a result, for n dependent variables and m external variables, the fundamental equations of the S-system representation take the form:

$$\begin{aligned} \frac{dX_i}{dt} &= \alpha_i X_1^{gi1} X_2^{gi2} \dots X_{n+m}^{g_{i,n+m}} - \beta_i X_1^{hi1} X_2^{hi2} \dots X_{n+m}^{h_{i,n+m}} \\ &= \alpha_i \prod_{j=1}^{n+m} X_j^{g_{ij}} - \beta_i \prod_{j=1}^{n+m} X_j^{h_{ij}} \qquad i = 1, 2, \dots, n. \end{aligned} \tag{2.2}$$

If a state variable X_j has no effect on the increase or degradation of X_i, its exponent g_{ij} or h_{ij}, respectively, is set to zero. The corresponding power-law $X_i^{g_{ij}}$ or $X_i^{h_{ij}}$ equals 1 and therefore can be omitted from the flux term. If a multiplier α_i or β_i is zero, the corresponding influx or efflux is absent.

2.2.2 Steady-state analysis

When the system reaches a steady-state, each dependent variable no longer changes with time as the rate of production and degradation of each dependent variable is equal. This situation is translated into mathematical terms by setting the time derivatives $\frac{dX_i}{dt}$ to zero resulting in a set of *non-linear* algebraic equations. For

each equation, the negative term can be added to both sides to yield the following expression:

$$\alpha_i \prod_{j=1}^{n+m} X_j^{g_{ij}} = \beta_i \prod_{j=1}^{n+m} X_j^{h_{ij}} \qquad i = 1, \ldots, n \tag{2.3}$$

Rearranging this equation one obtains:

$$\prod_{j=1}^{n+m} X_j^{(g_{ij}-h_{ij})} = (\beta_i/\alpha_i) \qquad i = 1, \ldots, n \tag{2.4}$$

By taking the logarithm of both sides of the equation this set of non-linear equations becomes a set of *linear* algebraic equations:

$$\sum_{j=1}^{n+m} a_{ij} y_j = b_i \qquad i = 1, \ldots, n \tag{2.5}$$

where $b_i = ln(\beta_i/\alpha_i)$, $y_j = ln(X_j)$ and $a_{ij} = (g_{ij} - h_{ij})$. These equations can also be expressed by conventional matrix notation:

$$[A]y] = b] \tag{2.6}$$

By partitioning the elements in the matrices corresponding to dependent and independent variables in equation 2.6, the following matrix equation is obtained:

$$[A_d : A_i] \begin{bmatrix} y_d \\ .. \\ y_i \end{bmatrix} = b] \tag{2.7}$$

The equation can be rewritten by separating the dependent and independent terms:

$$[A]_d \; y]_d + [A]_i \; y]_i = b] \tag{2.8}$$

or

$$[A]_d \; y]_d = -[A]_i \; y]_i + b] \tag{2.9}$$

As long as the determinant of $[A]_d$ is non-zero, the matrix has an inverse operator ($[A]_d^{-1} = [M]$). In these conditions, expression 2.9 can be rearranged to yield the familiar explicit steady-state solution for the S-system:

$$\begin{aligned} y]_d &= -[M][A]_i\ y]_i + [M]\ b] \\ &= [L]\ y]_i + [M]\ b] \\ &\quad\ \uparrow \qquad\quad \uparrow \\ &\quad slope \quad intercept \end{aligned} \tag{2.10}$$

where $[L] = -[M][A]_i$. Notice the linear dependence of the steady-state solutions in the logarithmic space to the logarithm of the independent variables (y_i) and the logarithm of the rate constants.

The steady-state flux through a given pool X_i can be calculated based on the aggregate rate law of either production or consumption[1] of X_i and replacing the values of each state variable by their explicit steady-state solution. For instance, the aggregate rate law of X_i production can be represented by:

$$V_i^+ = \alpha_i \prod_{j=1}^{n+m} X_j^{g_{ij}} \tag{2.11}$$

Taking logarithms and again taking advantage of the matrix notation the expression becomes:

$$\begin{aligned} ln(V_i^+)] &= (ln\alpha_i)] + [G]\ y] \\ &= (ln\alpha_i)] + [G]_d\ y]_d + [G]_i\ y]_i \end{aligned} \tag{2.12}$$

Replacing the explicit steady-state solutions given by expression 2.10, the steady-state solution of the flux through X_i is obtained:

$$\begin{aligned} ln(V_i^+)] &= [G]_i\ y]_i + [G]_d\{[L]\ y]_i + [M]\ b]\} + (ln\alpha_i)] \\ &= \{[G]_i + [G]_d\ [L]\}y]_i + \{[G]_d\ [M]\ b] + (ln\alpha_i)]\} \\ &\qquad\quad \uparrow \qquad\qquad\qquad \uparrow \\ &\qquad \{slope\} \qquad\qquad \{intercept\} \end{aligned} \tag{2.13}$$

The solution of the flux variables is also a linear function of the independent variables. It is interesting to note that both expressions 2.10 and 2.13 express the complete relationship between the steady-state values of the dependent variables and the values of both independent variables and structural parameters of the system.

[1] At steady state, production or influx to a given pool is equal to consumption or efflux from that same pool

2.2.3 Network and Sensitivity Theory

To obtain a clear understanding of the behaviour of a particular biological system it is important to distinguish between the influence exerted by independent variables that are determined by external factors and the parameters that characterize the underlying structure of the system. Independent variables pertain to external *stimuli*, relatively fixed concentrations of enzymes or metabolites that tend to remain constant under the conditions of study. Parameters can be thought as being physically or genetically determined by the system itself. We are usually interested in determining how a particular biological system (e.g. a cell) responds to external perturbations or different enzyme concentrations (independent variables), or for example, how it changes when different enzymatic activities caused by mutations or protein modifications alter the rate constants (parameters) of a given reaction. The responses of dependent variables and fluxes through the steady-state pools when changes in independent variables or parameters occur, can be determined using the methods described in network and sensitivity theory, respectively.

2.2.3.1 Log gains

When changes in independent variables occur, they are detected and propagated throughout the cell, influencing several cellular processes (dependent variables) to different degrees. The extent to which these inputs or signals are amplified or attenuated is given by the logarithmic gain factor [7]. For instance, when one of the independent variables is changed by a small (local) variation about its nominal operating value ($\Delta X_k/X_k$), while all other independent variables remain fixed, the corresponding variation of a particular dependent variable ($\Delta X_i/X_i$) is given by the log gain factor, which can be translated into the following expression:

$$\frac{\Delta X_i/X_i}{\Delta X_k/X_k} = L_{ik} \tag{2.14}$$

A log gain with a magnitude greater than 1 corresponds to amplification of the original signal. A value below 1 implies attenuation. A positive sign for the log gain indicates that X_i changes in the same direction as X_k, i.e., both increase in value or decrease. A value of zero indicates that there are no changes in the dependent variable when this particular signal changes, and a negative sign means that the changes are in opposite directions.

The log gain factors that characterize the systemic response to variation in a specific independent variable can also be determined by differentiating the explicit

steady-state solution (equation 2.10):

$$\begin{aligned} \frac{\partial y_i}{\partial y_k} &= \frac{\partial X_i}{\partial X_k} \cdot \frac{X_k}{X_i} = L_{ik} \\ &= L(X_i, X_k) \qquad i = 1, \ldots, n;\ k = n+1, \ldots, n+m \end{aligned} \tag{2.15}$$

Each log gain L_{ik} corresponds to the percentage change in a dependent variable X_i that results from an infinitesimal percent increase in an independent variable X_k, while all other independent variables remain constant. The matrix composed by all elements L_{ik} is equivalent to $[\mathrm{L}] = -[\mathrm{M}][\mathrm{A}]_i$ defined in expression 2.10. It is noteworthy to mention that log gains can be determined from direct experimental measurements of the intact system. Each element L_{ik} is analogous to the conventional gain or amplification factors described in linear network theory. This theory provides an explicit relationship between the log gain factors that characterize the systemic behaviour and the kinetic-order parameters that characterize the component processes. Thus, it establishes an important link between two types of experimental measurements: measurements of small variations in an independent variable, and measurements of small variations in the rate of an individual component process corresponding to small variations in the state variables that influence that process. Without network theory there would be no apparent relationship between these two different types of measurements.

The log gains for the flux variables can also be defined in a similar fashion. For example, when one of the independent variables is changed by a small (local) variation about its nominal operating value ($\Delta X_k/X_k$), while all other independent variables remain fixed, the corresponding variation of the flux through a particular pool ($\Delta V_i/V_i$) is given by:

$$\frac{\Delta V_i/V_i}{\Delta X_k/X_k} = L(V_i, X_k), \tag{2.16}$$

The systemic behaviour of the dependent fluxes in steady-state can be determined by differentiating expression 2.13:

$$L(V_i, X_k) = g_{ik} + \sum_{j=1}^{n} L(X_j, X_k) \qquad i = 1, \cdots, n;\ k = n+1, \cdots, n+m \tag{2.17}$$

2.2.3.2 Sensitivities

The standard factors that relate variations in dependent variables to changes in parameter values (rate constants and kinetic orders) are referred to as parameter sensitivities [7]. There are two classes of parameter sensitivities that deal in particular with either rate constants or kinetic orders.

Sensitivities to rate constants are defined as the change in dependent variable X_i or flux V_i in going from one steady-state to another as a result of an increase in a rate constant parameter β_k or a decrease in a rate constant parameter α_k. Again, in principle, sensitivities can be determined from direct experimental measurements of the intact system. As one of the rate constants is changed by a small (local) variation about its nominal operating value ($\Delta\beta_k/\beta_k$ or $\Delta\alpha_k/\alpha_k$), while independent variables and remaining parameters are fixed, the corresponding variation of a dependent variable ($\Delta X_i/X_i$) could be measured. The ratio between both variations yield the corresponding parameter sensitivity:

$$\frac{\Delta X_i/X_i}{\Delta\beta_k/\beta_k} = S_{X_i,\beta_k} \qquad i,k = 1,\cdots,n \tag{2.18}$$

or

$$\frac{\Delta X_i/X_i}{\Delta\alpha_k/\alpha_k} = S_{X_i,\alpha_k} \qquad i,k = 1,\cdots,n \tag{2.19}$$

The systemic response to changes in rate constant parameters can also be obtained by differentiating the steady-state solution (expression 2.10):

$$\begin{aligned} \frac{\partial y_i}{\partial b_k} &= \left(\frac{\partial X_i}{\partial \beta_k}\right)\cdot\frac{\beta_k}{X_i} = M_{ik} \\ &= S(X_i,\beta_k) \qquad i,k = 1,\ldots,n \end{aligned} \tag{2.20}$$

or

$$\begin{aligned} \frac{\partial y_i}{\partial b_k} &= -\left(\frac{\partial X_i}{\partial \alpha_k}\right)\cdot\frac{\alpha_k}{X_i} = -M_{ik} \\ &= S(X_i,\alpha_k) \qquad i,k = 1,\ldots,n \end{aligned} \tag{2.21}$$

These expressions represent mathematically the percent change in a dependent variable X_i that results from an infinitesimal percent change in a rate constant parameter β_k or α_k, with the independent variables and all other parameters held fixed. According to the latter expressions, sensitivities to rate-constants are given by the elements M_{ik} of the inverse matrix of $[A]_d$ defined above, and is part of the steady-state solution. These elements are equivalent to the conventional parameter sensitivities. It is interesting to note that $S(X_i,\beta_k) = -S(X_i,\alpha_k)$, and consequently the sum of all the rate constant sensitivities is zero:

$$\sum_{k=1}^{n}[S(X_i,\alpha_k) + S(X_i,\beta_k)] = 0 \qquad i = 1,\cdots,n \tag{2.22}$$

The same rationale can be applied to the dependent fluxes, and the corresponding systemic response of each steady-state flux (V_i) to changes in rate constant parameters is obtained by differentiating expression 2.13:

$$S(V_i,\beta_k) = \sum_{j=1}^{n} g_{ij}S(X_j,\beta_k) \qquad i,k = 1,\ldots,n; \tag{2.23}$$

and

$$S(V_i, \alpha_k) = \delta_{ik} + \sum_{j=1}^{n} g_{ij} S(X_j, \alpha_k) \qquad i, k = 1, \ldots, n; \tag{2.24}$$

where δ_{ik} is equal to 1 if $i = k$ and zero otherwise. In matrix form the expressions become:

$$[S(V^+, \beta)] = [G]_d [S(X, \beta)] \tag{2.25}$$

and

$$[S(V^+, \alpha)] = [I] + [G]_d [S(X, \alpha)] \tag{2.26}$$

The other class of parameter sensitivities describes the effect of changing the kinetic orders (h_{kp} or g_{hp}) on the steady-state of each dependent variable (X_i). These sensitivities can also, in principle, be determined experimentally by producing a small variation in the kinetic order parameters about their nominal operating value ($\Delta h_{kp}/h_{kp}$ or $\Delta g_{kp}/g_{kp}$), while independent variables and all remaining parameters are held constant, and measuring the corresponding variation of a dependent variable ($\Delta X_i/X_i$)). The ratio of these two variations yields the mathematical definition of kinetic order sensitivities:

$$\frac{\Delta X_i/X_i}{\Delta h_{kp}/h_{kp}} = S_{X_i, h_{kp}} \qquad i, k = 1, \cdots, n;\ p = 1, \cdots, n+m \tag{2.27}$$

or

$$\frac{\Delta X_i/X_i}{\Delta g_{kp}/g_{kp}} = S_{X_i, g_{kp}} \qquad i, k = 1, \cdots, n;\ p = 1, \cdots, n+m \tag{2.28}$$

The systemic response to changes in kinetic order parameters can also be obtained by differentiating the explicit steady-state solution (expression 2.10):

$$\begin{aligned} \frac{\partial y_i}{\partial ln(h_{kp})} &= \left(\frac{\partial X_i}{\partial h_{kp}}\right) \cdot \frac{h_{kp}}{X_i} = h_{kp} M_{ik} y_{p0} \\ &= S(X_i, h_{kp}) \qquad i, k = 1, \ldots, n;\ p = 1, \cdots, n+m \end{aligned} \tag{2.29}$$

or

$$\begin{aligned} \frac{\partial y_i}{\partial ln(g_{kp})} &= \left(\frac{\partial X_i}{\partial g_{kp}}\right) \cdot \frac{g_{kp}}{X_i} = -g_{kp} M_{ik} y_{p0} \\ &= S(X_i, g_{kp}) \qquad i, k = 1, \ldots, n;\ p = 1, \cdots, n+m \end{aligned} \tag{2.30}$$

where y_{p0} is the steady-state value of y_p. These expressions represent the percent change in a dependent variable X_i that results from an infinitesimal percent change in a kinetic order parameter h_{kp} or g_{kp}, when the independent variables and all other parameters remain constant. Notice that from expression 2.20, $M_{ik} = S(X_i, \beta_k)$. Replacing this equivalence in expression 2.29, the following relation is obtained:

$$S(X_i, h_{kp}) = h_{kp} S(X_i, \beta_k) y_{p0} \tag{2.31}$$

And from relation 2.21, it immediately follows that:

$$S(X_i, g_{kp}) = g_{kp} S(X_i, \alpha_k) y_{p0} \tag{2.32}$$

Again, the same rationale can be applied to the dependent fluxes, and the corresponding systemic response of each steady-state flux (V_i) to changes in kinetic order parameters is obtained by differentiating expression 2.13:

$$[S(V_i, h_{kp})/_{h_{kp}}] = \sum_{j=1}^{n} g_{ij} [S(X_j, h_{kp})/_{h_{kp}}] \qquad i, k = 1, \cdots, n; p = 1, \cdots, n+m \tag{2.33}$$

and

$$[S(V_i, g_{kp})/_{g_{kp}}] = \delta_{ik} y_p + \sum_{j=1}^{n} g_{ij} [S(X_j, g_{kp})/_{g_{kp}}] \qquad i, k = 1, \cdots, n; p = 1, \cdots, n+m \tag{2.34}$$

where δ_{ik} is equal to 1 if $i = k$ and zero otherwise. In matrix form the expressions become:

$$[S(V^+, h)_p] = [G]_d [S(X, h)_p] \tag{2.35}$$

and

$$[S(V^+, g)_p] = [I] y_p + [G]_d [S(X, g)_p] \tag{2.36}$$

References

[1] Savageau, M. A. (1999) Cellular and Molecular Networks. Micro/Immun 525 course, Winter Semester. Universtity of Michigan.

[2] Voit, E. (Editor) (1991) Van Nostrand Reinhold, New York.

[3] Voit, E. (Editor) (2000) *Computational analysis of biochemical systems. A practical guide for biochemists and molecular biologists.* Cambridge University Press, Cambridge, UK.

[4] Savageau, M. A. (1969) Biochemical Systems Analysis. I. Some mathematical properties of the rate law for the component enzymatic reactions. *J Theor Biol* **25**:365–9.

[5] Savageau, M. (1969) Biochemical Systems Analysis. II. The steady-state solutions for an n-pool system using a power-law approximation. *J Theor Biol* **25**:370–9.

[6] Savageau, M. (1970) Biochemical Systems Analysis. III. Dynamic solutions using a power-law approximation. *J Theor Biol* **26**:215–26.

[7] Savageau, M. (1971) Concepts relating the behavior of biochemical systems to their underlying molecular properties. *Arch Biochem Biophys* **145**:612–21.

Part II

Results

Chapter 3

Why does SOD overexpression sometimes enhance, sometimes decrease, hydrogen peroxide production? A minimalist explanation.[†]

Contents

[†]As published in Gardner *et. al* (2002) *Free Radic. Biol. Med.* **32**(12):1351-7

Summary

Toxic effects of superoxide dismutase (SOD) overexpression are commonly attributed to increased hydrogen peroxide (H_2O_2) production. Still, published experiments yield contradictory evidence on whether SOD overexpression increases or decreases H_2O_2 production. We analyzed this issue using a minimal mathematical model. The most relevant mechanisms of superoxide consumption are treated as pseudo first-order processes, and both superoxide production and the activity of enzymes other than SOD were considered constant. Even within this simple framework, SOD overexpression may increase, hold constant or decrease H_2O_2 production. At normal SOD levels, the outcome depends on the ratio between the rate of processes that consume superoxide without forming H_2O_2 and the rate of processes that consume superoxide with high (≥ 1) H_2O_2 yield. In cells or cellular compartments where this ratio is exceptionally low (< 1), a modest decrease in H_2O_2 production upon SOD overexpression is expected. Where the ratio is higher than unity, H_2O_2 production should increase, but at most linearly, with SOD activity. The results are consistent with the available experimental observations. According to the minimal model, only where most superoxide is eliminated through H_2O_2-free processes does SOD activity have the moderately large influence on H_2O_2 production observed in some experiments.

Abbreviations: $O_2^{\bullet -}$ - superoxide; H_2O_2 - hydrogen peroxide; SOD - superoxide dismutase; CuZnSOD - copper,zinc superoxide dismutase; MnSOD - manganese superoxide dismutase; GSH - glutathione;

3.1 Introduction

Though the role of superoxide dismutase (SOD) as antioxidant defense has been largely documented, it has also been reported that high SOD activities may induce toxic effects *in vivo*. This phenomenon has been observed in *Escherichia coli* [1, 2], *Saccharomyces cerevisiae* [3], cells of several mammals [4–7], tobacco [8] and other systems. The overexpression of CuZnSOD in several tissues has also been associated with various pathologies, such as Down's syndrome and Alzheimer's disease [9–11]. The toxicity observed in cells overexpressing SOD has been suggested to result from increased hydrogen peroxide (H_2O_2) concentration and ensuing increased oxidative damage by hydroxyl radicals [2–4, 7, 9, 12]. The experimental evidence for this explanation is contradictory, however. Increased H_2O_2 concentration was found in MnSOD- [13–15] and CuZnSOD-overexpressed human fibroblasts [16], as well as in CuZnSOD-overexpressed mouse epidermal cells [17]. Yet, the opposite was observed in mouse fibroblasts overexpressing CuZnSOD [18]. Previous attempts to rationalize the effect of changes of SOD activity on H_2O_2 production in terms of particular mechanisms of superoxide ($O_2^{\bullet -}$) production and consumption have also yielded contradictory conclusions. Assuming an irreversible production of $O_2^{\bullet -}$, in absence of other significant consumption processes, the effect of increasing SOD activity should be to decrease the steady state concentration of $O_2^{\bullet -}$ without increasing H_2O_2 production. *In vivo*, however, most $O_2^{\bullet -}$ is likely produced through reversible reactions [19]; namely, of ubisemiquinone with oxygen [20]. In these conditions, an increase in SOD concentration favors the forward direction (i.e., superoxide production) [19], consequently increasing H_2O_2 production [21]. In contrast, Liochev and Fridovich [22] suggested that because dismutation competes with reactions that convert $O_2^{\bullet -}$ into H_2O_2 at *higher* yields, SOD overexpression should decrease the *overall* yield – and thus also the production – of H_2O_2.

Altogether, these works suggest that as regards H_2O_2 production, the final outcome of SOD overexpression might depend on the balance of various processes of superoxide consumption. To further explore this hypothesis, we analyzed a minimal mathematical model comprised of the main processes of $O_2^{\bullet -}$ consumption. The results show that the outcome depends on the ratio between the rates of two types of $O_2^{\bullet -}$-consuming processes at normal SOD levels: those that do not form H_2O_2 and those that form one or more H_2O_2 molecules per $O_2^{\bullet -}$ consumed. Where the ratio is higher than unity, as expected in most cells, H_2O_2 production increases with SOD activity. In rarer cases where the ratio is lower than unity, H_2O_2 production should slightly decrease with increasing SOD activities.

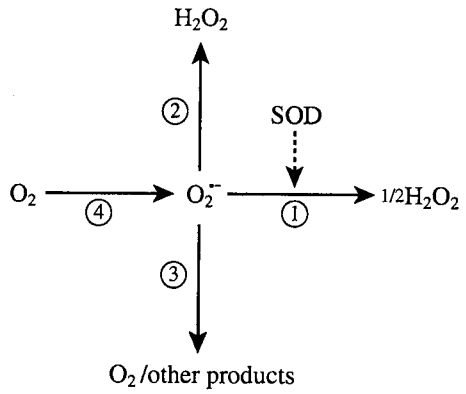

Figure 3.1: A simple model of $O_2^{\bullet-}$ production and consumption. Four processes are depicted: (1) dismutation reaction catalyzed by SOD produces 1/2 molecules of H_2O_2 per molecule of $O_2^{\bullet-}$; (2) processes of $O_2^{\bullet-}$ reduction that produce 1 or more molecules of H_2O_2 per molecule of $O_2^{\bullet-}$; (3) processes that consume $O_2^{\bullet-}$ but do not produce H_2O_2 and (4) $O_2^{\bullet-}$ generation.

3.2 Model Description

To describe the effect of SOD activity on the rate of H_2O_2 production, we considered a constant production of $O_2^{\bullet-}$, with rate v_4, and three classes of $O_2^{\bullet-}$-consuming mechanisms (Fig. 3.1). First, SOD catalyses the dismutation of $O_2^{\bullet-}$ into H_2O_2 and molecular oxygen with a yield of 1/2 molecules of H_2O_2 per molecule of $O_2^{\bullet-}$. Based on the kinetic scheme proposed by Fielden et al. [23], and considering that the concentration of SOD greatly exceeds that of $O_2^{\bullet-}$, we model $O_2^{\bullet-}$ dismutation as a pseudo first-order process. The rate expression is thus

$$v_1 = k_1[\mathrm{SOD}][O_2^{\bullet-}] \tag{3.1}$$

with k_1[SOD] playing the role of the pseudo first-order rate constant. Second, superoxide may act as an oxidant with yields of 1.0 or more molecules of H_2O_2 per molecule of $O_2^{\bullet-}$. This is the case of reactions between $O_2^{\bullet-}$ and the family of [4Fe-4S]-containing dehydratases (including the TCA-cycle enzyme aconitase) [24], which have unit H_2O_2 yield, and of chain oxidations (e.g., with hydroquinols [25] or thiols [26]), which may have higher H_2O_2 yields. Third, some reactions consume $O_2^{\bullet-}$ without producing H_2O_2. These include reactions between $O_2^{\bullet-}$ and ubiquinone (backward reaction of $O_2^{\bullet-}$ generation), nitric oxide, and cytochrome c^{3+}. As the co-reactants in the last two classes of processes are much more concentrated than superoxide itself, we treat these processes as following pseudo first-order kinetics:

$$\begin{aligned} v_2 &= k_2[O_2^{\bullet-}], \\ v_3 &= k_3[O_2^{\bullet-}] \end{aligned} \tag{3.2}$$

3.3 Results

To determine the influence of SOD concentration on the rate of H_2O_2 production, we now derive an expression for the rate of H_2O_2 production. As the physiological rates of the reactions described in this model are much faster than the processes governing changes in the activity of SOD, the system is considered to be at steady state. By definition, at steady state the rate of $O_2^{\bullet -}$ production equals the rate of $O_2^{\bullet -}$ consumption:

$$v_4 = v_1 + v_2 + v_3 \tag{3.3}$$

Substituting each rate by expressions 3.1 and 3.2, and solving the equation for $[O_2^{\bullet -}]$, the steady-state concentration of $O_2^{\bullet -}$ becomes:

$$O_2^{\bullet -} = \frac{v_4}{k_1[\mathrm{SOD}] + k_2 + k_3} \tag{3.4}$$

The overall rate of H_2O_2 production (v_H) is

$$v_H = \frac{1}{2}v_1 + v_2 = \frac{1}{2}k_1[\mathrm{SOD}][O_2^{\bullet -}] + k_2[O_2^{\bullet -}] \tag{3.5}$$

Replacing $[O_2^{\bullet -}]$ in the previous equation by its steady state expression (equation 3.4), we obtain:

$$v_H = v_4 \frac{\frac{1}{2}k_1[\mathrm{SOD}] + k_2}{k_1[\mathrm{SOD}] + k_2 + k_3} \tag{3.6}$$

The logarithmic gain [27] of the rate of H_2O_2 production to the concentration of SOD,

$$\begin{aligned} L(v_H, [\mathrm{SOD}]) &= \frac{d\log(v_H)}{d\log([\mathrm{SOD}])} = \frac{dv_H}{d[\mathrm{SOD}]} \cdot \frac{[\mathrm{SOD}]}{v_H} \\ &= \frac{k_1[\mathrm{SOD}](k_3 - k_2)}{(k_1[\mathrm{SOD}] + k_2 + k_3) \cdot (k_1[\mathrm{SOD}] + 2k_2)}, \end{aligned} \tag{3.7}$$

Table 3.1: Dependence of H_2O_2 Production on SOD Concentration

	Change in [SOD][a]	
Rate of v_2 vs. v_3	↑	↓
$v_2 < v_3$	↑	↓
$v_2 = v_3$	=	=
$v_2 > v_3$	↓	↑

[a] (↑) increase; (↓) decrease and (=) no change.

provides a concise way of describing how changes in SOD concentration affect the rate of H_2O_2 production. Positive values of L indicate that v_H increases with [SOD],

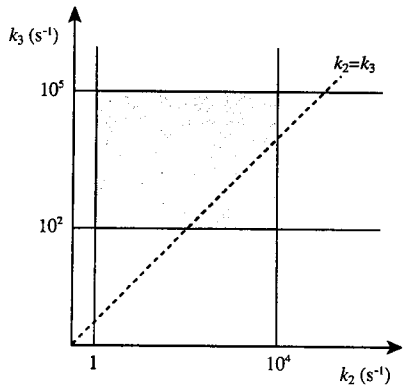

Figure 3.2: Predicting the direction of changes in H_2O_2 production from the values of k_2 and k_3. The shaded area represents the ranges of values estimated from the literature, as explained in the text. Region above dotted line: H_2O_2 production changes in the same direction as [SOD]; region below dotted line: H_2O_2 production changes in the opposite direction as [SOD].

whereas negative values indicate the opposite. A log gain of 0.5 indicates that a 1% increase in [SOD] causes 0.5% increase in v_H. As follows from equation 3.7, the log gain has the sign of $k_3 - k_2$. Hence, when the concentration of SOD increases, the rate of H_2O_2 production (v_H) may increase, decrease or remain unchanged, depending on the difference between the rate constant for $O_2^{\bullet-}$ reduction (k_2) and the rate constant for H_2O_2-free $O_2^{\bullet-}$ consumption (k_3) (Table 3.1). This result may be understood as follows. As SOD concentration increases, the steady state concentration of $O_2^{\bullet-}$ decreases and the flux of $O_2^{\bullet-}$ consumption shifts from v_2 and v_3 to v_1. The outcome on the *overall* production of H_2O_2 therefore depends on whether the increase of the rate of H_2O_2 production through dismutation (v_1) is higher or lower than its decrease through the $O_2^{\bullet-}$-reducing pathway (v_2). To illustrate this point, consider a system mostly free of SOD, and where the main pathway of $O_2^{\bullet-}$ reduction is through inactivation of dehydratases with a yield of 1 molecule of H_2O_2 per molecule of $O_2^{\bullet-}$. Addition of SOD may then lead to the following situations, depending on the balance between k_2 and k_3. (a) $k_2 = k_3$: addition of SOD decreases v_2 and v_3 by the same amount, i.e., exactly *half* of the increase through v_1. As SOD generates H_2O_2 at *half* the yield of the dehydratase inactivation, the overall production of H_2O_2 remains unchanged. (b) $k_2 > k_3$: v_2 decreases by less than half of the increase in v_1 and consequently the overall production of H_2O_2 decreases. (c) $k_2 < k_3$: the production of H_2O_2 increases with the concentration of SOD.

If the overall pseudo first-order rate constants k_2 and k_3 are known, one can predict the effect of changes in SOD activity on H_2O_2 production in particular physiological settings (Fig. 3.2). An extensive search of the available data [28] revealed only a few substances that are both reactive and abundant enough *in vivo* to compete with SOD for superoxide under physiological conditions. Reactions involving the iron-sulfur clusters of dehydratases, ascorbate and reduced glutathione (GSH) may

contribute significantly to v_2 in most cells. Rate constants between superoxide and various dehydratases are in the range $10^6 - 10^7$ $M^{-1}s^{-1}$ [reviewed in 24]. Considering the concentrations of susceptible dehydratases in the range $1 - 100$ μM [29], k_2 should lie in the range $1 - 10^3$ s^{-1}. The rate constant for the reaction with ascorbate is 2.7×10^5 $M^{-1}s^{-1}$ [30]. Ascorbate concentrations in the millimolar range [31] thus contribute 10^2 s^{-1} to k_2. There are widely discrepant determinations of the rate constant for the reaction of superoxide with GSH and other thiols. Considering the highest rate constant reported for GSH, 6.7×10^5 $M^{-1}s^{-1}$ [32], and intracellular concentrations in the range $1 - 10$ mM [33], an upper limit of 10^4 s^{-1} is found for the contribution of GSH to k_2.

As regards k_3, the rate constant for the backward reaction of $O_2^{\bullet -}$ production is one of the main contributors and occurs in most cells. From Fig. 4 in [20] a second-order rate constant for the backward reaction of $O_2^{\bullet -}$ can be estimated as 4.2×10^8 $M^{-1}s^{-1}$, which is close to the value estimated in aqueous solution between superoxide and quinone [34]. As ubiquinone concentrations in tissues of a wide variety of organisms are in the range $0.3 - 200$ μM [35], k_3 should lie in the range $10^2 - 10^5$ s^{-1}. Superoxide also reacts with nitric oxide with a rate constant of 1.9×10^{10} $M^{-1}s^{-1}$ [36]. Considering a concentration of nitric oxide in the range of $10 - 100$ nM [37], this reaction would give a contribution of $10^2 - 10^3$ s^{-1} to k_3. It may therefore be very significant in some cells. On the other hand, ferricytochrome c, which is present at concentrations up to 5 mM in the mitochondrial intermembrane space, oxidizes superoxide to oxygen with a second-order rate constant of 2.6×10^5 $M^{-1}s^{-1}$ [38]. Assuming that superoxide readily permeates the outer mitochondrial membrane and that the volume of the mitochondrial intermembrane space is at most 1% of the cytoplasm volume, one finds 10 s^{-1} as an upper estimate for the contribution of the reaction of superoxide with cytochrome c^{3+} to k_3. This contribution is therefore negligible.

From the estimates above, one predicts that in most systems $O_2^{\bullet -}$ is consumed faster through v_3 than through v_2. Therefore, H_2O_2 production should most often change in the same direction as SOD activity (Fig. 3.2). The opposite may happen, however, in systems where the concentration of co-reactants involved in $O_2^{\bullet -}$-consuming reactions that contribute to v_2 are high and/or the concentration of co-reactants contributing to v_3 are low.

In the framework of the minimal model, significant increases of H_2O_2 production upon SOD overexpression occur only in systems where, at normal SOD levels, most of the superoxide is consumed without H_2O_2 production (i.e., $v_3 \gg v_1 + v_2$) (Fig. 3.3). Yet, changes in H_2O_2 production are always less than proportional to changes in SOD activity ($|L| < 1$). In systems where H_2O_2 production decreases in response to SOD overexpression, the factor of decrease is always small as compared to the factor of SOD overexpression (L is never lower than $-1/6$).

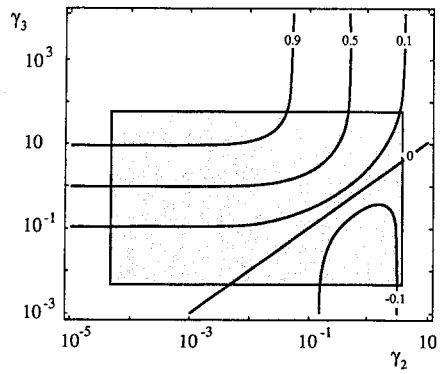

Figure 3.3: Contour plot of log gains of the rate of H_2O_2 production to the concentration of SOD. γ_2 and γ_3 are the ratios $k_2/(k_1[\text{SOD}])$ and $k_3/(k_1[\text{SOD}])$, respectively. The shaded area represents the ranges of values estimated from the literature, as shown in Fig. 3.2; values of k_1 and [SOD] used were $\sim 10^9\ \text{M}^{-1}\text{s}^{-1}$ [39] and $\sim 2 - 20\ \mu\text{M}$ [40, 41].

The minimal model presented above does not account for $O_2^{\bullet-}$ regulation of its own production. Several mechanisms of feedback inhibition have been proposed. These include aconitase inactivation, which decreases the flow of reducing equivalents into the respiratory chain [42], and proton leakage by $O_2^{\bullet-}$, which decreases the level of reduction of respiratory chain components [42, 43]. The recent findings that $O_2^{\bullet-}$ activates the uncoupling proteins UCP1, UCP2 and UCP3, resulting in mild-proton leakage [44], strongly supports the latter hypothesis. In presence of this feeback inhibition, SOD overexpression will lower the concentration of $O_2^{\bullet-}$, consequently lifting the inhibition and increasing the rate of $O_2^{\bullet-}$ generation. In the Appendix we assess how this regulation affects the response of H_2O_2 production to changes of SOD activity. For strong inhibitions, L is always positive, meaning that H_2O_2 production changes in the same direction as SOD concentration. The maximum value of the logarithmic gain, however, remains the same (+1), i.e., changes in H_2O_2 production are still at most proportional to changes in SOD.

3.4 Discussion

It is usually assumed that an increase in SOD activity elicits an increase in H_2O_2 production. Our analysis, however, shows that even without accounting for changes in the activity of other enzymes, SOD overexpression may also decrease or have no effect on H_2O_2 production. The outcome depends on the ratio between the rates of $O_2^{\bullet-}$ reduction (v_2) and the rates of the non-H_2O_2-producing reactions (v_3) at normal levels of SOD expression. As the balance between these two processes differs among cellular systems and depends on physiological conditions various outcomes are expected to occur, explaining the contradictory experimental results so far reported.

According to the minimal model, and given the estimated ranges for the rate constants of reactions contributing to v_2 and v_3 SOD overexpresssion is more prone to induce H_2O_2 overproduction than the opposite (Fig. 3.2). This is even more so where superoxide inhibits its own production. These results are consistent with the available experimental observations. Whereas various studies report increased H_2O_2 production in cells overexpressing SOD [13–17], only one reports decreased H_2O_2 production [18].

Irrespective of parameter values, however, the minimal model predicts that where H_2O_2 production decreases with increasing SOD activity, the factor of decrease is always small as compared to the factor of SOD overexpression (log gain smaller than $-1/6$). Where H_2O_2 production increases with SOD activity, the factor of increase is always lower than the factor of SOD overexpression (log gain lower than 1). These results are also consistent with the experimental data. Teixeira et al. [18] reported a 0.86-fold decrease in H_2O_2 concentration in mouse fibroblasts with a 2.3-fold increase in SOD activity, corresponding to a log gain of -0.11. In mitochondria of human fibrosarcoma cells, a 4.6-fold MnSOD overexpression increased the concentration of H_2O_2 1.6-fold [13]. Assuming that the concentration of H_2O_2 is proportional to H_2O_2 production, this response corresponds to a log gain of ~0.17. In mouse epidermal cells, a 2.3-fold CuZnSOD overexpression increased the concentration of H_2O_2 1.95-fold [17]. As the activity of catalase did not change significantly, the log gain for H_2O_2 production in this case is ~0.73.

High log gains for H_2O_2 production as estimated from [17] are only achievable within the framework of the minimal model if the normal cells eliminate most of the superoxide through processes that do not yield H_2O_2 (Fig. 3.3). Nevertheless, part of the observed increase in H_2O_2 production might also be due, for instance, to increased levels of superoxide-susceptible [4Fe-4S] clusters upon SOD overexpression.

The minimal model may serve as a "null hypothesis" in the inference of the mechanisms of oxidative damage elicited by SOD overexpression. According to this model, if the rate of oxidative damage is proportional to the rate of H_2O_2 production, the percent increase in the rate of damage will not exceed the percent increase in SOD activity. More pronounced increases of the rate of damage, if observed, could have two explanations. One is a significant departure from first-order kinetics by the considered mechanisms of superoxide consumption. The other explanation is the contribution of mechanisms that the minimal model does not account for and that are sensitive to small variations about the normal levels of H_2O_2. For example, the participation of superoxide and H_2O_2 in signal transduction and in transcriptional control of various genes, which is probably relevant for the response of the rate of oxidative damage to modulations of SOD activity [45, 46] and should be considered in more detailed analyses. Our aim, however, is to point out the explanatory power of the basic chemistry of superoxide consumption *in vivo*, as

condensed in the minimal model, and to highlight the usefulness of this model as starting point to understand the role of the aforementioned mechanisms.

References

[1] Bloch, C. and Ausubel, F. (1986) Paraquat-mediated selection for mutations in the manganese-superoxide dismutase gene *sodA*. *J Bacteriol* **168**:795–8.

[2] Scott, M.; Meshnick, S. and Eaton, J. (1989) Superoxide dismutase amplifies organismal sensitivity to ionizing radiation. *J Biol Chem* **264**:2498–501.

[3] Costa, V.; Reis, E.; Quintanilha, A. and Moradas-Ferreira, P. (1993) Acquisition of ethanol tolerance in *Saccharomyces cerevisiae*: The key role of the mitochondrial superoxide dismutase. *Arch Biochem Biophys* **300**:608–614.

[4] Elroy-Stein, O.; Bernstein, Y. and Groner, Y. (1986) Overproduction of human Cu/Zn-superoxide dismutase in transfected cells: Extenuation of paraquat-mediated cytotoxicity and enhancement of lipid peroxidation. *EMBO J* **5**:615–622.

[5] Omar, B.; Gad, N.; Jordan, M.; Striplin, S.; Russell, W.; Downey, J. and McCord, J. (1990) Cardioprotection by Cu,Zn-superoxide dismutase is lost at high doses in the reoxygenated heart. *Free Radic Biol Med* **9**:465–71.

[6] Omar, B. and McCord, J. (1990) The cardioprotective effect of Mn-superoxide dismutase is lost at high doses in the postischemic isolated rabbit heart. *Free Radic Biol Med* **9**:473–8.

[7] Amstad, P.; Peskin, A.; Shah, G.; Mirault, M.; Moret, R.; Zbinden, I. and Cerutti, P. (1991) The balance between Cu,Zn-superoxide dismutase and catalase affects the sensitivity of mouse epidermal cells to oxidative stress. *Biochemistry* **30**:9305–13.

[8] Bowler, C.; Slooten, L.; Vandenbranden, S.; De Rycke, R.; Botterman, J.; Sybesma, C.; Van Montagu, M. and Inze, D. (1991) Manganese superoxide dismutase can reduce cellular damage mediated by oxygen radicals in transgenic plants. *EMBO J* **10**:1723–32.

[9] Kedziora, J. and Bartosz, G. (1988) Down's syndrome: A pathology involving the lack of balance of reactive oxygen species. *Free Radic Biol Med* **4**:317–30.

[10] Lohr, J. (1991) Oxygen radicals and neuropsychiatric illness. Some speculations. *Arch Gen Psychiatry* **48**:1097–106.

[11] Elroy-Stein, O. and Groner, Y. (1988) Impaired neurotransmitter uptake in PC12 cells overexpressing human Cu/Zn-superoxide dismutase–implication for gene dosage effects in down syndrome. *Cell* **52**:259–67.

[12] Ceballos-Picot, I.; Nicole, A. and Sinet, P. (1992) Cellular clones and transgenic mice overexpressing copper-zinc superoxide dismutase: Models for the study of free radical metabolism and aging. In I. Emerit and B. Chance (Editors), *Free radicals and aging*, 89–98. Basel:Birkhauser Verlag, Switzerland.

[13] Wenk, J.; Brenneisen, P.; Wlaschek, M.; Poswig, A.; Briviba, K.; Oberley, T. and Scharffetter-Kochanek, K. (1999) Stable overexpression of manganese superoxide dismutase in mitochondria identifies hydrogen peroxide as a major oxidant in the AP-1-mediated induction of matrix-degrading metalloprotease-1. *J Biol Chem* **274**:25869–76.

[14] Rodriguez, A.; Carrico, P.; Mazurkiewicz, J. and Melendez, J. (2000) Mitochondrial or cytosolic catalase reverses the MnSOD-dependent inhibition of proliferation by enhancing respiratory chain activity, net ATP production, and decreasing the steady state levels of H_2O_2. *Free Radic Biol Med* **29**:801–13.

[15] Ranganathan, A.; Nelson, K.; Rodriguez, A.; Kim, K.; Tower, G.; Rutter, J.; Brinckerhoff, C.; Huang, T.; Epstein, C.; Jeffrey, J. and Melendez, J. (2001) Manganese superoxide dismutase signals matrix metalloproteinase expression via H_2O_2-dependent ERK1/2 activation. *J Biol Chem* **276**:14264–70.

[16] de Haan JB; Cristiano, F.; Iannello, R.; Bladier, C.; Kelner, M. and Kola, I. (1996) Elevation in the ratio of Cu/Zn-superoxide dismutase to glutathione peroxidase activity induces features of cellular senescence and this effect is mediated by hydrogen peroxide. *Hum Mol Genet* **5**:283–92.

[17] Schmidt, K.; Amstad, P.; Cerutti, P. and Baeuerle, P. (1995) The roles of hydrogen peroxide and superoxide as messengers in the activation of transcription factor NF-kappa B. *Chem Biol* **2**:13–22.

[18] Teixeira, H.; Schumacher, R. and Meneghini, R. (1998) Lower intracellular hydrogen peroxide levels in cells overexpressing CuZn-superoxide dismutase. *Proc Natl Acad Sci U S A* **95**:7872–5.

[19] Winterbourn, C.; French, J. and Claridge, R. (1978) Superoxide dismutase as an inhibitor of reactions of semiquinone radicals. *FEBS Lett* **94**:269–272.

[20] Cadenas, E.; Boveris, A.; Ragan, C. and Stoppani, A. (1977) Production of superoxide radicals and hydrogen peroxide by NADH-ubiquinone reductase and ubiquinol-cytochrome *c* reductase from beef-heart mitochondria. *Arch Biochem Biophys* **180**:248–257.

[21] Forman, H. and Boveris, A. (1982) Superoxide radical and hydrogen peroxide in mitochondria. In W. Pryor (Editor), *Free radicals in Biology*, 65–90. Academic Press, New York.

[22] Liochev, S. and Fridovich, I. (1994) The role of $O_2^{\bullet -}$ in the production of $HO^{\bullet}$: In vitro and in vivo. *Free Radic Biol Med* **16**:29–33.

[23] Fielden, E.; Roberts, P.; Bray, R.; Lowe, D.; Mautner, G.; Rotilio, G. and Calabrese, L. (1974) Mechanism of action of superoxide dismutase from pulse radiolysis and electron paramagnetic resonance. Evidence that only half the active sites function in catalysis. *Biochem J* **139**:49–60.

[24] Gardner, P. (1997) Superoxide-driven aconitase Fe-S center cycling. *Biosci Rep* **17**:33–42.

[25] Ollinger, K.; Buffinton, G.; Ernster, L. and Cadenas, E. (1990) Effect of superoxide dismutase on the autoxidation of substituted hydro- and semi-naphthoquinones. *Chem Biol Interact* **73**:53–76.

[26] Munday, R. (1985) Toxicity of aromatic disulphides. I. Generation of superoxide radical and hydrogen peroxide by aromatic disulphides in vitro. *J Appl Toxicol* **5**:402–8.

[27] Savageau, M. (1971) Concepts relating the behavior of biochemical systems to their underlying molecular properties. *Arch Biochem Biophys* **145**:612–21.

[28] Ross, A.; Mallard, W.; Helman, W.; Buxton, G.; Huie, R. and Neta, P. (1998) NDRL-NIST Solution Kinetics Database - Ver. 3. Tech. rep., Notre Dame Radiation Laboratory, Notre Dame, IN and NIST Standard Reference Data, Gaithersburg, MD.

[29] Keyer, K. and Imlay, J. (1997) Inactivation of dehydratase [4Fe-4S] clusters and disruption of iron homeostasis upon cell exposure to peroxynitrite. *J Biol Chem* **272**:27652–9.

[30] Nishikimi, M. (1975) Oxidation of ascorbic acid with superoxide anion generated by the xanthine-xanthine oxidase system. *Biochem Biophys Res Commun* **63**:463–8.

[31] Hornig, D. (1975) Distribution of ascorbic acid, metabolites and analogues in man and animals. *Ann N Y Acad Sci* **258**:103–18.

[32] Asada, K. and Kanematsu, S. (1976) Reactivity of thiols with superoxide radicals. *Agric Biol Chem* **40**:1891 – 1892.

[33] Forman, H. and Liu, R.-M. (1997) Glutathione cycling in oxidative stress. In L. Clerch and D. Massaro (Editors), *Oxygen, gene expression, and cellular function*, 99–121. Marcel Dekker, New York.

[34] Willson, R. (1971) Pulse radiolysis studies of electron transfer in aqueous quinone solutions. *Trans Faraday Soc* **67**:3020–3029.

[35] Crane, F. (1965) Distribution of ubiquinones. In R. A. Morton (Editor), *Biochemistry of quinones*, 183–206. Academic Press, New York.

[36] Kissner, R.; Nauser, T.; Bugnon, P.; Lye, P. and Koppenol, W. (1997) Formation and properties of peroxynitrite as studied by laser flash photolysis, high-pressure stopped-flow technique, and pulse radiolysis. *Chem Res Toxicol* **10**:1285–92.

[37] Giulivi, C. (1998) Functional implications of nitric oxide produced by mitochondria in mitochondrial metabolism. *Biochem J* **332**:673–679.

[38] Butler, J.; Koppenol, W. and Margoliash, E. (1982) Kinetics and mechanism of the reduction of ferricytochrome c by the superoxide anion. *J Biol Chem* **257**:10747–50.

[39] Forman, H. and Fridovich, I. (1973) Superoxide dismutase: A comparison of rate constants. *Arch Biochem Biophys* **158**:396–400.

[40] Hartz, J.; Funakoshi, S. and Deutsch, H. (1973) The levels of superoxide dismutase and catalase in human tissues as determined immunochemically. *Clin Chim Acta* **46**:125–32.

[41] Tyler, D. (1975) Polarographic assay and intracellular distribution of superoxide dismutase in rat liver. *Biochem J* **147**:493–504.

[42] Skulachev, V. (1996) Role of uncoupled and non-coupled oxidations in maintenance of safely low levels of oxygen and its one-electron reductants. *Q Rev Biophys* **29**:169–202.

[43] Liu, S. (1997) Generating, partitioning, targeting and functioning of superoxide in mitochondria. *Biosci Rep* **17**:259–72.

[44] Echtay, K.; Roussel, D.; St-Pierre, J.; Jekabsons, M.; Cadenas, S.; Stuart, J.; Harper, J.; Roebuck, S.; Morrison, A.; Pickering, S.; Clapham, J. and Brand, M. (2002) Superoxide activates mitochondrial uncoupling proteins. *Nature* **415**:96–9.

[45] Suzuki, Y.; Forman, H. and Sevanian, A. (1997) Oxidants as stimulators of signal transduction. *Free Radic Biol Med* **22**:269–85.

[46] Gonzalez-Flecha, B. and Demple, B. (2000) Genetic responses to free radicals. Homeostasis and gene control. *Ann N Y Acad Sci* **899**:69–87.

[47] Savageau, M. A. (1969) Biochemical Systems Analysis. I. Some mathematical properties of the rate law for the component enzymatic reactions. *J Theor Biol* **25**:365–9.

[48] Voit, E. (Editor) (2000) *Computational analysis of biochemical systems. A practical guide for biochemists and molecular biologists.* Cambridge University Press, Cambridge, UK.

Appendix A

A.1 Inclusion of a negative feedback of $O_2^{\bullet-}$ on its own production

To represent the rate of change of $O_2^{\bullet-}$ with a general feedback mechanism on its own production, we use the S-system representation [47, 48]:

$$\frac{dX_1}{dt} = \alpha_1 X_1^{g_{11}} - \beta_1 X_1^{h_{11}} \tag{A.1}$$

In this representation, all reactions that contribute to the production of a chemical species are aggregated in a positive term, and all the reactions contributing to consumption are aggregated in a negative term. In this case, X_1 is the concentration of $O_2^{\bullet-}$; α_1 and β_1 are the aggregated rate constants of reactions producing and consuming $O_2^{\bullet-}$, respectively. In the minimal model, $O_2^{\bullet-}$ production is constant, and therefore the "rate constant" is equivalent to the rate of production ($\alpha_1 = v_4$). The aggregated rate constant of consumption is the sum of all rate constants contributing to $O_2^{\bullet-}$ consumption ($\beta_1 = k_1[\mathrm{SOD}] + k_2 + k_3$). Symbols g_{11} and h_{11} are the kinetic orders of X_1 with respect to production and consumption, respectively. For a simple mass action reaction, the kinetic orders correspond to the molecularity of the reaction. As the present model considers pseudo first-order $O_2^{\bullet-}$ consumption, $h_{11} = 1$. Without feedback, $O_2^{\bullet-}$ production does not depend on the concentration of $O_2^{\bullet-}$, and so $g_{11} = 0$. A negative feedback of $O_2^{\bullet-}$ on its own production is modeled by ascribing a negative real number to g_{11}. The steady state expression for $[O_2^{\bullet-}]$ then becomes:

$$[O_2^{\bullet-}] = \left(\frac{\alpha_1}{k_1[\mathrm{SOD}] + k_2 + k_3}\right)^{\frac{1}{1-g_{11}}} \tag{A.2}$$

The rate of H_2O_2 production with a negative feedback mechanism is determined by replacing A.2 into expression 3.5. The log gain can then be calculated:

$$L_f(v_H, \text{SOD}) = \frac{k_1[\text{SOD}](k_3 - k_2 - g_{11}(k_1[\text{SOD}] + k_2 + k_3))}{(1 - g_{11}) \cdot (k_1[\text{SOD}] + k_2 + k_3) \cdot (k_1[\text{SOD}] + 2k_2)} \tag{A.3}$$

For very strong inhibitions, L_f becomes:

$$\lim_{g_{11} \to -\infty} L_f(v_H, \text{SOD}) = \frac{k_1[\text{SOD}]}{(k_1[\text{SOD}] + 2k_2)} \tag{A.4}$$

Expressions A.3 and A.4 can be compared with equation 3.7.

Chapter 4

Identification of possible mechanisms leading to amplification of H_2O_2-mediated oxidative damage when SOD is overexpressed.

Contents

Summary

In spite of the evidence that SOD overexpression may lead to deleterious effects, the mechanisms underlying these observations remain unclear. According to the minimal model described in Chapter 3, H_2O_2 increases at most linearly with SOD activity, suggesting that additional mechanisms may contribute to the prooxidative effects of SOD overexpression. To assess the effects of SOD overexpression on the rate of H_2O_2-mediated oxidative damage, which is not necessarily proportional to H_2O_2 production, we have extended the minimal model to include oxidative damage formation through Fenton reactions, a pathway of damage repair, and H_2O_2 removal by peroxidases and/or catalases. We then analyzed all possible feedforward and feedback interactions of $O_2^{\bullet -}$, H_2O_2, and oxidative damage on the rates of production and depletion of each pool. The analysis was based on well-established methods in Biochemical Systems Theory, which makes only minimal assumptions about the mechanisms of physiological processes. Using qualitative and quantitative criteria we identified a few physiologically plausible interactions that when present render the system prone to supralinear increases in the rate of oxidative damage when SOD activity is increased. We report those interactions and describe the physiological conditions whereby amplification of H_2O_2-mediated oxidative damage can be observed when SOD is overexpressed. Our results show that increasing SOD activity in different types of cells or subcellular compartments may produce quite different responses on the rate of oxidative damage. In addition, when SOD activity is increased, the presence of some interactions allow amplification of oxidative damage without significant changes in H_2O_2 concentration, suggesting that changes in these two concentrations are not necessarily correlated.

Abbreviations: SOD - superoxide dismutase; $O_2^{\bullet -}$ - superoxide; H_2O_2 - hydrogen peroxide; ROS - reactive oxygen species; Zwf - glucose-6-phosphate dehydrogenase; Ahp - alkyl hydroperoxide reductase; NADPH - reduced nicotinamide adenine dinucleotide phosphate; IRP - iron regulatory protein; BST - Biochemical Systems Theory;

4.1 Introduction

Despite strong evidence that elevated SOD activities can produce deleterious effects [1–18], the mechanism(s) underlying these observations are still far from understood. The most common explanation has been attributed to the exacerbation of H_2O_2 formation as a consequence of the dismutation reaction. However, there is contradictory evidence on whether H_2O_2 production is increased at higher steady-state activities of SOD [19, 20]. With a minimal model (Chapter 3 or [21]) we have shown that when the steady-state activity of SOD is increased H_2O_2 production may increase, decrease or remain constant depending on the physiological conditions. The outcome does not depend on the rate of dismutation. An increase in the rate of H_2O_2 production is only observed if the overall rate of H_2O_2-generating processes with higher stoichiometries than the dismutation reaction is below the overall rate of non-H_2O_2 producing reactions. In these conditions, the minimal model predicts that the rate of H_2O_2 production increases at most linearly with SOD. If one were to assume that the rate of oxidative damage is proportional to H_2O_2, for example *via* Fenton reaction, the minimal model would also predict an increase of oxidative damage at most linear with SOD. However, the rate of hydroxyl-mediated damage is not necessarily proportional to H_2O_2. For example, Liochev and Fridovich [12] proposed that the growth inhibition observed in *Escherichia coli* cells overexpressing SOD can be due to a decrease in $O_2^{\bullet-}$-mediated induction of glucose-6-phosphate dehydrogenase (E.C.: 1.1.1.49) (Zwf) consequently reducing NADPH availability. Yet, reduction of NADPH may significantly diminish the NADPH-dependent H_2O_2-reducing activity of alkyl hydroperoxide reductase (E.C.: 1.6.4.x) (Ahp), which is the main H_2O_2 scavenger in *E. coli* [22]. This would leave more H_2O_2 available for Fenton reactions and increase hydroxyl radical-mediated oxidative damage. In conditions where an increase in SOD activity significantly stimulates H_2O_2 production, if the rate of H_2O_2 reduction by Ahp is much higher than consumption through the Fenton reaction a supralinear increase in oxidative damage could be observed in cells overexpressing SOD. Similar interactions may also elicit a supralinear increase in H_2O_2-mediated oxidative damage when SOD activity is increased. For instance, assuming a slight positive feedback of oxidative damage products on their own production, it is conceivable that exacerbation of SOD activity can lead to supralinear increases in oxidative damage with only moderate alterations in the rate of H_2O_2 production.

To address these questions, we performed a systematic analysis looking for possible mechanisms that may account for supralinear changes in H_2O_2-mediated oxidative damage and/or changes in H_2O_2 steady-state concentrations. For this purpose, the minimal model from Chapter 3 [21] was extended to include oxidative damage formation, mainly by hydroxyl radicals ($HO^{\bullet}$) produced by H_2O_2 through the Fenton reaction, and a pathway of damage repair or removal. We then introduced and

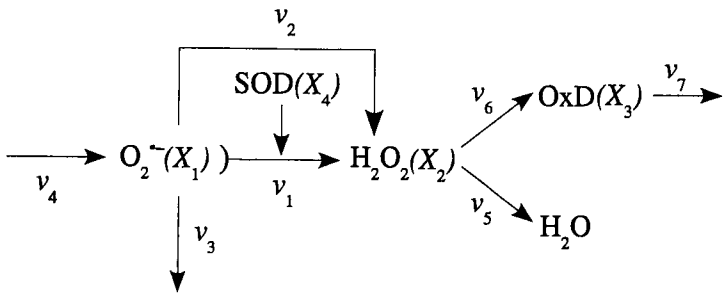

Figure 4.1: Graph representation of the reference model, which is an extension of the minimal model, using conventional symbols and in parentheses the respective S-system representation. Symbols are also described in Table 4.1. Minimal model in Chapter 3 [21] describes fluxes v_1 to v_4. The reference model takes additionaly into account two pathways of H_2O_2 consumption, through i) reduction to water (v_5) and ii) oxidative damage formation (v_6), and a pathway of damage removal or repair (v_7).

analyzed every possible interaction of $O_2^{\bullet -}$, H_2O_2 and oxidative damage on each flux considered in the model. This was done using well-established techniques in Biochemical Systems Theory (BST) (see Chapter 2 or [23]) that allow one to make minimal assumptions about the mechanisms involved in each process. Every interaction is considered generically as a positive or negative feedforward or feedback mechanism. A single parameter determines the overall kinetic order of each process with respect to each effector. This parameter therefore determines the type of kinetics involved, such as saturable, linear, cooperative, etc. For each interaction, we evaluated the influence of SOD on the steady-state concentrations of both H_2O_2 and oxidative damage. We found that, under physiological conditions, there are a few interactions that may lead to supralinear changes in H_2O_2 and oxidative damage concentrations when SOD activity is increased. Additionally, in conditions, for instance, where $O_2^{\bullet -}$ can induce the expression of enzymes responsible for damage removal/repair, an increase in SOD activity may lead to supralinear increases in oxidative damage without changes in H_2O_2 steady-state concentrations. This result implies that changes in H_2O_2 and oxidative damage are not necessarily correlated.

4.2 Methods

4.2.1 Reference Model

The minimal model (Chapter 3 or [21]), was extended to include oxidative damage formation and removal (Fig. 4.1). In the present work, oxidative damage can be understood as any oxidative product formed in macromolecules by direct action of H_2O_2 or indirectly by action of $HO^{\bullet}$, which is produced through Fenton reactions. The pathway of removal or repair of oxidative damage therefore depends on the

Table 4.1: Conversion table from conventional to S-systems symbols

Variable type	Variable name (symbol)	Symbol in S-system
Dependent	Superoxide ($O_2^{\bullet -}$)	X_1
	Hydrogen peroxide (H_2O_2)	X_2
	Oxidative Damage (OxD)	X_3
Independent	Superoxide dismutase (SOD)	X_4

type of damage considered. It may include enzymes responsible for DNA repair, lipid hydroperoxide removal from membranes, reactivation of proteins damaged by $HO^{\bullet}$, etc. A pathway of H_2O_2 detoxification was also considered, where H_2O_2 is reduced to water by peroxidases or catalase.

The following equations translate how $O_2^{\bullet -}$ (X_1), H_2O_2 (X_2), and oxidative damage (X_3) levels change in time using the S-system representation (see Table 4.1 for meaning of symbols):

$$\begin{aligned} \dot{X}_1 &= \alpha_1 - \beta_1 X_1^{h_{11}} X_4^{h_{14}} \\ \dot{X}_2 &= \alpha_2 X_1^{g_{21}} X_4^{g_{24}} - \beta_2 X_2^{h_{22}} \\ \dot{X}_3 &= \alpha_3 X_2^{g_{32}} - \beta_3 X_3^{h_{33}} \end{aligned} \tag{4.1}$$

Here, SOD (X_4) is an independent variable and therefore is a constant term in the equations. According to the S-system representation, changes in each dependent variable are defined as the difference between all influxes and all effluxes. Each term is constituted by the product of all variables that contribute to the corresponding process. At steady-state, the changes in each variable are equal to zero, where influx to a given pool equals its efflux. The steady-state solutions can be computed using the methods described in Chapter 2.

To evaluate the amount of variation in H_2O_2 and damage concentrations upon changes in SOD activity we determined the logarithmic gain of state variables X_2 and X_3 with respect to X_4 - $L(X_2, X_4)$ and $L(X_3, X_4)$, respectively (details on how to calculate log gains are also given in Chapter 2):

$$L(X_2, X_4) = \frac{g_{24}}{h_{22}} - \frac{h_{14} g_{21}}{h_{11} h_{22}} \tag{4.2}$$

$$L(X_3, X_4) = L(X_2, X_4) \cdot \frac{g_{32}}{h_{33}} \tag{4.3}$$

Just as we did with the minimal model (Chapter 3 or [21]) we assume that reactions

consuming superoxide (X_1) and forming hydrogen peroxide (X_2) follow pseudo first-order mass action kinetics. In other words, the consumption term of $\dot{X}_1$ and the production term of $\dot{X}_2$ are proportional to the concentration of X_1. The kinetic orders associated to X_1 in both these terms, h_{11} and g_{21}, are therefore set to 1. The parameter h_{22} is the average kinetic order of the overall consumption of X_2 weighted by the contributions of each process to the overall rate. A small fraction of X_2 is consumed through the Fenton reaction, which exhibits first-order kinetics with respect to X_2. Most X_2, however, is consumed through the detoxification pathway. Catalase [24, 25] and glutathione peroxidase [26], which are major contributers to the detoxification pathway, display first-order kinetics with respect to X_2 in *in vivo* conditions. Therefore, given that the two pathways of X_2 consumption (i.e., *via* detoxification or oxidative damage formation) display the same linear kinetics, the kinetic order for X_2 consumption is set to 1 ($h_{22} = 1$). The parameter g_{32} is the kinetic order of oxidative damage formation by X_2, which includes the Fenton reaction and direct oxidative damage by X_2 that can also be approximated to first-order kinetics with respect to X_2. Thus, $g_{32} = 1$. As long as the availability of the co-factors of the enzymes involved in removal or repair of oxidative damage (X_3) is not a limiting factor, the kinetics of these processes can also be approximated to first-order kinetics with respect to X_3 (i.e., $h_{33} = 1$). With all kinetic orders equal to 1 except for h_{14} and g_{24}, we arrive at a simpler expression for $L(X_2, X_4)$ and $L(X_3, X_4)$:

$$L(X_2, X_4) = g_{24} - h_{14} \tag{4.4}$$

$$L(X_3, X_4) = g_{24} - h_{14} \tag{4.5}$$

The two parameters h_{14} and g_{24} are the average kinetic orders of the overall consumption of X_1 and production of X_2 with respect to X_4, weighted by the contributions of each reaction rate to the overall rate. As the kinetic order of the dismutation reaction with respect to X_4 is 1, if for instance, most of $O_2^{\bullet -}$ disappears through dismutation, $h_{14} \simeq 1$. On the other hand, if all three processes of $O_2^{\bullet -}$ consumption contribute equally to the overall consumption rate, $h_{14} = 1/3 \times 1 + 1/3 \times 0 + 1/3 \times 0 = 1/3$. Thus, the actual values of h_{14} and g_{24} depend on the contributions of each process rate to the overall rate of $O_2^{\bullet -}$ consumption and H_2O_2 formation.

4.2.1.1 Evaluating h_{14} and g_{24} for different contributions of each process to the overall rate of $O_2^{\bullet -}$ consumption and H_2O_2 production

The average kinetic orders of superoxide (X_1) consumption and H_2O_2 (X_2) formation relative to X_4, h_{14} and g_{24}, are dependent on the contribution of the individual processes to the overall rate of X_1 consumption and X_2 production, respectively.

Table 4.2: Possible extreme *cases* regarding contribution of v_1, v_2, and v_3 to the total flux of X_1 consumption or X_2 production.

	$v_1 \gg v_2$	$v_1 = v_2$	$v_1 \ll v_2$
$v_1 \gg v_3$	*case* 1 $\begin{cases} v_2 \gg v_3 \\ v_2 = v_3 \\ v_2 \ll v_3 \end{cases}$	*case* 4 $\rightarrow v_2 \gg v_3$	*case* 7 $\rightarrow v_2 \gg v_3$
$v_1 = v_3$	*case* 2 $\rightarrow v_2 \ll v_3$	*case* 5 $\rightarrow v_2 = v_3$	*case* 8 $\rightarrow v_2 \gg v_3$
$v_1 \ll v_3$	*case* 3 $\rightarrow v_2 \ll v_3$	*case* 6 $\rightarrow v_2 \ll v_3$	*case* 9 $\begin{cases} v_2 \gg v_3 \\ v_2 = v_3 \\ v_2 \ll v_3 \end{cases}$

Table 4.2 shows all the possible combinations of contributions of each individual flux v_1, v_2, and v_3, which are explored separately. The values of h_{14} and g_{24} used in the models presented throughout this work will be based on these different combinations that are given by the each following *case*:

Case 1 ($v_1 \gg v_2$; $v_1 \gg v_3$) Whether $v_2 \gg v_3$, $v_2 = v_3$, or $v_2 \ll v_3$, most of the flux of H_2O_2 production ($^1/_2 v_1 + v_2$) and superoxide consumption ($v_1 + v_2 + v_3$) is through dismutation (v_1). As the kinetic order of dismutation relative to X_4 is 1, both h_{14} and g_{24} are 1. From expressions 4.4 and 4.5 we compute a log gain of ~ 0 for $L(X_2, X_4)$ and $L(X_3, X_4)$.

Case 2 ($v_1 \gg v_2$; $v_1 = v_3$; $v_2 \ll v_3$) In terms of X_1 consumption, though the flux is equally distributed by both v_1 and v_3, the kinetic orders of v_1 and v_3 relative to X_4 are 1 and zero, respectively. Thus, $h_{14} \simeq 50\% \times 1 + 50\% \times 0 \simeq 0.5$. As for X_2 production, the flux is mainly through dismutation and therefore $g_{24} \simeq 1$. The resulting log gains are $L(X_2, X_4) = L(X_3, X_4) \simeq 0.5$.

Case 3 ($v_1 \gg v_2$; $v_1 \ll v_3$; $v_2 \ll v_3$) Most superoxide (X_1) is consumed through v_3 and most H_2O_2 (X_2) is produced by dismutation (v_1). As the kinetic order of v_3 relative to X_4 is zero, then $h_{14} \simeq 0$. In contrast, $g_{24} \simeq 1$ because v_1 is proportional to X_4. In this case the log gains are $L(X_2, X_4) = L(X_3, X_4) \simeq 1$.

Case 4 ($v_1 = v_2$; $v_1 \gg v_3$; $v_2 \gg v_3$) In this case, the flux of superoxide (X_1) consumption is equally distributed between v_1 and v_2. As the kinetic order of v_1 relative to X_4 is 1 and the kinetic order of v_2 relative to X_4 is zero, then $h_{14} \simeq 50\% \times 1 + 50\% \times 0 \simeq 0.5$. In terms of X_2 production, v_1 produces half of the X_2 that v_2 produces (due to the stoichiometric factor), producing a slightly different relation for the average kinetic order of v_2 relative to X_4:

$g_{24} \simeq 33\% \times 1 + 67\% \times 0 \simeq 1/3$. Replacing these values in expressions 4.4 and 4.5 results in $L(X_2, X_4) = L(X_3, X_4) \simeq 1/2 - 1/3 \simeq -1/6$.

Case 5 ($v_1 = v_2$; $v_1 = v_3$; $v_2 = v_3$) Each process contributes equally to the consumption of superoxide (X_1). Therefore, $h_{14} \simeq 33\% \times 1 + 33\% \times 0 + 33\% \times 0 \simeq 1/3$. As both v_1 and v_2 are the same, they each contribute with $1/3$ and $2/3$, respectively, to the overall rate of H_2O_2 (X_2) production. Again, $g_{24} \simeq 33\% \times 1 + 67\% \times 0 \simeq 1/3$. This results in $L(X_2, X_4) = L(X_3, X_4) \simeq 1/3 - 1/3 \simeq 0$.

Case 6 ($v_1 = v_2$; $v_1 \ll v_3$; $v_2 \ll v_3$) Superoxide (X_1) is mostly consumed through v_3. As the kinetic order of v_3 relative to X_4 is zero, $h_{14} \simeq 0$. Though little H_2O_2 (X_2) is produced in this case, a third of the overall production of X_2 is through v_1 and two thirds through v_2, resulting in $g_{24} \simeq 33\% \times 1 + 67\% \times 0 \simeq 1/3$. One obtains $L(X_2, X_4) = L(X_3, X_4) \simeq 1/3 - 0 \simeq 1/3$.

Case 7 ($v_1 \ll v_2$; $v_1 \gg v_3$; $v_2 \gg v_3$) The flux through the dismutation reaction is minimal, and most superoxide (X_1) consumed and H_2O_2 (X_2) produced is through v_2. As the kinetic order of v_2 relative to X_4 is zero, h_{14} and g_{24} are close to zero. Therefore, $L(X_2, X_4) = L(X_3, X_4) \simeq 0$.

Case 8 ($v_1 \ll v_2$; $v_1 = v_3$; $v_2 \gg v_3$) The same situation as *case* 7 above, though in this case $v_1 = v_3$. Thus, $L(X_2, X_4) = L(X_3, X_4) \simeq 0$.

Case 9 ($v_1 \ll v_2$; $v_1 \ll v_3$) Whether $v_2 \gg v_3$, $v_2 = v_3$, or $v_2 \ll v_3$, the overall flux of H_2O_2 (X_2) production is given by v_2, and therefore $g_{24} \simeq 0$. Though in terms of superoxide (X_1) consumption the flux may change between v_2 and v_3 depending on their individual contributions, the kinetic orders of v_2 and v_3 relative to X_4 are zero, and so h_{14} is always approximately to zero. The resulting log gains are $L(X_2, X_4) = L(X_3, X_4) \simeq 0$.

These nine *cases* represent the limits of the log gains as presented in Fig. 3 in Chapter 3 [21], which is expected as the log gains $L(X_2, X_4)$ and $L(X_3, X_4)$ are the same as the log gain calculated in the minimal model for H_2O_2 production when SOD is overexpressed.

4.2.2 Model Variants

The reference model has 3 variables × 7 reactions = 21 different possible interactions that can either be positive or negative (Examples in Fig. 4.2). Each interaction is considered separately as a model variant, and the logarithmic gains of H_2O_2 and damage with respect to SOD concentration were determined for each of these 21 model variants. Given that for each model variant either a new parameter is introduced or the existing ones are changed to account for the new interaction,

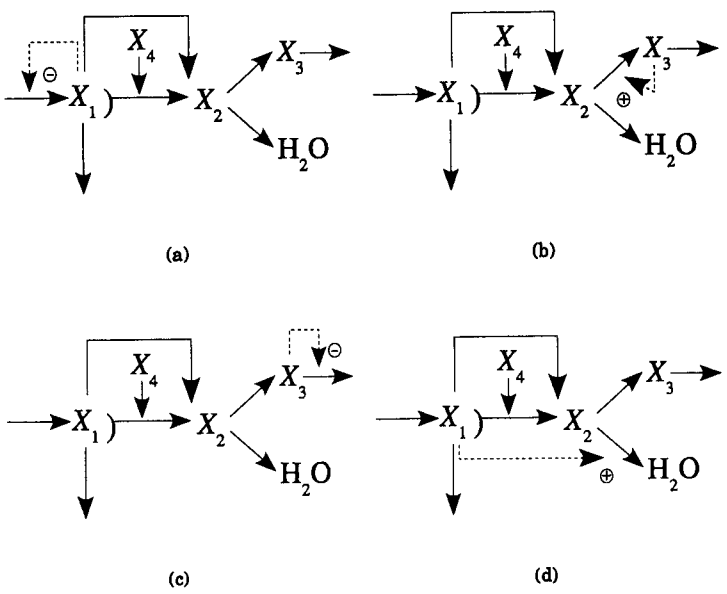

Figure 4.2: Twenty one different interactions are possible by the 3 dependent variables on the 7 reactions considered in the extended minimal model. Each interaction may be either negative or positive. Four examples of model variants are shown here, with different signs: (a) (Negative) feedback mechanism of superoxide (X_1) on its own production; (b) (positive) feedback of damage on its formation; (c) (negative) feedforward mechanism of damage on processes of damage repair; and (d) (positive) feedforward of superoxide (X_1) on processes of H_2O_2 detoxification.

the task of ascertaining whether the log gains are greater than 1 may become unfeasible. However, we know that in the reference model the log gain $L(X_2, X_4)$ is the same as in the minimal model reported in [21], whose absolute value is always less than 1 (i.e., without amplification). The reference model can therefore be used as a reference system and compared to each model variant. A variant that shows log gains greater than those obtained in the reference system represents a candidate mechanism of H_2O_2 or damage amplification when SOD is overexpressed. However, to compare two different models, an adequate controlled method must be used. We employed the concepts of internal equivalence used in mathematically controlled comparisons [27] where it is assumed that both systems being compared differ only in the single specific process that characterizes the alternative model. The values of parameters that characterize the unaltered processes of the alternative model (model variant) are assumed to be strictly identical to the corresponding parameters of the reference or control system (reference model). With the parameter values differing only in the altered process, the system is allowed to reach a different steady-state which can be directly compared with the control system. Differences in steady-states and log gains may therefore be attributed only to differences in the parameters pertaining to the altered process.

4.3 Results

The values of the log gains for all twenty one model variants are presented in Table 4.3. Each interaction is analysed separately considering the possibility of both activation and inhibition mechanisms. To illustrate the approach, the first interaction is explored with some detail and the remaining twenty possible interactions are described more briefly. Table 4.18 on page 104 summarizes the interactions that are capable of producing amplification of H_2O_2 and H_2O_2-mediated damage concentrations when SOD activity is augmented.

Table 4.3: Log gains for all 21 alternative models. $L_{ij}^{(2)}$ and $L_{ij}^{(3)}$ are the log gains of X_2 and X_3 with respect to X_4, respectively. Subscript ij corresponds to the model variant where X_i acts as an effector on v_j.

	X_1	X_2	X_3
v_1	$L_{11}^{(2)} = g_{24} - h_{14}\frac{g_{21}}{h_{11}}$	$L_{21}^{(2)} = \frac{g_{24}-h_{14}}{1+h_{12}-g_{22}}$	$L_{31}^{(2)} = \frac{g_{24}-h_{14}}{1+h_{13}-g_{23}}$
	$L_{11}^{(3)} = g_{24} - h_{14}\frac{g_{21}}{h_{11}}$	$L_{21}^{(3)} = \frac{g_{24}-h_{14}}{1+h_{12}-g_{22}}$	$L_{31}^{(3)} = \frac{g_{24}-h_{14}}{1+h_{13}-g_{23}}$
v_2	$L_{12}^{(2)} = g_{24} - h_{14}\frac{g_{21}}{h_{11}}$	$L_{22}^{(2)} = \frac{g_{24}-h_{14}}{1+h_{12}-g_{22}}$	$L_{32}^{(2)} = \frac{g_{24}-h_{14}}{1+h_{13}-g_{23}}$
	$L_{12}^{(3)} = g_{24} - h_{14}\frac{g_{21}}{h_{11}}$	$L_{22}^{(3)} = \frac{g_{24}-h_{14}}{1+h_{12}-g_{22}}$	$L_{32}^{(3)} = \frac{g_{24}-h_{14}}{1+h_{13}-g_{23}}$
v_3	$L_{13}^{(2)} = g_{24} - h_{14}\frac{1}{h_{11}}$	$L_{23}^{(2)} = \frac{g_{24}-h_{14}}{1+h_{12}}$	$L_{33}^{(2)} = \frac{g_{24}-h_{14}}{1+h_{13}}$
	$L_{13}^{(3)} = g_{24} - h_{14}\frac{1}{h_{11}}$	$L_{23}^{(3)} = \frac{g_{24}-h_{14}}{1+h_{12}}$	$L_{33}^{(3)} = \frac{g_{24}-h_{14}}{1+h_{13}}$
v_4	$L_{14}^{(2)} = g_{24} - \frac{h_{14}}{1-g_{11}}$	$L_{24}^{(2)} = \frac{g_{24}-h_{14}}{1-g_{12}}$	$L_{34}^{(2)} = \frac{g_{24}-h_{14}}{1-g_{13}}$
	$L_{14}^{(3)} = g_{24} - \frac{h_{14}}{1-g_{11}}$	$L_{24}^{(3)} = \frac{g_{24}-h_{14}}{1-g_{12}}$	$L_{34}^{(3)} = \frac{g_{24}-h_{14}}{1-g_{13}}$
v_5	$L_{15}^{(2)} = g_{24} - h_{14}(1-h_{21})$	$L_{25}^{(2)} = \frac{g_{24}-h_{14}}{h_{22}}$	$L_{35}^{(2)} = \frac{g_{24}-h_{14}}{1+h_{23}}$
	$L_{15}^{(3)} = g_{24} - h_{14}(1-h_{21})$	$L_{25}^{(3)} = \frac{g_{24}-h_{14}}{h_{22}}$	$L_{35}^{(3)} = \frac{g_{24}-h_{14}}{1+h_{23}}$
v_6	$L_{16}^{(2)} = g_{24} - h_{14}(1-h_{21})$	$L_{26}^{(2)} = \frac{g_{24}-h_{14}}{h_{22}}$	$L_{36}^{(2)} = \frac{(g_{24}-h_{14})(1-g_{33})}{1+h_{23}-g_{33}}$
	$L_{16}^{(3)} = g_{24} - h_{14}(1-h_{21}+g_{31})$	$L_{26}^{(3)} = \frac{g_{24}-h_{14}}{h_{22}} \cdot g_{32}$	$L_{36}^{(3)} = \frac{g_{24}-h_{14}}{1+h_{23}-g_{33}}$
v_7	$L_{17}^{(2)} = g_{24} - h_{14}$	$L_{27}^{(2)} = g_{24} - h_{14}$	$L_{37}^{(2)} = g_{24} - h_{14}$
	$L_{17}^{(3)} = g_{24} - h_{14}(1-h_{31})$	$L_{27}^{(3)} = (g_{24}-h_{14}).(1-h_{32})$	$L_{37}^{(3)} = \frac{g_{24}-h_{14}}{h_{33}}$

4.3.1 Superoxide (X_1) as an effector...

4.3.1.1 ...of the dismutation reaction (v_1)

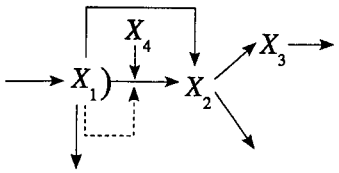

$$\begin{aligned}
\dot{X}_1 &= \alpha_1 - \beta_1 X_1^{h_{11}} X_4^{h_{14}} \\
\dot{X}_2 &= \alpha_2 X_1^{g_{21}} X_4^{g_{24}} - \beta_2 X_2^{h_{22}} \\
\dot{X}_3 &= \alpha_3 X_2^{g_{32}} - \beta_3 X_3^{h_{33}}
\end{aligned}$$

Figure 4.3: Graph depicting a positive or negative interaction of superoxide (X_1) on the dismutation reaction (v_1), and its S-system representation. This model variant is described by the same S-system as that of the reference model and no new parameters are introduced, except that h_{11} and g_{21} take different values.

This model variant, which includes a feedforward mechanism where superoxide (X_1) interacts indirectly on the dismutation reaction, is described by the same S-system as that of the reference model (Fig 4.3). The log gains of X_2 and X_3 with respect to X_4 (represented by the superscript (2) and (3), respectively) derived from this model are therefore the same as expressions 4.2 and 4.3:

$$L_{11}^{(2)} = \frac{g_{24}}{h_{22}} - \frac{h_{14}g_{21}}{h_{11}h_{22}} \tag{4.6}$$

$$L_{11}^{(3)} = \frac{g_{24}g_{32}}{h_{22}h_{33}} - \frac{h_{14}g_{21}g_{32}}{h_{11}h_{22}h_{33}} \tag{4.7}$$

The indices of $L_{11}^{(2)}$ and $L_{11}^{(3)}$ - "11" - identify the model variant, which in this case is where X_1 is an effector of v_1. According to the internal equivalence criterioncriterion, though both alternative and reference systems are described by the same S-system, only the values taken by the parameters related to the influence of X_1 on the dismutation reaction, h_{11} and g_{21}, are different from the reference model. The log gain expressions are then simplified to (see Table 4.3):

$$L_{11}^{(2)} = L_{11}^{(3)} = g_{24} - h_{14}\frac{g_{21}}{h_{11}} \tag{4.8}$$

The difference between this model variant and the reference model will obviously depend on the new values h_{11} and g_{21}, i.e., on the sign and strength of the new interaction. As these two kinetic orders are already 1 in the reference model (representing linear kinetics), an extra negative interaction can yield a positive kinetic order of the flux of dismutation (v_1) with respect to superoxide (X_1), though always lower than 1. A kinetic order greater than 1 is observed only for positive interactions, which might display, for instance, cooperative kinetics with respect to X_1. As

Table 4.4: Case by case analysis of the log gains $L_{11}^{(2)}$ and $L_{11}^{(3)}$.

cases	h_{14}	g_{24}	h_{11}	g_{21}	$L_{11}^{(2)} = L_{11}^{(3)}$
1	1	1	γ	γ	0
2	$1/2$	1	$\frac{1+\gamma}{2}$	γ	$\frac{1}{1+\gamma}$
3	0	1	1	γ	1
4	$1/2$	$1/3$	$\frac{1+\gamma}{2}$	$\frac{2+\gamma}{3}$	$-\frac{1}{3} \cdot \frac{1}{1+\gamma}$
5	$1/3$	$1/3$	$\frac{2+\gamma}{3}$	$\frac{2+\gamma}{3}$	0
6	0	$1/3$	1	$\frac{2+\gamma}{3}$	$1/3$
7	0	0	1	1	0
8	0	0	1	1	0
9	0	0	1	1	0

in the reference model, given that v_1 is not the only flux contributing to the rate of X_1 consumption, the effect of X_1 on the overall kinetic order of X_1 consumption (h_{11}) and X_2 production (g_{21}) will depend on the different contributions of v_1, v_2 and v_3 on these processes (i.e., on the different *cases* defined in section 4.2.1.1). To determine the effect of the new interaction of X_1 on the overall kinetic orders h_{11} and g_{21} we defined γ as the new kinetic order of the affected reaction (in this case v_1) with respect to the effector (in this case X_1). We were then able to analyse the log gains as a function of the kinetic order of the new interaction for every *case* where v_1, v_2 and v_3 contribute differently to the overall rate of X_1 consumption and X_2 production (Table 4.4). The same definition will be used throughout the remaining model variants. As mentioned in Chapter 2, kinetic orders for most biological processes are in the range $[-4, 4]$, so it would be expected in this particular case for an extra inhibitory interaction of X_1 on v_1 to be represented by $-4 \leq \gamma < 1$ (corresponding to saturable or negative cooperative kinetics for X_1), an extra activating interaction displaying saturable kinetics by $0 < \gamma < 1$ (corresponding to positive saturable kinetics for X_1) and an extra positive interaction displaying cooperative kinetics by $1 < \gamma \leq 4$ (corresponding to positive cooperative kinetics for X_1).

The influence of SOD (X_4) on the steady-state concentrations X_2 and X_3 is independent of the sign and strength of the new interaction and equal to that in the reference model for every *case* except for *cases* 2 and 4 (Table 4.4). For example, in *cases* 1 and 5, the new interaction has the same effect on the consumption rate of X_1 as on the production rate of X_2, which translates into $h_{11} = g_{21}$. Thus, the influence of X_4 on both X_2 and X_3 is equivalent to the one obtained in the reference

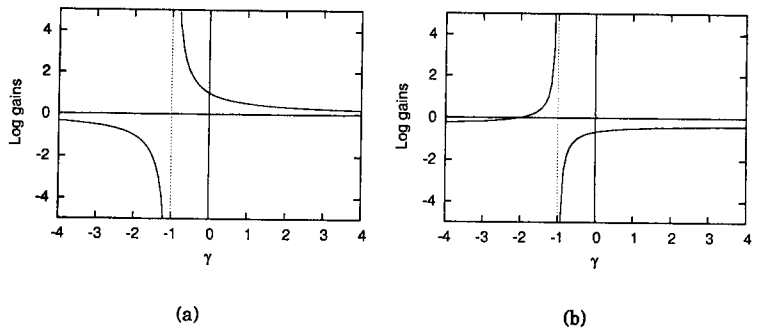

Figure 4.4: Log gains $L_{11}^{(2)}$ and $L_{11}^{(3)}$ calculated for different values of γ where (a) $v_1 \gg v_2$ and $v_1 = v_3$ (*case* 2); (b) $v_1 = v_2$ and $v_1 \gg v_3$ (*case* 4). Note that the plots are not representing how the steady-state behaviour of the system changes as a function of γ. Changing the strength of the interaction alters the contributions of the rates of each process towards the overall rate of X_1 depletion and X_2 formation yielding different values for h_{14} and g_{24}. Instead, what the plots are showing is: given a certain fixed relationship between the rates of each process contributing to X_1 consumption and X_2 production (consequently fixing the values for all kinetic orders including h_{14} and g_{14}), what will be $L(X_2, X_4)$ or $L(X_3, X_4)$ for different values of γ?

model. In *cases* 3 and 6, most of the flux of X_1 consumption is through v_3 and the strength and sign of the new interaction have negligible effects on the log gains. The new interaction has also little effect on the log gains when the dismutation reaction (the pathway being affected by the interaction) has negligible flux as seen in *cases* 7, 8 and 9.

In contrast, in *cases* 2 and 4 the log gains are greatly influenced by the strength and sign of the feedforward mechanism (Fig. 4.4). In *case* 2, v_2 is negligible and the rates of X_1 consumption v_1 and v_3 are equal. With activating cooperative kinetics for X_1, given by a new positive feedforward mechanism ($\gamma > 1$), the log gains $L(X_2, X_4)$ and $L(X_3, X_4)$ decrease with the strength of the extra interaction (Fig. 4.4a). In these conditions, for a stronger positive feedforward interaction, the same change in X_4 has less effect on depleting X_1 and less of the flux will be transfered from v_3 to v_1. Conversely, saturating kinetics for X_1, given by a weak negative feedforward mechanism, has an effect in the same direction as increasing X_4, leading to positive log gains greater than 1 (positive amplification). However, if the extra interaction of X_1 on the dismutation reaction represents a stronger negative feedforward mechanism, i.e., negative cooperative kinetics for X_1 ($\gamma \leq -1$) the system can no longer reach a stable positive steady-state. The point at which this occurs ($\gamma = -1$) is a bifurcation point. The local stability of the steady-states can be checked by analysing the eigenvalues of the system. If the real parts of all the eigenvalues are negative, the nominal steady-state is locally stable. If one of the eigenvalues has a positive real part, there is no stable positive steady-state. For

this model variant the eigenvalues are:

$$\begin{aligned}\lambda_1 &= -\frac{1}{2}(1+\gamma)\cdot X_4^{\frac{2h_{14}}{1+\gamma}}\cdot\alpha_1^{\frac{\gamma-1}{1+\gamma}}\cdot\beta_1^{\frac{2}{1+\gamma}}\\ \lambda_2 &= -\beta_2\\ \lambda_3 &= -\beta_3\end{aligned}$$

We can easily see that all eigenvalues are negative except when $\gamma \leq -1$. This means that the left branches of the graphs depicted in Fig. 4.4 represent unstable steady-states and should therefore be discarded. Though the right branch in Fig. 4.4a represents stable steady-states, amplification (log gain> 1) is only seen in the region close to the bifurcation point (dashed line, $\gamma = -1$). In these regions the system is highly sensitive to changes in parameters or control variables such as SOD, and thus log gains such as $L^{(2)}$ and $L^{(3)}$ are expected to be very high. However, biological systems tend to evolve away from conditions where small fluctuations of signals or other parameters cause drastic changes in steady-state concentrations. Highly sensitive systems are frail because small changes in environmental parameters such as temperature, pH or ionic strength could have unpredictable and uncontrollable effects. Therefore, to further assess the physiological plausibility of the model variants in conditions where they present amplification of oxidative damage close to a bifurcation point, we analysed the log gains of the steady-state concentrations with respect to external factors, such as oxidative load. In this model, oxidative load is given by the input of radical species, i.e., the rate of superoxide production. In natural occurring settings, cells or subcellular compartments should be able to sustain reasonable variations in oxidative load without significant changes in the steady-state concentrations. It is reasonable to assume then that the log gain of the steady-state concentrations with respect to changes in the rate of $O_2^{\bullet-}$ production should be low ($|L(X_i, \alpha_1)| < 2$). These log gains are calculated using the methodology described in Chapter 2, and can be expressed differently for each model variant depending on whether X_1 acts as an effector:

$$L(X_i, \alpha_1) = \frac{g_{24} - L(X_i, X_4)}{h_{14}} \tag{4.9}$$

or whether X_2 or X_3 act as effectors:

$$L(X_i, \alpha_1) = \frac{L(X_i, X_4)}{g_{24} - h_{14}} \tag{4.10}$$

with X_i representing $O_2^{\bullet-}$, H_2O_2 or oxidative damage. The same argument could be used in terms of the log gain of the rate of oxidative damage production with respect to changes in oxidative load ($|L(V_3^+, \alpha_1)| < 2$). However, in this case $L(V_3^+, \alpha_1)$ for different model variants is equal either to $L(X_2, \alpha_1)$ or $L(X_3, \alpha_1)$, and thus just a particular case of the results obtained using $L(X_i, \alpha_1)$. Model variants that present

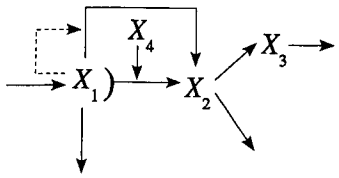

$$\begin{aligned}\dot{X}_1 &= \alpha_1 - \beta_1 X_1^{h_{11}} X_4^{h_{14}} \\ \dot{X}_2 &= \alpha_2 X_1^{g_{21}} X_4^{g_{24}} - \beta_2 X_2^{h_{22}} \\ \dot{X}_3 &= \alpha_3 X_2^{g_{32}} - \beta_3 X_3^{h_{33}}\end{aligned}$$

Figure 4.5: Graph depicting a positive or negative interaction of superoxide (X_1) on the superoxide reductive pathway (v_2), and its S-system representation. As in the previous model variant, the S-system is identical to that describing the reference model, though h_{11} and g_{21} are different.

amplification of oxidative damage and H_2O_2 when $|L(X_i, \alpha_1)| < 2$ are considered to be physiologically plausible. When $|(L(X_i, \alpha_1)| > 2$ steady-state concentrations are very influenced by changes in oxidative load. Because lower gains of concentrations and productions of reactive oxygen species (ROS) and oxidative damage can be achieved by other variants that might easily have evolved from such systems, organisms with such poor design are unlikely to have survived natural selection to present day. Model variants that show amplification only in these conditions are thus discarded from our analysis as implausible. For *case* 2 in this particular model variant and according to equation 4.9, the log gains $L_{11}(X_i, \alpha_1)$ are:

$$L_{11}(X_i, \alpha_1) = \begin{bmatrix} 1/h_{11} \\ g_{21}/h_{11} \\ g_{21}/h_{11} \end{bmatrix} \tag{4.11}$$

From these log gains, one can determine that $|L_{11}(X_i, \alpha_1)| < 2$ only where $\gamma > 0$, i.e., where there is no amplification of oxidative damage or H_2O_2 (Fig. 4.4a). Thus, *case* 2 does not present amplification under physiologically plausible settings.

In *case* 4 (Fig. 4.4b) the same arguments can be used as in *case* 2, except that now v_3 is negligible and $v_1 = v_2$. Thus, when the flux is transfered from v_2 to v_1 as a consequence of an increase in X_4, the production of X_2 is decreased more than it is increased due to the different stoichiometries. The resulting dependency towards γ is the opposite of *case* 2, i.e., it leads to negative log gains smaller than -1. This "negative amplification", though out of the scope of this work, may also be interesting for future analysis as it corresponds to situations in which small increases in SOD lead to larger decreases in oxidative damage or in which small decreases in SOD activity lead to larger increases in oxidative damage.

4.3.1.2 ...of its reductive pathway (v_2)

This model variant is also described by the same S-system as the reference model, although with different parameters (Fig. 4.5). The simplified log gains $L(X_2, X_4)$

Table 4.5: Case by case analysis of the log gains $L_{12}^{(2)}$ and $L_{12}^{(3)}$.

cases	h_{14}	g_{24}	h_{11}	g_{21}	$L_{12}^{(2)} = L_{12}^{(3)}$
1	1	1	1	1	0
2	$1/2$	1	1	1	$1/2$
3	0	1	1	1	1
4	$1/2$	$1/3$	$\frac{1+\gamma}{2}$	$\frac{1+2\gamma}{3}$	$-\frac{1}{3} \cdot \frac{\gamma}{1+\gamma}$
5	$1/3$	$1/3$	$\frac{2+\gamma}{3}$	$\frac{1+2\gamma}{3}$	$\frac{1}{3} \cdot \frac{1-\gamma}{2+\gamma}$
6	0	$1/3$	1	$\frac{1+2\gamma}{3}$	0
7	0	0	γ	γ	0
8	0	0	γ	γ	0
9	0	0	γ, $\frac{1+\gamma}{2}$ or 1[a]	γ	0

[a] For $v_2 \gg v_3$, $v_2 = v_3$, $v_2 \ll v_3$, respectively.

and $L(X_3, X_4)$ are thus the same as expression 4.8:

$$L_{12}^{(2)} = L_{12}^{(3)} = g_{24} - h_{14}\frac{g_{21}}{h_{11}} \tag{4.12}$$

However, h_{11} and g_{21} take different values for the same *cases* as in the previous model variant. The parameter γ is now related to the strength of the interaction of X_1 on its reductive pathway, v_2 (Table 4.5).

There are two *cases*, 4 and 5, that show positive amplification with stable steady-states for, $-1 < \gamma < -3/4$ and $-2 < \gamma < -5/4$, respectively. The stability was assessed by determining the eigenvalues (not shown) that indicate positive stable steady-states for $\gamma > -1$ and $\gamma > -2$ in *cases* 4 and 5, respectively. Given that amplification is seen close to a bifurcation point, $L_{12}(X_i, \alpha_1)$ was calculated and found to be large ($|L_{12}(X_i, \alpha_1)| > 2$) in the regions showing amplification. Activating interactions do not show any amplification and stronger negative feedforward kinetics produce unstable steady-states.

4.3.1.3 ...of its non H_2O_2-producing consumption pathway (v_3)

As in the previous model variants, the S-system is identical to that in the reference model (Fig. 4.6). In this case, however, the new interaction has no direct effect on processes producing X_2 and the value of g_{21} remains the same as in the reference

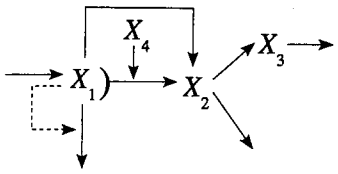

$$\begin{aligned}\dot{X}_1 &= \alpha_1 - \beta_1 X_1^{h_{11}} X_4^{h_{14}} \\ \dot{X}_2 &= \alpha_2 X_1^{g_{21}} X_4^{g_{24}} - \beta_2 X_2^{h_{22}} \\ \dot{X}_3 &= \alpha_3 X_2^{g_{32}} - \beta_3 X_3^{h_{33}}\end{aligned}$$

Figure 4.6: Graph depicting a positive or negative interaction of superoxide (X_1) on the non H_2O_2-producing pathway (v_3), and its S-system representation. Though this model variant has the same S-system representation as the reference model, h_{11} is different

Table 4.6: Case by case analysis of the log gains $L_{13}^{(2)}$ and $L_{13}^{(3)}$.

cases	h_{14}	g_{24}	h_{11}	$L_{13}^{(2)} = L_{13}^{(3)}$
1	1	1	1	0
2	$1/2$	1	$\frac{1+\gamma}{2}$	$\frac{\gamma}{1+\gamma}$
3	0	1	γ	1
4	$1/2$	$1/3$	1	$-1/6$
5	$1/3$	$1/3$	$\frac{2+\gamma}{3}$	$\frac{1}{3} \cdot \frac{\gamma-1}{2+\gamma}$
6	0	$1/3$	γ	$1/3$
7	0	0	1	0
8	0	0	1	0
9	0	0	1, $\frac{1+\gamma}{2}$ or γ[a]	0

[a] For $v_2 \gg v_3$, $v_2 = v_3$, $v_2 \ll v_3$, respectively.

model. With $g_{21} = 1$, the simplified log gains are:

$$L_{13}^{(2)} = L_{13}^{(3)} = g_{24} - h_{14}\frac{1}{h_{11}} \tag{4.13}$$

The log gains for each *case* are presented in Table 4.6. The only *cases* which could potentially exhibit positive amplification are *cases* 2 and 5. However, according to the eigenvalue expressions (not shown) positive amplification only occurs in regions without positive stable steady-states.

4.3.1.4 ...of its own production (v_4)

When X_1 acts as an effector of its own production, a new parameter g_{11} is introduced that expresses the strength and sign of the effect of X_1 on its own production

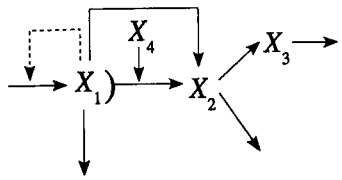

$$\begin{aligned}\dot{X}_1 &= \alpha_1 X_1^{g11} - \beta_1 X_1^{h11} X_4^{h14}\\ \dot{X}_2 &= \alpha_2 X_1^{g21} X_4^{g24} - \beta_2 X_2^{h22}\\ \dot{X}_3 &= \alpha_3 X_2^{g32} - \beta_3 X_3^{h33}\end{aligned}$$

Figure 4.7: Graph depicting a positive or negative interaction of superoxide (X_1) on its own production (v_4), and its S-system representation. A new parameter is introduced, g_{11}, while all other parameters remain the same as in the reference model.

Table 4.7: Case by case analysis of the log gains $L_{14}^{(2)}$ and $L_{14}^{(3)}$.

cases	h_{14}	g_{24}	$L_{14}^{(2)} = L_{14}^{(3)}$ $(g_{11} = \gamma)$
1	1	1	0
2	1/2	1	$\frac{1}{2} \cdot \frac{1-2\gamma}{1-\gamma}$
3	0	1	1
4	1/2	1/3	$-\frac{1}{6} \cdot \frac{1+2\gamma}{1-\gamma}$
5	1/3	1/3	$-\frac{1}{3} \cdot \frac{\gamma}{1-\gamma}$
6	0	1/3	1/3
7	0	0	0
8	0	0	0
9	0	0	0

rate (Fig. 4.7). The calculated log gains are:

$$L_{14}^{(2)} = \frac{g_{24}}{h_{22}} - \frac{g_{21} h_{14}}{(h_{11} - g_{11}) h_{22}} \tag{4.14}$$

$$L_{14}^{(3)} = \left(\frac{g_{24}}{h_{22}} - \frac{g_{21} h_{14}}{(h_{11} - g_{11}) h_{22}} \right) \frac{g_{32}}{h_{33}} \tag{4.15}$$

Maintaining the same values for all kinetic orders as those in the reference model, expressions 4.14 and 4.15 are simplified to:

$$L_{14}^{(2)} = L_{14}^{(3)} = g_{24} - \frac{h_{14}}{1 - g_{11}} \tag{4.16}$$

In this case, γ is g_{11} and a value of zero means no effective interaction (equal to the reference system), while positive or negative values represent activation or inhibition, respectively. In Table 4.7, the various values of h_{14} and g_{24} are taken into consideration and the log gains are determined for each different *case*. According

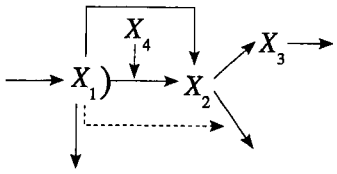

$$\begin{aligned}\dot{X}_1 &= \alpha_1 - \beta_1 X_1^{h_{11}} X_4^{h_{14}} \\ \dot{X}_2 &= \alpha_2 X_1^{g_{21}} X_4^{g_{24}} - \beta_2 X_1^{h_{21}} X_2^{h_{22}} \\ \dot{X}_3 &= \alpha_3 X_2^{g_{32}} - \beta_3 X_3^{h_{33}}\end{aligned}$$

Figure 4.8: Graph depicting a positive or negative interaction of superoxide (X_1) on the pathway that leads to H_2O_2 detoxification (v_5), and its S-system representation. A new parameter is introduced, h_{21}, while all other parameters remain the same as in the reference model.

to the eigenvalue expressions for this model variant (not shown), positive stable steady-states are only achieved for $\gamma < 1$, i.e., for saturable kinetics or negative cooperativity. Under these circumstances, no positive amplification is observed.

4.3.1.5 ...of H_2O_2 reduction to water (v_5)

The model variant describing the effect of X_1 on the pathway of H_2O_2 detoxification to water (Fig. 4.8), contains a new parameter that is not present in the reference model (h_{21}). The log gain expressions are the following:

$$L_{15}^{(2)} = \frac{g_{24}}{h_{22}} - \frac{h_{14}(g_{21} - h_{21})}{h_{11}h_{22}} \tag{4.17}$$

$$L_{15}^{(3)} = \left(\frac{g_{24}}{h_{22}} - \frac{h_{14}(g_{21} - h_{21})}{h_{11}h_{22}}\right)\frac{g_{32}}{h_{33}} \tag{4.18}$$

Except for h_{21}, all other parameters remain unchanged from the reference model and the log gains can be simplified to:

$$L_{15}^{(2)} = L_{15}^{(3)} = g_{24} - h_{14} + h_{14}h_{21} \tag{4.19}$$

The impact of the new interaction on the sensitivity of X_2 and X_3 towards changes in X_4 is given by the strength and sign of the effector mechanism (γ). A negative interaction (inhibition) is given by γ in the range $[-4, 0[$ and a positive interaction (activation) in the range $]0, 4]$. Given that the S-system does not distinguish between this model variant from the one where X_1 is affecting the consumption of X_2 through the oxidative damage pathway, the contribution of each process to the overall consumption of X_2 must also be considered. The three possible scenarios or *cases* are where $v_5 \gg v_6$, $v_5 = v_6$ and $v_5 \ll v_6$, and represented by $h_{21} = \gamma$, $h_{21} = \gamma/2$ and $h_{21} = 0$, respectively. The latter *case* is of no interest, because when $v_5 \ll v_6$, the new interaction has no influence on the behaviour of the system and the log gains are the same as in the reference model. The remaining two scenarios are evaluated based on the values of h_{14} and g_{24} (Table 4.8) for each of the 9 *cases*

Table 4.8: Case by case analysis of the log gains $L_{15}^{(2)}$ and $L_{15}^{(3)}$.

			$L_{15}^{(2)} = L_{15}^{(3)}$		
			$v_5 \gg v_6$	$v_5 = v_6$	$v_5 \ll v_6$
cases	h_{14}	g_{24}	$(h_{21} = \gamma)$	$(h_{21} = \gamma/2)$	$(h_{21} = 0)$
1	1	1	γ	$\gamma/2$	0
2	$1/2$	1	$1/2 + \gamma/2$	$1/2 + \gamma/4$	$1/2$
3	0	1	1	1	1
4	$1/2$	$1/3$	$-1/6 + \gamma/3$	$-1/6 + \gamma/6$	$-1/6$
5	$1/3$	$1/3$	$\gamma/3$	$\gamma/6$	0
6	0	$1/3$	$1/3$	$1/3$	$1/3$
7	0	0	0	0	0
8	0	0	0	0	0
9	0	0	0	0	0

described previously. All eigenvalues for this particular model variant (not shown) present negative real parts independently of γ. In other words, the system has positive stable steady-states for any given value of γ. Positive amplification is found for *cases* 1, 2, 4 and 5 where $v_5 \gg v_6$, and for *cases* 1 and 2 where $v_5 = v_6$. Considering the log gains of the steady-state concentrations with respect to α_1 ($L_{15}(X_i, \alpha_1)$), we find that positive amplification of X_2 and X_3 in this model variant is likely to be observed under physiological conditions only in *cases* 1 and 2 where $1 < \gamma \leq 3$ ($v_5 \gg v_6$) and $2 < \gamma \leq 4$ ($v_5 = v_6$). One of the possible mechanisms that may account for the induction of the rate of H_2O_2 detoxification by $O_2^{\bullet -}$ was mentioned in the introduction of this chapter. Superoxide can activate the gene encoding Zwf (glucose-6-phosphate dehydrogenase). An increase in Zwf activity can augment NADPH availability which could lead to an increase in the NADPH-dependent activity of Ahp, the main H_2O_2 scavenger in *E. coli*. However, values of γ between 1 and 4 mean that for this mechanism to account for amplification of oxidative damage the flux of H_2O_2 detoxification has to display cooperative kinetics with respect to $O_2^{\bullet -}$.

4.3.1.6 ...of the oxidative damage production pathway (v_6)

When X_1 interacts with the processes leading to oxidative damage formation, v_6 (Fig. 4.9), the impact on the steady-state concentration of X_2 will be different from

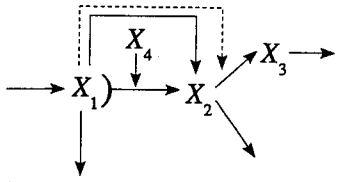

$$\begin{aligned}
\dot{X}_1 &= \alpha_1 - \beta_1 X_1^{h_{11}} X_4^{h_{14}} \\
\dot{X}_2 &= \alpha_2 X_1^{g_{21}} X_4^{g_{24}} - \beta_2 X_1^{h_{21}} X_2^{h_{22}} \\
\dot{X}_3 &= \alpha_3 X_1^{g_{31}} X_2^{g_{32}} - \beta_3 X_3^{h_{33}}
\end{aligned}$$

Figure 4.9: Graph depicting a positive or negative interaction of superoxide (X_1) on the oxidative damage production pathway (v_6), and its S-system representation. Two new parameters are introduced, h_{21} and g_{31}, while the remaining parameters are the same as in the reference model.

that on the steady-state concentration of X_3. Two new parameters are introduced in this model variant, h_{21} and g_{31}, related to the consumption of X_2 and the production of X_3, respectively. The log gains for this model are:

$$L_{16}^{(2)} = \frac{g_{24}}{h_{22}} - \frac{h_{14}(g_{21} - h_{21})}{h_{11}h_{22}} \tag{4.20}$$

$$L_{16}^{(3)} = \frac{g_{24}g_{32}}{h_{22}h_{33}} - \frac{h_{14}g_{32}(g_{21} - h_{21})}{h_{11}h_{22}h_{33}} - \frac{h_{14}g_{31}}{h_{11}h_{22}h_{33}} \tag{4.21}$$

Again, the parameter values are the same as the reference model, except for h_{21} and g_{31} that will take values in the range $[-4, 4]$, except for zero that indicates no interaction. The log gains are simplified to:

$$L_{16}^{(2)} = g_{24} - h_{14} + h_{14}h_{21} \tag{4.22}$$

$$L_{16}^{(3)} = g_{24} - h_{14} + h_{14}(h_{21} - g_{31}) \tag{4.23}$$

The kinetic order g_{31} always takes the value of γ corresponding to the strength and sign of the interaction, while h_{21} will take values depending on the contribution of v_6 to the overall consumption of X_2, as in the previous model variant. However, in this case h_{21} takes the values 0, $\gamma/2$ and γ where $v_5 \gg v_6$, $v_5 = v_6$, and $v_5 \ll v_6$, respectively. The log gains that result from each of these three situations in the 9 *cases* are shown in Table 4.9.

These expressions are similar to the log gains obtained in the previous model variant. In the first situation ($v_5 \gg v_6$) there is no amplification for X_2 ($L_{16}^{(2)}$ takes the same values as $L(X_2, X_4)$ in the reference model). As for X_3, positive amplification is seen for cases 1, 2, 3 and 4. Although according to the eigenvalues (not shown) the system presents positive stable steady-states for every γ in these *cases*, the criterion of plausibility that $|L_{16}(X_i, \alpha_1)| < 2$ is only fulfilled for *cases* 1 and 2 with γ in the range $[-3, -1[$. The inhibitory influence of superoxide on the flux of the Fenton reaction can be illustrated by the reported down-regulation of the mRNA binding activity of the iron regulatory protein (IRP-1) by superoxide that leads to increased sequestration and reduced cellular uptake of labile "free" iron [28]. Interestingly, in these conditions, the log gain of X_2 is between $0 - 0.5$ and

Table 4.9: Case by case analysis of the log gains L_{16}^{2} and L_{16}^{3}.

		$L_{16}^{(2)}$			$L_{16}^{(3)}$		
cases	$g_{24} - h_{14}$	$v_5 \gg v_6$ $(h_{21} = 0)$	$v_5 = v_6$ $(h_{21} = \gamma/2)$	$v_5 \ll v_6$ $(h_{21} = \gamma)$	$v_5 \gg v_6$ $(h_{21} - g_{31} = -\gamma)$	$v_5 = v_6$ $(h_{21} - g_{31} = -\gamma/2)$	$v_5 \ll v_6$ $(h_{21} - g_{31} = 0)$
1	0	0	$\gamma/2$	γ	$-\gamma$	$-\gamma/2$	0
2	$1/2$	$1/2$	$1/2 + \gamma/4$	$1/2 + \gamma/2$	$1/2 - \gamma/2$	$1/2 - \gamma/4$	$1/2$
3	1	1	1	1	1	1	1
4	$-1/6$	$-1/6$	$-1/6 + \gamma/6$	$-1/6 + \gamma/3$	$-1/6 - \gamma/3$	$-1/6 - \gamma/6$	$-1/6$
5	0	0	$\gamma/6$	$\gamma/3$	$-\gamma/3$	$-\gamma/6$	0
6	$1/3$	$1/3$	$1/3$	$1/3$	$1/3$	$1/3$	$1/3$
7	0	0	0	0	0	0	0
8	0	0	0	0	0	0	0
9	0	0	0	0	0	0	0

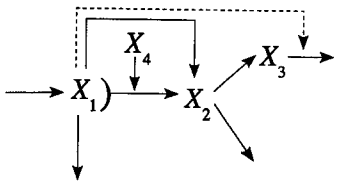

$$\begin{aligned}
\dot{X}_1 &= \alpha_1 - \beta_1 X_1^{h_{11}} X_4^{h_{14}} \\
\dot{X}_2 &= \alpha_2 X_1^{g_{21}} X_4^{g_{24}} - \beta_2 X_2^{h_{22}} \\
\dot{X}_3 &= \alpha_3 X_2^{g_{32}} - \beta_3 X_1^{h_{31}} X_3^{h_{33}}
\end{aligned}$$

Figure 4.10: Graph depicting a positive or negative interaction of superoxide (X_1) on the pathway of oxidative damage removal (v_7), and its S-system representation. A new parameter is introduced, h_{31}, while all other parameters remain equal to the reference model.

independent of γ, implying that there may be amplification of oxidative damage without significant increases in H_2O_2.

Where $v_5 = v_6$, both X_2 and X_3 do not present positive amplification under physiologically plausible conditions given by the ranges of γ where $|L_{16}(X_i, \alpha_1)| < 2$.

If $v_5 \ll v_6$, $L_{16}^{(3)}$ is equal to the reference model and there is no amplification for X_3. However, X_2 can be amplified in the same way as in the previous model variant where $v_5 \gg v_6$, i.e., in *cases* 1 and 2 with values of γ within the range $]1, 3]$.

4.3.1.7 ...of damage removal pathway (v_7)

To model the interaction of X_1 on the pathway of damage removal (Fig. 4.10) X_1 is introduced in the S-system equations in the consumption term of X_3. The new kinetic order accounting for the influence of X_1 on the consumption of X_3 (v_7) is h_{31}, and represents the strength and sign of the interaction. The log gains for this model variant are:

$$L_{17}^{(2)} = \frac{g_{24}}{h_{22}} - \frac{h_{14} g_{21}}{h_{11} h_{22}} \tag{4.24}$$

$$L_{17}^{(3)} = \frac{g_{24} g_{32}}{h_{22} h_{33}} - \frac{h_{14}(g_{32} g_{21} - h_{22} h_{31})}{h_{11} h_{22} h_{33}} \tag{4.25}$$

$L_{17}^{(2)}$ is equal to the reference model, meaning that there is no amplification for X_2. Taking into account the values of the kinetic orders of the processes that remain unaltered by the new interaction, $L_{17}^{(3)}$ can be simplified to:

$$L_{17}^{(3)} = g_{24} - h_{14} + h_{14} h_{31} \tag{4.26}$$

The latter expression is equivalent to expression 4.19, and positive amplification will be observed for the same *cases* and in the same conditions as observed in that model variant where $h_{21} = \gamma$ (see Table 4.8), i.e., in *cases* 1 and 2 with γ in the range $]1, 3]$. This interaction can be exemplified by the reported activation of DNA repair enzyme endonuclease IV by $O_2^{\bullet -}$ through the SoxRS regulon in *E. coli*

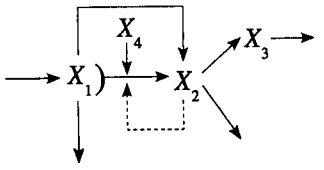

$$\begin{aligned}\dot{X}_1 &= \alpha_1 - \beta_1 X_1^{h_{11}} X_2^{h_{12}} X_4^{h_{14}} \\ \dot{X}_2 &= \alpha_2 X_1^{g_{21}} X_2^{g_{22}} X_4^{g_{24}} - \beta_2 X_2^{h_{22}} \\ \dot{X}_3 &= \alpha_3 X_2^{g_{32}} - \beta_3 X_3^{h_{33}}\end{aligned}$$

Figure 4.11: Graph depicting a positive or negative interaction of H_2O_2 (X_2) on the dismutation reaction (v_1), and its S-system representation. Two new parameters are introduced, h_{12} and g_{22}, while all other parameters remain the same as in the reference model.

[29, 30]. As in the previous model variants, amplification is only observed if the interaction of $O_2^{\bullet -}$ on the rate of oxidative damage repair (v_7) displays cooperative kinetics with respect to $O_2^{\bullet -}$.

4.3.2 Hydrogen peroxide (X_2) as an effector...

4.3.2.1 ...of the dismutation reaction (v_1)

This model variant introduces two new parameters at the level of X_1 consumption, h_{12}, and X_2 production, g_{22} (Fig. 4.11). The log gains for this model variant are:

$$L_{21}^{(2)} = \frac{g_{24}h_{11} - g_{21}h_{14}}{g_{21}h_{12} + h_{11}h_{22} - g_{22}h_{11}} \tag{4.27}$$

$$L_{21}^{(3)} = \frac{g_{24}h_{11} - g_{21}h_{14}}{g_{21}h_{12} + h_{11}h_{22} - g_{22}h_{11}} \cdot \frac{g_{32}}{h_{33}} \tag{4.28}$$

The log gains are simplified after attributing to the parameters the same values as in the extended model:

$$L_{21}^{(2)} = L_{21}^{(3)} = \frac{g_{24} - h_{14}}{1 + h_{12} - g_{22}} \tag{4.29}$$

A value of zero for both h_{12} and g_{22} yields the reference model, with no interaction. Yet, these two parameters are not identical as the processes that participate in the consumption of X_1 are not equivalent to those involved in the formation of X_2. Once again, invoking the parameter γ as the kinetic order of the affected processes (v_1) with respect to the effector (X_2), it is possible to determine the log gains for each of the *cases* defined in Table 4.2. From the nine possible *cases*, three of them (2, 3 and 6) show positive amplification only for activating interactions ($\gamma > 0$) in the stable positive steady-state region. Yet, this positive amplification is only seen close to a bifurcation point as strong positive cooperativity leads to non-positive steady-states. However, according to our condition of physiological plausibility ($|L_{21}(X_i, \alpha_1)| < 2$) *case* 3 can still present positive amplification when the interaction exhibits saturable kinetics ($0 < \gamma \leq 1/2$). Induction of both manganese and copper-zinc SODs by H_2O_2 has been observed [31], which may account for the inductive interaction of X_2 on v_1.

Table 4.10: Case by case analysis of the log gains $L_{21}^{(2)}$ and $L_{21}^{(3)}$.

cases	h_{14}	g_{24}	h_{12}	g_{22}	$L_{21}^{(2)} = L_{21}^{(3)}$
1	1	1	γ	γ	0
2	$1/2$	1	$\gamma/2$	γ	$\frac{1}{2-\gamma}$
3	0	1	0	γ	$\frac{1}{1-\gamma}$
4	$1/2$	$1/3$	$\gamma/2$	$\gamma/3$	$-\frac{1}{6+\gamma}$
5	$1/3$	$1/3$	$\gamma/3$	$\gamma/3$	0
6	0	$1/3$	0	$\gamma/3$	$\frac{1}{3-\gamma}$
7	0	0	0	0	0
8	0	0	0	0	0
9	0	0	0	0	0

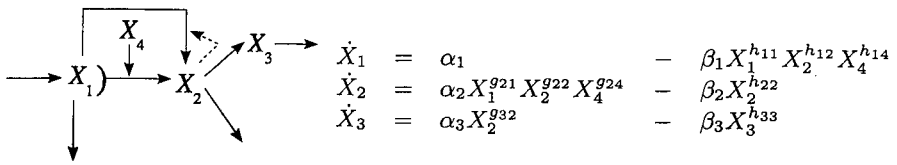

Figure 4.12: Graph depicting a positive or negative interaction of H_2O_2 (X_2) on the superoxide reduction pathway (v_2), and its S-system representation. Two new parameters are introduced, h_{12} and g_{22}, while all other parameters remain the same as in the reference model.

4.3.2.2 ...of the superoxide reduction pathway (v_2)

This model variant is described by the same S-system as the previous model variant (Fig. 4.12). The difference lies on the values that h_{12} and g_{22} take, because the interaction is now on the superoxide (X_1) reduction pathway (v_2), instead of the dismutation reaction (v_1). The log gains are therefore the same as the previous model variant:

$$L_{22}^{(2)} = L_{22}^{(3)} = \frac{g_{24} - h_{14}}{1 + h_{12} - g_{22}} \tag{4.30}$$

Positive amplification is observed only in *case* 6 for $1 < \gamma < 3/2$, under stable steady-state conditions(see Table 4.11). However, where $L_{22}(X_i, \alpha_1) < 2$, no amplification is observed.

Table 4.11: Case by case analysis of the log gains $L_{22}^{(2)}$ and $L_{22}^{(3)}$.

cases	h_{14}	g_{24}	h_{12}	g_{22}	$L_{22}^{(2)} = L_{22}^{(3)}$
1	1	1	0	0	0
2	$1/2$	1	0	0	$1/2$
3	0	1	0	0	1
4	$1/2$	$1/3$	$\gamma/2$	$2\gamma/3$	$-\frac{1}{6-\gamma}$
5	$1/3$	$1/3$	$\gamma/3$	$2\gamma/3$	0
6	0	$1/3$	0	$2\gamma/3$	$\frac{1}{3-2\gamma}$
7	0	0	γ	γ	0
8	0	0	γ	γ	0
9	0	0	γ, $\gamma/2$, or 0[a]	γ	0

[a] For $v_2 \gg v_3$, $v_2 = v_3$, $v_2 \ll v_3$, respectively.

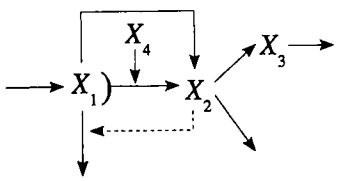

$$\begin{aligned}
\dot{X}_1 &= \alpha_1 - \beta_1 X_1^{h_{11}} X_2^{h_{12}} X_4^{h_{14}} \\
\dot{X}_2 &= \alpha_2 X_1^{g_{21}} X_4^{g_{24}} - \beta_2 X_2^{h_{22}} \\
\dot{X}_3 &= \alpha_3 X_2^{g_{32}} - \beta_3 X_3^{h_{33}}
\end{aligned}$$

Figure 4.13: Graph depicting a positive or negative interaction of H_2O_2 (X_2) on the superoxide consumption through the non H_2O_2-producing processes (v_3), and its S-system representation. A new parameter is introduced, h_{12}, while all other parameters remain the same as in the reference model.

4.3.2.3 ...of superoxide consumption through the non H_2O_2-producing processes (v_3)

The interaction of X_2 on v_3 does not affect the production of X_2 directly, and thus only one parameter, h_{21}, is introduced in this model variant (Fig. 4.13). The simplified log gains are:

$$L_{23}^{(2)} = L_{23}^{(3)} = \frac{g_{24} - h_{14}}{1 + h_{12}} \tag{4.31}$$

The existence of a negative feedback of X_2 on v_3 may lead to positive amplification both of X_2 and X_3 in *cases* 2, 3 and 6 under stable steady-state conditions. However, amplification is only seen close to a bifurcation point as too strong negative cooperative kinetics leads to the loss of positive stable steady-states. After applying our plausibility criterion ($|L_{23}(X_i, \alpha_1)| < 2$) only *case* 3 presents positive amplification when the interaction displays inhibiting saturable kinetics ($-1/2 \leq \gamma < 0$).

Table 4.12: Case by case analysis of the log gains $L_{23}^{(2)}$ and $L_{23}^{(3)}$.

cases	h_{14}	g_{24}	h_{12}	$L_{23}^{(2)} = L_{23}^{(3)}$
1	1	1	0	0
2	$1/2$	1	$\gamma/2$	$\frac{1}{2+\gamma}$
3	0	1	γ	$\frac{1}{1+\gamma}$
4	$1/2$	$1/3$	0	$-1/6$
5	$1/3$	$1/3$	$\gamma/3$	0
6	0	$1/3$	γ	$\frac{1}{3+3\gamma}$
7	0	0	0	0
8	0	0	0	0
9	0	0	0, $\gamma/2$, or γ[a]	0

[a] For $v_2 \gg v_3$, $v_2 = v_3$, $v_2 \ll v_3$, respectively.

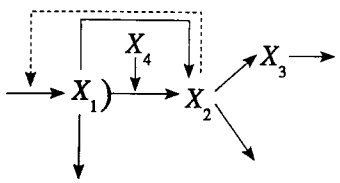

$$\begin{aligned}
\dot{X}_1 &= \alpha_1 X_2^{g12} - \beta_1 X_1^{h11} X_4^{h14} \\
\dot{X}_2 &= \alpha_2 X_1^{g21} X_4^{g24} - \beta_2 X_2^{h22} \\
\dot{X}_3 &= \alpha_3 X_2^{g32} - \beta_3 X_3^{h33}
\end{aligned}$$

Figure 4.14: Graph depicting a positive or negative interaction of H_2O_2 (X_2) on the superoxide formation pathway (v_4), and its S-system representation. A new parameter is introduced, g_{12}, while all other parameters remain the same as in the reference model.

4.3.2.4 ...of superoxide formation (v_4)

The feedback mechanism of X_2 on the pathway of superoxide production (v_4) is characterized by the extra parameter g_{12} (Fig. 4.14). The calculated log gains for this model variant are:

$$L_{24}^{(2)} = \frac{g_{24}h_{11} - g_{21}h_{14}}{h_{11}h_{22} - g_{21}g_{12}} \tag{4.32}$$

$$L_{24}^{(3)} = \frac{g_{24}h_{11} - g_{21}h_{14}}{h_{11}h_{22} - g_{21}g_{12}} \cdot \frac{g_{32}}{h_{33}} \tag{4.33}$$

Maintaining the same values for all kinetic orders as those in the reference model, expressions 4.32 and 4.33 are simplified to:

$$L_{24}^{(2)} = L_{24}^{(3)} = \frac{g_{24} - h_{14}}{1 - g_{12}} \tag{4.34}$$

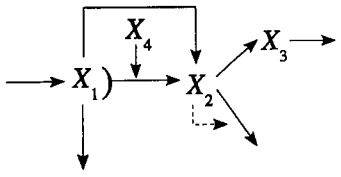

$$\begin{aligned}
\dot{X}_1 &= \alpha_1 - \beta_1 X_1^{h_{11}} X_4^{h_{14}} \\
\dot{X}_2 &= \alpha_2 X_1^{g_{21}} X_4^{g_{24}} - \beta_2 X_2^{h_{22}} \\
\dot{X}_3 &= \alpha_3 X_2^{g_{32}} - \beta_3 X_3^{h_{33}}
\end{aligned}$$

Figure 4.15: Graph depicting a positive or negative interaction of H_2O_2 (X_2) on the detoxification pathway through reduction of H_2O_2 to water (v_5), and its S-system representation. The topology of the S-system representation is identical to the reference model. However, h_{22} takes different values.

The log gain for this model variant is the log gain of the reference model divided by $1 - g_{12}$. The eigenvalues for this system (not shown) indicate that positive stable steady-states are found where $g_{12} < 1$. Positive amplification can be observed in *cases* where the log gain in the reference model is not already zero. However, where $|L_{24}(X_i, \alpha_1)| < 2$, only *case* 3 shows positive amplification with the interaction displaying saturable kinetics ($0 < \gamma \leq 1/2$).

4.3.2.5 ...of its detoxification through reduction to water (v_5)

When one considers the kinetics of the detoxification pathway (v_5) with respect to X_2 to be non-linear (saturating or cooperative), the new model variant is still described by the same S-system as that of the reference model (Fig. 4.15). The log gains $L_{25}^{(2)}$ and $L_{25}^{(3)}$ are therefore formally similar to those calculated for the reference model (see expressions 4.2 and 4.3). However, due the new interaction on v_5, the exponent h_{22} is no longer 1. Positive cooperativity is given by $h_{22} > 1$, and saturating or negative cooperativity kinetics by $h_{22} < 1$. The simplified log gains can be represented by the following expressions:

$$L_{25}^{(2)} = L_{25}^{(3)} = \frac{g_{24} - h_{14}}{h_{22}} \tag{4.35}$$

Besides the 9 different *cases* that relate to the different contributions to the flux of X_1 consumption, the distinct contributions of v_5 and v_6 to the overall consumption of X_2 must also be considered (Table 4.13). In the case where most of the flux of X_2 consumption is through v_6 ($v_5 \ll v_6$) the system is identical to the reference model in the same conditions, i.e., $h_{22} = 1$. Therefore, in these conditions the log gains are the same as in the reference model, in which there is no amplification. As for the other two scenarios ($v_5 \gg v_6$ and $v_5 = v_6$), based on the eigenvalues, when the extra interaction displays positive cooperativity ($\gamma > 1$) the model variant presents positive stable steady-states though without amplification. Conversely, positive amplification is seen when the extra interaction exhibits negative cooperativity or v_5 is reaching saturation with X_2. Stronger inhibiting cooperativity leads to the

Table 4.13: Case by case analysis of the log gains $L_{25}^{(2)}$ and $L_{25}^{(3)}$.

			$L_{25}^{(2)} = L_{25}^{(3)}$		
			$v_5 \gg v_6$	$v_5 = v_6$	$v_5 \ll v_6$
cases	h_{14}	g_{24}	$(h_{22} = \gamma)$	$(h_{22} = (1+\gamma)/2)$	$(h_{22} = 1)$
1	1	1	0	0	0
2	$1/2$	1	$1/2\gamma$	$\frac{1}{\gamma+1}$	$1/2$
3	0	1	$1/\gamma$	$\frac{2}{\gamma+1}$	1
4	$1/2$	$1/3$	$-1/6\gamma$	$-\frac{1}{3} \cdot \frac{1}{\gamma+1}$	$-1/6$
5	$1/3$	$1/3$	0	0	0
6	0	$1/3$	$1/3\gamma$	$\frac{2}{3} \cdot \frac{1}{\gamma+1}$	$1/3$
7	0	0	0	0	0
8	0	0	0	0	0
9	0	0	0	0	0

disappearance of positive stable steady-states, indicating that this amplification may only be observed close to a bifurcation point. Still, where $|L_{25}(X_i, \alpha_1)| < 2$, there is positive amplification for *case* 3. This can be observed for $1/2 \leq \gamma < 1$ where $v_5 \gg v_6$, and for $-1 \leq \gamma < -1/2$ where $v_5 = v_6$. Since γ is already 1 without the extra interaction the values of γ in these ranges can arise if the extra interaction displays either activating or inhibiting saturable kinetics. H_2O_2 has been observed to induce the expression of genes encoding enzymes capable of reducing it to water. These include, for instance, Ahp and hydroperoxidase I (product of the *katG* gene) in *E. coli* [32], and catalase, cytochrome c peroxidase and thioredoxin peroxidase in the yeast *Saccharomyces cerevisiae* [31].

4.3.2.6 ...of the oxidative damage formation pathway (v_6)

This model variant is also described by the same S-system as the reference model and one expects the log gain expressions to be equivalent to expressions 4.2 and 4.3 (Fig. 4.16). However, in contrast to the previous model variant, the flux of X_3 production is also being influenced by this new interaction. Therefore, both h_{22} and g_{32} are different from the reference model. Replacing the values of the kinetic orders that remain the same as in the reference model, the following simplified log

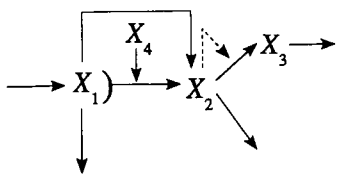

$$\begin{aligned}\dot{X}_1 &= \alpha_1 - \beta_1 X_1^{h_{11}} X_4^{h_{14}} \\ \dot{X}_2 &= \alpha_2 X_1^{g_{21}} X_4^{g_{24}} - \beta_2 X_2^{h_{22}} \\ \dot{X}_3 &= \alpha_3 X_2^{g_{32}} - \beta_3 X_3^{h_{33}}\end{aligned}$$

Figure 4.16: Graph depicting a positive or negative interaction of H_2O_2 (X_2) on the flux of oxidative damage formation by H_2O_2 (v_6), and its S-system representation. Though the S-system representation is identical to the reference model, h_{22} and g_{32} take different values.

gain expressions are obtained:

$$L_{26}^{(2)} = \frac{g_{24} - h_{14}}{h_{22}} \tag{4.36}$$

$$L_{26}^{(3)} = \frac{g_{24} - h_{14}}{h_{22}} \cdot g_{32} \tag{4.37}$$

The influence of the new interaction on X_2 is accounted for in h_{22}. However, X_3 is influenced both by the consumption of X_2 and its own production and thus changes in X_3 are dependent on both h_{22} and g_{32}. Expression 4.36 is equivalent to the log gain expressions obtained for the previous model. However, in this case, h_{22} takes different values than in the previous model variant when the same contributions to the overall rate of X_2 depletion are considered. For simplicity, each of these situations ($v_5 \gg v_6$, $v_5 = v_6$, and $v_5 \ll v_6$) will again be presented separately.

$v_5 \gg v_6$ ($h_{22} = 1$, $g_{32} = \gamma$): Most of the flux of X_2 depletion is through the detoxifying pathway, and the interaction is negligible, approximating it to the reference model in the same conditions. Yet, there are differences between this model variant and the reference model regarding the log gain of X_3 with respect to X_4 (Table 4.14). The eigenvalues in this particular situation are always negative and independent of γ, and thus there is always a positive stable steady-state. To be consistent, the plausibility criterion ($|L_{26}(X_i, \alpha_1)| < 2$) was applied and positive amplification of oxidative stress is observed in *case* 3 where $1 < \gamma \leq 2$, i.e., where the Fenton reaction displays activating cooperative kinetics with respect to H_2O_2. Though H_2O_2 has also been reported to inhibit IRP-1 [28], others have shown that treatment of cell cultures with H_2O_2 actually stimulate the RNA-binding activity of IRP [33, 34] consequently increasing the levels of intracellular "free" iron. Whether this pathway occurs *in vivo* still remains to be established, though if true it could account for the effect of H_2O_2 enhancing the rate of the Fenton reaction with non-linear kinetics.

$v_5 = v_6$ ($h_{22} = \frac{1+\gamma}{2}$, $g_{32} = \gamma$): The flux is equally distributed through both processes of X_2 depletion and therefore X_3 production will now be influenced differently by changes in X_4 than in the reference model. The eigenvalues determined for this model variant indicate that positive stable steady-states are found for values of

Table 4.14: Case by case analysis of the log gains $L_{26}^{(2)}$ and $L_{26}^{(3)}$.

		$L_{26}^{(2)}$			$L_{26}^{(3)}$		
cases	$g_{24} - h_{14}$	$v_5 \gg v_6$ $(h_{22} = 1)$	$v_5 = v_6$ $(h_{22} = \frac{1+\gamma}{2})$	$v_5 \ll v_6$ $(h_{22} = \gamma)$	$v_5 \gg v_6$ $(g_{32}/h_{22} = \gamma)$	$v_5 = v_6$ $(g_{32}/h_{22} = \frac{2\gamma}{1+\gamma})$	$v_5 \ll v_6$ $(g_{32}/h_{22} = 1)$
1	0	0	0	0	0	0	0
2	$1/2$	$1/2$	$\frac{1}{1+\gamma}$	$1/2\gamma$	$\gamma/2$	$\frac{\gamma}{1+\gamma}$	$1/2$
3	1	1	$\frac{2}{1+\gamma}$	$1/\gamma$	γ	$\frac{2\gamma}{1+\gamma}$	1
4	$-1/6$	$-1/6$	$-\frac{1}{3} \cdot \frac{1}{1+\gamma}$	$-1/6\gamma$	$-\gamma/6$	$-\frac{1}{3} \cdot \frac{\gamma}{1+\gamma}$	$-1/6$
5	0	0	0	0	0	0	0
6	$1/3$	$1/3$	$\frac{2}{3} \cdot \frac{1}{1+\gamma}$	$1/3\gamma$	$\gamma/3$	$\frac{2}{3} \cdot \frac{\gamma}{1+\gamma}$	$1/3$
7	0	0	0	0	0	0	0
8	0	0	0	0	0	0	0
9	0	0	0	0	0	0	0

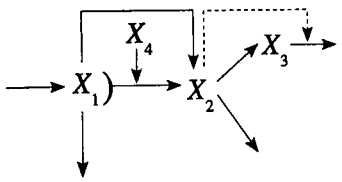

$$\begin{aligned}
\dot{X}_1 &= \alpha_1 - \beta_1 X_1^{h_{11}} X_4^{h_{14}} \\
\dot{X}_2 &= \alpha_2 X_1^{g_{21}} X_4^{g_{24}} - \beta_2 X_2^{h_{22}} \\
\dot{X}_3 &= \alpha_3 X_2^{g_{32}} - \beta_3 X_2^{h_{32}} X_3^{h_{33}}
\end{aligned}$$

Figure 4.17: Graph depicting a positive or negative interaction of H_2O_2 (X_2) on the flux of oxidative damage repair (v_7), and its S-system representation. A new parameter is introduced, h_{32}, while all remaining parameters are the same as in the reference model.

$h_{22} > 0$. As the average kinetic order of the overall consumption rate of X_2 with respect to X_2 is $h_{22} = \frac{1+\gamma}{2}$, the positive stable steady-states will be observed for $\gamma > -1$. Positive amplification of both X_2 and X_3 are indeed found in this region (though close to $\gamma = -1$ in the case of X_2). Considering $|L_{26}(X_i, \alpha_1)| < 2$, positive amplification is found for X_2 and X_3 only in *case* 3, for $0 \leq \gamma < 1$ and $1 < \gamma \leq 4$, respectively.

$v_5 \ll v_6$ ($h_{22} = \gamma$ and $g_{32} = \gamma$): In this case, the flux of X_2 consumption is mostly through the oxidative damage formation pathway. The average kinetic order of X_2 consumption with respect to X_2 is now determined mainly by the reaction on which the interaction is taking effect corresponding to $h_{22} = \gamma$. As the real parts of the eigenvalues are all negative for $h_{22} > 0$, the system will present positive stable steady-states for $\gamma > 0$. Interestingly, although there may be amplification of X_2 in this region, changes in X_3 are equivalent to that observed in the reference model. At steady-state, the flux of X_2 consumption, which is equivalent in the present case to X_3 production, must be equal to the overall flux of X_2 production. Thus, changes in X_3 production elicited by variations in X_4 must match the changes observed in the rate of X_2 production. The latter corresponds to unaltered processes with respect to the reference model and therefore the changes are the same as in the reference model. As for X_2, positive amplification is observed for *cases* 2, 3 and 6, though where $|L_{26}(X_i, \alpha_1)| < 2$, only *case* 3 presents positive amplification of X_2 for $1/2 \leq \gamma < 1$.

4.3.2.7 ...damage removal pathway (v_7)

In this model variant, X_2 interacts on the pathway of oxidative damage removal or repair (Fig. 4.17), characterized by the new exponent h_{32}. The log gains measuring changes in X_2 and X_3 with respect to variations in X_4 are determined:

$$L_{27}^{(2)} = \frac{g_{24}}{h_{22}} - \frac{g_{21} h_{14}}{h_{11} h_{22}} \tag{4.38}$$

$$L_{27}^{(3)} = \left(\frac{g_{24}}{h_{22} h_{33}} - \frac{h_{14} g_{21}}{h_{11} h_{22} h_{33}}\right) \cdot (g2.3_{32} - h_{32}) \tag{4.39}$$

Table 4.15: Case by case analysis of the log gain $L_{27}^{(3)}$.

cases	h_{14}	g_{24}	$L_{27}^{(3)}$ $(h_{32} = \gamma)$
1	1	1	0
2	$1/2$	1	$\frac{1}{2} \cdot (1 - \gamma)$
3	0	1	$(1 - \gamma)$
4	$1/2$	$1/3$	$-\frac{1}{6} \cdot (1 - \gamma)$
5	$1/3$	$1/3$	0
6	0	$1/3$	$\frac{1}{3} \cdot (1 - \gamma)$
7	0	0	0
8	0	0	0
9	0	0	0

The steady-state concentration of X_2 does not depend on the downstream concentrations, i.e., on X_3. As X_2 is only affecting the depletion of X_3 the log gain $L_{27}^{(2)}$is unaffected and is equivalent to the log gain obtained in the reference model. In contrast, $L_{27}^{(3)}$ is dependent on the new parameter h_{32}. Replacing the values known for the parameters in the reference model the following simplified expression for $L_{27}^{(3)}$ is obtained:

$$L_{27}^{(3)} = (g_{24} - h_{14}) \cdot (1 - h_{32}) \tag{4.40}$$

All eigenvalues determined for this particular model variant (not shown) have negative real parts and are independent of h_{32}. Positive amplification is observed for inhibitory kinetics, and where $|L_{27}(X_i, \alpha_1)| < 2$ amplification is only found in *case* 3 for $-1 \leq \gamma < 0$. Considering the weak inhibitory interaction, it may be possible that direct oxidation of enzymes responsible for oxidative damage repair by H_2O_2 may occur *in vivo*. At least *in vitro*, oxidative stress repair enzymes such as glutathione peroxidase [35] and possibly phospholipid hydroperoxide glutathione peroxidase, seem to be degraded preferentially by proteases after exposure to H_2O_2 and independently of hydroxyl radicals.

4.3.3 Amount of damage (X_3) as an effector...

4.3.3.1 ...of the dismutation reaction (v_1)

This model variant (Fig. 4.18) is equivalent to the model where X_2 acts as an effector of v_1. The log gains obtained are equivalent (Table 4.3) and amplification

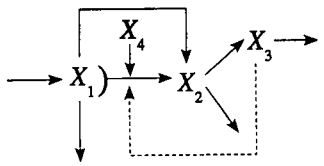

$$\dot{X}_1 = \alpha_1 - \beta_1 X_1^{h_{11}} X_3^{h_{13}} X_4^{h_{14}}$$
$$\dot{X}_2 = \alpha_2 X_1^{g_{21}} X_3^{g_{23}} X_4^{g_{24}} - \beta_2 X_2^{h_{22}}$$
$$\dot{X}_3 = \alpha_3 X_2^{g_{32}} - \beta_3 X_3^{h_{33}}$$

Figure 4.18: Graph depicting a positive or negative interaction of the amount of damage (X_3) on the flux of dismutation (v_1), and its S-system representation. Two new parameters are introduced, h_{13} and g_{23}, while all remaining parameters are identical to the extended minimal model.

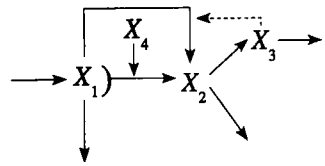

$$\dot{X}_1 = \alpha_1 - \beta_1 X_1^{h_{11}} X_3^{h_{13}} X_4^{h_{14}}$$
$$\dot{X}_2 = \alpha_2 X_1^{g_{21}} X_3^{g_{23}} X_4^{g_{24}} - \beta_2 X_2^{h_{22}}$$
$$\dot{X}_3 = \alpha_3 X_2^{g_{32}} - \beta_3 X_3^{h_{33}}$$

Figure 4.19: Graph depicting a positive or negative interaction of the amount of damage (X_3) on the flux of superoxide reduction pathway (v_2), and its S-system representation. Two new parameters are introduced, h_{13} and g_{23}, while all other parameters remain identical to the extended minimal model.

is observed for the same conditions (see section 4.3.2.1, for details).

4.3.3.2 ...of the superoxide reduction reaction (v_2)

This model variant (Fig. 4.19) is equivalent to the model where X_2 acts as an effector of v_2. The log gains obtained are equivalent (Table 4.3) and amplification is observed for the same conditions (see section 4.3.2.2, for details).

4.3.3.3 ...of superoxide consumption through the non H_2O_2-producing reactions (v_3)

This model variant (Fig. 4.20) is equivalent to the model where X_2 acts as an effector of v_3. The log gains obtained are equivalent (Table 4.3) and amplification

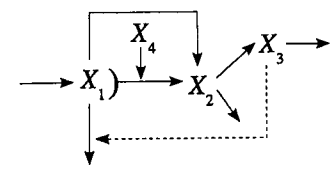

$$\dot{X}_1 = \alpha_1 - \beta_1 X_1^{h_{11}} X_3^{h_{13}} X_4^{h_{14}}$$
$$\dot{X}_2 = \alpha_2 X_1^{g_{21}} X_3^{g_{23}} X_4^{g_{24}} - \beta_2 X_2^{h_{22}}$$
$$\dot{X}_3 = \alpha_3 X_2^{g_{32}} - \beta_3 X_3^{h_{33}}$$

Figure 4.20: Graph depicting a positive or negative interaction of the amount of damage (X_3) on the pathway of superoxide consumption that does not produce H_2O_2 (v_3), and its S-system representation. Two new parameters are introduced, h_{13} and g_{23}, while all other parameters remain identical to the extended minimal model.

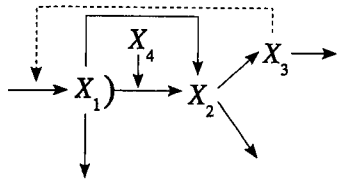

$$\begin{aligned}\dot{X}_1 &= \alpha_1 X_3^{g13} - \beta_1 X_1^{h11} X_4^{h14}\\ \dot{X}_2 &= \alpha_2 X_1^{g21} X_4^{g24} - \beta_2 X_2^{h22}\\ \dot{X}_3 &= \alpha_3 X_2^{g32} - \beta_3 X_3^{h33}\end{aligned}$$

Figure 4.21: Graph depicting a positive or negative interaction of the amount of damage (X_3) on the pathway of superoxide formation (v_4), and its S-system representation. A new parameter is introduced, g_{13}, while all other parameters remain the same as in the extended minimal model.

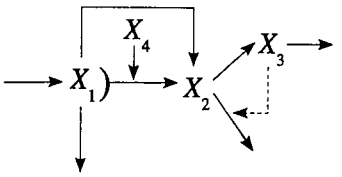

$$\begin{aligned}\dot{X}_1 &= \alpha_1 - \beta_1 X_1^{h11} X_4^{h14}\\ \dot{X}_2 &= \alpha_2 X_1^{g21} X_4^{g24} - \beta_2 X_2^{h22} X_3^{h23}\\ \dot{X}_3 &= \alpha_3 X_2^{g32} - \beta_3 X_3^{h33}\end{aligned}$$

Figure 4.22: Graph depicting a positive or negative interaction of the amount of damage (X_3) on the pathway of H_2O_2 detoxification (v_5), and its S-system representation. A new parameter is introduced, h_{23}, while all other parameters remain unchanged from the reference model.

is observed for the same conditions (see section 4.3.2.3, for details).

4.3.3.4 ...of the superoxide generating reaction (v_4)

This model variant (Fig. 4.21) is equivalent to the model where X_2 acts as an effector of v_4. The log gains obtained are equivalent (Table 4.3) and amplification is observed for the same conditions (see section 4.3.2.4, for details).

4.3.3.5 ...of H_2O_2 consumption through reduction to water (v_5)

The interaction of X_3 on the flux of H_2O_2 detoxification has to be analyzed considering the balance between both fluxes of H_2O_2 depletion. A new parameter is introduced, h_{23}, which is the kinetic order of the overall consumption of X_2 with respect to X_3 (Fig 4.22). The general expressions for the log gains are:

$$L_{35}^{(2)} = (g_{24} - \frac{h_{14}g_{21}}{h_{11}}) \cdot \frac{h_{33}}{g_{32}h_{23} + h_{22}h_{33}} \tag{4.41}$$

$$L_{35}^{(3)} = (g_{24} - \frac{h_{14}g_{21}}{h_{11}}) \cdot \frac{g_{32}}{g_{32}h_{23} + h_{22}h_{33}} \tag{4.42}$$

All parameters, except for h_{23} take the same values as in the reference model,

Table 4.16: Case by case analysis of the log gains $L_{35}^{(2)}$ and $L_{35}^{(3)}$.

cases	h_{14}	g_{24}	$L_{35}^{(2)} = L_{35}^{(3)}$	
			$h_{23} = \gamma$	$h_{23} = \gamma/2$
1	1	1	0	0
2	$1/2$	1	$\frac{1}{2} \cdot \frac{1}{1+\gamma}$	$\frac{1}{2+\gamma}$
3	0	1	$\frac{1}{1+\gamma}$	$\frac{2}{2+\gamma}$
4	$1/2$	$1/3$	$-\frac{1}{6} \cdot \frac{1}{1+\gamma}$	$-\frac{1}{3} \cdot \frac{1}{2+\gamma}$
5	$1/3$	$1/3$	0	0
6	0	$1/3$	$\frac{1}{3} \cdot \frac{1}{1+\gamma}$	$\frac{2}{3} \cdot \frac{1}{2+\gamma}$
7	0	0	0	0
8	0	0	0	0
9	0	0	0	0

thereby simplifying the expressions:

$$L_{35}^{(2)} = L_{35}^{(3)} = \frac{g_{24} - h_{14}}{1 + h_{23}} \tag{4.43}$$

The kinetic order of v_5 with respect to the effector X_3 is γ. Positive interactions are given by $\gamma > 0$ and negative interactions by $\gamma < 0$. The relationship between γ and h_{23} depends on the relative contributions of the fluxes of H_2O_2 consumption. When most of the flux is through the X_2 detoxification pathway ($v_5 \gg v_6$), the kinetic order of the overall consumption of X_2 with respect to X_3 is the actual kinetic order of the interaction and thus $h_{23} = \gamma$. If, however, both fluxes of X_2 depletion contribute equally to the overall rate of consumption ($v_5 = v_6$), the kinetic order is only half of the one observed in the previous case, $h_{23} = \gamma/2$. Finally, if the flux through v_5 is negligible ($v_5 \ll v_6$), then the new interaction has little effect on the overall consumption of X_2 and the system behaves identically to the reference model under the same conditions ($h_{23} = 0$) (Table 4.16). This latter case shows lack of amplification and is not discussed further. Taking into consideration the eigenvalues for this model variant, stable positive steady-states are only found where $h_{23} > -1$. Within this range, positive amplification where $|L_{35}(X_i, \alpha_1)| < 2$ is only predicted in *case* 3 for $-1/2 \leq \gamma < 0$ ($v_5 \gg v_6$) and $-1 \leq \gamma < 0$ ($v_5 = v_6$). It seems conceivable that products of oxidative damage may inhibit H_2O_2 detoxification. For instance, direct DNA oxidation by hydroxyl radicals can reduce the efficiency of transcription or translation of genes and/or enzymes involved in H_2O_2 detoxification. Given

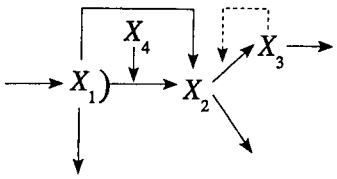

$$\begin{aligned}
\dot{X}_1 &= \alpha_1 - \beta_1 X_1^{h_{11}} X_4^{h_{14}} \\
\dot{X}_2 &= \alpha_2 X_1^{g_{21}} X_4^{g_{24}} - \beta_2 X_2^{h_{22}} X_3^{h_{23}} \\
\dot{X}_3 &= \alpha_3 X_2^{g_{32}} X_3^{g_{33}} - \beta_3 X_3^{h_{33}}
\end{aligned}$$

Figure 4.23: Graph depicting a positive or negative interaction of the amount of damage (X_3) on the pathway of damage formation through H_2O_2 (v_6), and its S-system representation. Two parameters are introduced, h_{23} and g_{33}, while the remaining parameters are unchanged from the reference model.

that a modest inhibition suffices to cause amplification, these situations suggest plausible causes for amplification under physiological conditions.

4.3.3.6 ...of oxidative damage formation pathway (v_6)

This model variant is represented by the interaction of X_3 on the flux of H_2O_2 consumption through the Fenton reaction (v_6) (Fig. 4.23). In contrast to the previous model, the amount of damage influences both H_2O_2 consumption and its own formation. This is represented in the S-system by introducing X_3 raised to its kinetic order in the consumption term of X_2 and the production term of X_3. Two new parameters are thus introduced, h_{23} and g_{33}. The general expressions for the log gains are:

$$L_{36}^{(2)} = (g_{24} - \frac{h_{14}g_{21}}{h_{11}}) \cdot \frac{h_{33} - g_{33}}{g_{32}h_{23} + h_{22}(h_{33} - g_{33})} \tag{4.44}$$

$$L_{36}^{(3)} = (g_{24} - \frac{h_{14}g_{21}}{h_{11}}) \cdot \frac{g_{32}}{g_{32}h_{23} + h_{22}(h_{33} - g_{33})} \tag{4.45}$$

Taking into account the values of the parameters that remain unchanged from the reference model, the log gains are simplified to:

$$L_{36}^{(2)} = \frac{g_{24} - h_{14}}{1 + h_{23} - g_{33}} \cdot (1 - g_{33}) \tag{4.46}$$

$$L_{36}^{(3)} = \frac{g_{24} - h_{14}}{1 + h_{23} - g_{33}} \tag{4.47}$$

As there is an alternative pathway of X_2 depletion, h_{23} will take different values depending on the balance between both fluxes contributing to X_2 consumption. Considering γ as the strength of the interaction, h_{23} takes the values 0, $\gamma/2$ and γ where $v_5 \gg v_6$, $v_5 = v_6$ and $v_5 \ll v_6$, respectively, while g_{33} always takes the value of γ. Again, for simplicity these cases are considered separately:

$v_5 \gg v_6$ ($h_{23} = 0$, $g_{33} = \gamma$): Most of the flux of X_2 depletion is through the detoxifying pathway, and the interaction is negligible regarding X_2 consumption and thus

Table 4.17: Case by case analysis of the log gains $L_{36}^{(2)}$ and $L_{36}^{(3)}$.

		$L_{36}^{(2)}$			$L_{36}^{(3)}$		
cases	$g_{24} - h_{14}$	$v_5 \gg v_6$ $(h_{23} = 0)$	$v_5 = v_6$ $(h_{23} = \gamma/2)$	$v_5 \ll v_6$ $(h_{23} = \gamma)$	$v_5 \gg v_6$ $(h_{23} = 0)$	$v_5 = v_6$ $(h_{23} = \gamma/2)$	$v_5 \ll v_6$ $(h_{23} = \gamma)$
1	0	0	0	0	0	0	0
2	$1/2$	$1/2$	$\frac{1-\gamma}{2-\gamma}$	$\frac{1-\gamma}{2}$	$\frac{1}{2} \cdot \frac{1}{1-\gamma}$	$\frac{1}{2-\gamma}$	$1/2$
3	1	1	$\frac{2-2\gamma}{2-\gamma}$	$1-\gamma$	$\frac{1}{1-\gamma}$	$\frac{2}{2-\gamma}$	1
4	$-1/6$	$-1/6$	$-\frac{1}{3} \cdot \frac{1-\gamma}{2-\gamma}$	$\frac{\gamma-1}{6}$	$-\frac{1}{6} \cdot \frac{1}{1-\gamma}$	$-\frac{1}{3} \cdot \frac{1}{2-\gamma}$	$-1/6$
5	0	0	0	0	0	0	0
6	$1/3$	$1/3$	$\frac{2}{3} \cdot \frac{1-\gamma}{2-\gamma}$	$\frac{1-\gamma}{3}$	$\frac{1}{3} \cdot \frac{1}{1-\gamma}$	$\frac{2}{3} \cdot \frac{1}{2-\gamma}$	$1/3$
7	0	0	0	0	0	0	0
8	0	0	0	0	0	0	0
9	0	0	0	0	0	0	0

$L_{36}^{(2)}$ is equivalent to $L(X_2, X_4)$ in the reference model. Yet, there are differences between this model variant and the reference model regarding the log gain of X_3 with respect to X_4 (Table 4.17). The eigenvalues in this particular situation always show negative real parts as long as $g_{33} - h_{23} < 1$, which corresponds to where $\gamma < 1$. Amplification is observed for weak positive feedback displaying saturable kinetics (close to $\gamma = 1$). Where $|L_{36}(X_i, \alpha_1)| < 2$, only *case* 3 presents positive amplification of X_3 for $0 < \gamma \leq 1/2$. Here also seems plausible that oxidative damage may have a slight positive feedback on its own formation, which in turn, can cause amplification under plausible conditions. Direct damage to proteins and DNA can, for example, cause rises in intracellular calcium, which can consequently activate nucleases and proteases causing further damage to DNA and reduce enzyme activity [36].

$v_5 = v_6$ ($h_{23} = \frac{\gamma}{2}$, $g_{33} = \gamma$): The flux is equally distributed through both processes of X_2 depletion. Thus, the log gains of X_2 and X_3 with respect to X_4 are now different from the reference model (Table 4.17). As in the previous case, the eigenvalues indicate the existence of positive stable steady-states where $g_{33} - h_{23} < 1$ corresponding to $\gamma < 2$. Positive amplification of oxidative damage (X_3) is found in this region close to $\gamma = 2$. Though, where $|L_{36}(X_i, \alpha_1)| < 2$, positive amplification is only observed in *case* 3 for a weak positive feedback displaying linear or saturable kinetics, i.e., for $0 < \gamma \leq 1$. In contrast, positive amplification of X_2 is observed only in *case* 3 but for a negative feedback exhibiting either saturable, linear or cooperative kinetics, i.e., for $-4 \leq \gamma < 0$.

$v_5 \ll v_6$ ($h_{23} = \gamma$ and $g_{33} = \gamma$): In this particular case, the eigenvalues always display negative real parts independently of γ. As in the model variant described in section 4.3.2.6, given that the flux of X_2 consumption is the same as the flux of X_3 production, the latter will display the same steady-state changes as the flux of X_2 production , which are equal to those observed in the reference model. This implies that there is no amplification of X_3 in these conditions. Conversely, X_2 is amplified though only in *case* 3, and where $|L_{36}(X_i, \alpha_1)| < 2$ positive amplification is found for a negative feedback displaying inhibiting saturable kinetics or where v_6 is inversely proportional to X_3 ($-1 \leq \gamma < 0$).

4.3.3.7 ...damage removal (v_7)

Though the S-system is formally the same as that of the reference model, the exponent h_{33} corresponding to the kinetic order of X_3 relative to flux of damage repair, is no longer equal to 1 but can take any value between -4 and 4. As the flux of repair is downstream of X_2 it does not have any effect on the log gain of X_2 when changes in X_4 occur, i.e., $L_{37}^{(2)}$ is equivalent to the one obtained with the reference

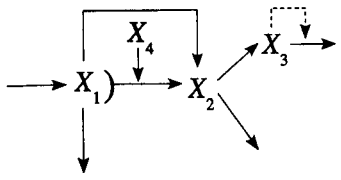

$$\begin{aligned}\dot{X}_1 &= \alpha_1 - \beta_1 X_1^{h_{11}} X_4^{h_{14}} \\ \dot{X}_2 &= \alpha_2 X_1^{g_{21}} X_4^{g_{24}} - \beta_2 X_2^{h_{22}} \\ \dot{X}_3 &= \alpha_3 X_2^{g_{32}} - \beta_3 X_3^{h_{33}}\end{aligned}$$

Figure 4.24: Graph depicting a positive or negative interaction of the amount of damage (X_3) on the pathway of damage removal (v_7), and its S-system representation. Though the system is described by the same S-system than that of the reference model, h_{33} takes different values.

model. The log gain of X_3 with respect to changes in X_4 is:

$$L_{37}^{(3)} = \frac{g_{24} - h_{14}}{h_{33}} \tag{4.48}$$

This expression is similar to the one obtained in the model variant where X_2 affects its consumption through the detoxification pathway (see section 4.3.2.5). As in this model variant $h_{33} = \gamma$, the system will show positive amplification in the same conditions as in the model variant described in section 4.3.2.5 where $h_{22} = \gamma$, i.e., in *case* 3 where v_7 reaches saturation with X_3 ($1/2 \leq \gamma < 1$). Though we considered for simplification the kinetics of oxidative damage removal to be linear, it is also plausible that these processes may exhibit saturable kinetics. However, even considering linear kinetics for these processes of damage removal, increased deficiency in DNA repair due to oxidative damage to proteases and repair enzymes may produce saturable kinetics.

4.4 Discussion

We showed previously that according to a minimal model H_2O_2 production increases at most linearly with SOD activity. However, as mentioned in the previous chapter, the minimal model served as a "null hypothesis" in the inference of the mechanisms of oxidative damage elicited by SOD overexpression. Supralinear increases in oxidative damage, if observed, could be due to additional mechanisms not considered in the minimal model. In the present work, we extended the minimal model to take into account these additional mechanisms and assess whether the existence of these interactions could account for a supralinear increase in H_2O_2-mediated oxidative damage without significant changes in H_2O_2. Our results are summarized in Table 4.18, which identifies possible mechanisms that may be responsible for amplification of H_2O_2-mediated oxidative damage when SOD activity is increased under physiological conditions. Plausible physiological conditions are restricted to where a positive stable steady-state exists in which all concentrations show moderate log gains with respect to changes in oxidative load (i.e., $|L(X_i, \alpha_1)| < 2$).

Table 4.18: Amplification of oxidative damage (X_3) and H_2O_2 (X_2) under plausible physiological conditions†

	Oxidative Damage (X_3)			Hydrogen Peroxide (X_2)		
	Effect of X_1	Effect of X_2	Effect of X_3	Effect of X_1	Effect of X_2	Effect of X_3
v_1	-	*case* 3 / S(+)	*case* 3 / S(+)	-	*case* 3 / S(+)	*case* 3 / S(+)
v_2	-	-	-	-	-	-
v_3	-	*case* 3 / S(−)	*case* 3 / S(−)	-	*case* 3 / S(−)	*case* 3 / S(−)
v_4	-	*case* 3 / S(+)	*case* 3 / S(+)	-	*case* 3 / S(+)	*case* 3 / S(+)
v_5	*cases* 1 and 2 / C(+)	*case* 3 / S(+)	*case* 3 / S(−)	*cases* 1 and 2 / C(+)	*case* 3 / S(+)	*case* 3 / S(−)
v_6	*cases* 1 and 2 / C(−)	*case* 3 / C(+)	*case* 3 / S(+)	-	-	-
v_7	*cases* 1 and 2 / C(+)	*case* 3 / S(−)	*case* 3 / S(+)	-	-	-

† The *cases* and the type of kinetics in which positive amplification is observed for each model variant are presented. (S) saturable or (C) cooperative kinetics of the affected flux with respect to the effector; (+) and (−) represent activation and inhibition, respectively. Conditions of physiological plausibility are explained in text.

We find that amplification of H_2O_2 (X_2) and H_2O_2-mediated oxidative damage (X_3) are only observed under moderate $L(X_i, \alpha_1)$ in *cases* 1-3, i.e., where the H_2O_2 is produced mainly through the superoxide dismutation reaction ($v_1 \gg v_2$). While amplification in *cases* 1 and 2 ($v_1 = v_3$) is only found when X_1 acts as effector, mechanisms mediated by X_2 and X_3 show physiologically plausible amplification only in *case* 3 ($v_1 \ll v_3$). Interestingly, *cases* 1 and 2 are where X_1 displays greater variations when SOD activity is increased while *case* 3 is where X_2 and X_3 suffer a greater change with SOD activity.

We also find amplification where H_2O_2 is produced equally through v_1 and v_2 (*cases* 4-6), though in these *cases* the log gains of the steady-state concentrations with respect to changes in oxidative load were always high ($|L(X_i, \alpha_1)| > 2$), and are not likely to be observed in physiological conditions. This may be due to the moderate influence of X_1, X_2 or X_3 on each interaction when SOD is increased in *cases* 4-6 (given by the low absolute log gains of the concentrations with respect to SOD in the reference model), compared to similar conditions in *cases* 1-3. To display the same amplification as in *cases* 1-3, the log gains of the effector concentrations with respect to SOD would have to be of similar magnitude in the presence of each interaction. This only occurs where the system is generally more sensitive to other parameters or external factors such as oxidative load.

We did not find amplification in conditions where H_2O_2 is mostly produced through the superoxide reductive pathway (v_2) (*cases* 7-9). This is not surprising given that in these conditions variations in any of the variable pools considered in this model are negligible when SOD activity is increased. Nonetheless, according to the minimal model presented in the previous chapter [21], the rates of processes of superoxide reduction are likely to be always lower than the dismutation rate ($v_2 \ll v_1$), and therefore *cases* 7-9 are not physiologically relevant.

As for the flux ratios of H_2O_2 consumption, although we have found positive amplification where $v_5 \leq v_6$ we have not considered these cases as occurring under physiological conditions and therefore are not included in Table 4.18. Typically *in vivo*, the rates of enzyme-catalysed detoxification of H_2O_2 are a few orders of magnitude higher than those observed for the Fenton reaction ($v_5 \gg v_6$). Considering for instance, glutathione peroxidase concentrations in rat liver cytosol is 1.2-5.8 μM [37–39] and a second-order rate constant of the reaction between the enzyme and H_2O_2 to be 5×10^7 $M^{-1}s^{-1}$ [24], the resulting pseudo first-order rate constant will be $60 - 290$ s^{-1}. Catalase concentrations reported in liver, 1.2 μM [24] and heart mitochondria, 0.24 μM [40] and a second-order rate constant for the reaction with H_2O_2 of 4.6×10^7 $M^{-1}s^{-1}$[24], yields a pseudo first-order rate constant of 11-55 s^{-1}. As the rate constant of the reaction between EDTA-, ATP- or citrate-ferrous iron chelates and H_2O_2 is 10^4 $M^{-1}s^{-1}$ [41, 42], a concentration of labile iron $> 10^{-2}$ M would be required to compete with glutathione peroxidase and/or catalase. For comparison, physiological concentrations of labile iron are believed

to be lower than 10^{-6} M. Therefore, amplification in conditions where $v_5 = v_6$ or $v_5 \ll v_6$ are not considered to be physiologically relevant and are not presented in Table 4.18.

From Table 4.18 we can also see that in the model variants where the fluxes $v_1 - v_4$ display non-linear kinetics with respect to X_1, the system does not present physiologically plausible amplification ($|L(X_i, \alpha_1)| > 2$), while it does so when X_1 influences the fluxes $v_5 - v_7$ or even when X_2 or X_3 affect the fluxes v_1, v_3 and v_4.

The model variants where X_1, X_2 and X_3 act on v_2 also do not present amplification under physiologically plausible conditions. Under conditions where the variable pools exert a higher influence on v_2 (*cases* 1-3), which is where all other model variants can present amplification under physiological conditions, the rate of v_2 compared to the dismutation is negligible. Thus, the interaction on v_2 under these circumstances is undetectable.

It is interesting to note that amplification in model variants where X_1 acts as an effector is observed due to the attenuation of the beneficial effects of superoxide. These interactions may be regarded as protective stratagems to ameliorate oxidative injury or induce resistance to oxidative stress. Increasing SOD will reduce the steady-state concentration of $O_2^{\bullet -}$ consequently diminishing the capacity of the system to protect itself against the oxidative load, and may lead to amplification of oxidative damage. In the absence of such interactions there would be no amplification of oxidative damage as the log gains of X_3 with respect to SOD would be equivalent to that of X_2 (between $0 - \frac{1}{2}$). Interestingly, in *cases* 1 and 2 the log gain of X_2 with respect to SOD is always between $0 - \frac{1}{2}$ and is independent of the kinetics displayed by the extra interaction. In systems where superoxide can significantly decrease the flux of the Fenton reaction or induce oxidative removal/repair, amplification of H_2O_2-mediated damage can be observed without significant changes in H_2O_2 levels. However, the kinetics displayed by the interaction must be cooperative with respect to superoxide (Table 4.18).

On the other hand, in model variants where X_2 and X_3 act as effectors, amplification is observed for weaker interactions corresponding to saturable kinetics (except for the model variant where X_2 has an extra interaction on the Fenton reaction, v_6). Among these interactions, it is worth mentioning the effects of the products of H_2O_2-mediated oxidative damage on the fluxes of H_2O_2 consumption and oxidative damage formation. When SOD activity is augmented, the concentration of proteins damaged by hydroxyl radicals that are involved in H_2O_2 detoxification may increase. Mutations in genes encoding catalases, peroxidases or transcription factors responsible for inducing H_2O_2 detoxification may also rise, reducing the expression of these proteins. Together, these events can divert the steady-state flux of H_2O_2 consumption from the detoxification to the damage pathway (i.e., from v_5 to v_6). Assuming saturable kinetics for the overall mechanism with respect to the

concentration of oxidative damage, these events could lead to amplification of both H_2O_2 and oxidative damage concentrations when SOD activity is increased. In addition, damage to proteins involved in maintenance of essential ion gradients such as calcium, copper or iron can lead to imbalances in ion homeostasis. Increased intracellular free iron and copper concentrations leads to higher rates of Fenton reactions, while higher calcium concentrations stimulate proteases and nucleases that further damage proteins and DNA [36]. This secondary damage can also include endonucleases or other repair enzymes that may further reduce the capacity to remove the products of oxidative damage. Assuming also saturable kinetics for these mechanisms with respect to oxidative damage products, increasing SOD activity can lead to amplification of H_2O_2-mediated oxidative damage with only a linear increase in H_2O_2. Still, amplification due to these interactions is predicted to occur only where $O_2^{\bullet-}$ is mostly consumed through the non-H_2O_2 producing pathway ($v_3 \gg v_1, v_2$).

Many interactions that we considered implausible to occur in well-performing biological systems may still occur under anomalous conditions and should therefore not be entirely discarded. Mutations, infrequent pathologies, experimental handling, and other artificial interventions, can all give rise or significantly increase the importance of interactions that are not relevant under physiological settings. The kinetic orders describing each interaction should not be viewed as immutable parameters. For instance, the distinct kinetics of the various processes that govern the consumption of a particular metabolite and the balance between those processes is what determines the magnitude of the overall kinetic order. This was seen in the Methods section where each extreme condition was defined in terms of the balance between the different processes of $O_2^{\bullet-}$ consumption, exhibiting significant differences in the kinetic order of X_4 relative to the overall consumption rate of $O_2^{\bullet-}$. All the other fluxes in the reference model were assumed to follow pseudo-first order kinetics. Additional interactions with variable kinetics changes the overall kinetic order of the effectors on the rate of the affected processes. The kinetics of these interactions are themselves determined by the various processes that may contribute to them. Hence, changes in environmental conditions, such as oxidative stress, can change the balance of the different processes contributing to the interaction and lead to variations in the kinetic order of the effector (the strength of the interaction). For instance, in metal-induced stress, where labile iron and copper concentrations are significantly increased, the flux ratio between v_5 and v_6 may change in favor of the Fenton reaction. Under these circumstances, the conditions $v_5 = v_6$ or even $v_5 \ll v_6$ would have to be considered. Assuming the existence of interactions were the different flux ratios between v_5 and v_6 can lead to different outcomes in terms of amplification, an increase in SOD activity could no longer produce a supralinear increase in H_2O_2-mediated oxidative damage and even lead to amplification of H_2O_2, which would not occur under physiological con-

ditions.

In conclusion, using a mathematical approach we were able in this work to identify possible mechanisms that may lead to H_2O_2-mediated damage to cellular components increasing supralinearly with increasing SOD activity. We have also identified the physiological conditions in which these may be observed. The supralinear increase in H_2O_2-mediated damage may be accompanied by a similar increase in H_2O_2, by a linear increase or even sublinear changes in H_2O_2 concentration. This shows that these two concentrations need not be correlated. Therefore, caution should be used to avoid over-interpretations of experimental data based on changes of only one of these concentrations. Given that the physiological relevance of each interaction studied here may vary among different tissues, cellular or subcellular compartments, the mechanisms leading to amplification of oxidative damage in each given instance must be assessed in the specific physiological or pathological context. However, it is also clear that the number of interactions and the complexity of their kinetics require further assessment by means of quantitative experiments. Evaluation of the types of kinetics of the most important interactions involved in ROS metabolism, assessment of the balance and relevance of each of these interactions, together with our work, can provide a powerful framework to help identify the causes of the prooxidative effects of SOD in various biological systems.

References

[1] Bloch, C. and Ausubel, F. (1986) Paraquat-mediated selection for mutations in the manganese-superoxide dismutase gene *sodA*. *J Bacteriol* **168**:795–8.

[2] Elroy-Stein, O.; Bernstein, Y. and Groner, Y. (1986) Overproduction of human Cu/Zn-superoxide dismutase in transfected cells: Extenuation of paraquat-mediated cytotoxicity and enhancement of lipid peroxidation. *EMBO J* **5**:615–622.

[3] Scott, M.; Meshnick, S. and Eaton, J. (1987) Superoxide dismutase-rich bacteria. Paradoxical increase in oxidant toxicity. *J Biol Chem* **262**:3640–5.

[4] Elroy-Stein, O. and Groner, Y. (1988) Impaired neurotransmitter uptake in PC12 cells overexpressing human Cu/Zn-superoxide dismutase–implication for gene dosage effects in down syndrome. *Cell* **52**:259–67.

[5] Kedziora, J. and Bartosz, G. (1988) Down's syndrome: A pathology involving the lack of balance of reactive oxygen species. *Free Radic Biol Med* **4**:317–30.

[6] Scott, M.; Meshnick, S. and Eaton, J. (1989) Superoxide dismutase amplifies organismal sensitivity to ionizing radiation. *J Biol Chem* **264**:2498–501.

[7] Omar, B.; Gad, N.; Jordan, M.; Striplin, S.; Russell, W.; Downey, J. and McCord, J. (1990) Cardioprotection by Cu,Zn-superoxide dismutase is lost at high doses in the reoxygenated heart. *Free Radic Biol Med* **9**:465–71.

[8] Omar, B. and McCord, J. (1990) The cardioprotective effect of Mn-superoxide dismutase is lost at high doses in the postischemic isolated rabbit heart. *Free Radic Biol Med* **9**:473–8.

[9] Amstad, P.; Peskin, A.; Shah, G.; Mirault, M.; Moret, R.; Zbinden, I. and Cerutti, P. (1991) The balance between Cu,Zn-superoxide dismutase and catalase affects the sensitivity of mouse epidermal cells to oxidative stress. *Biochemistry* **30**:9305–13.

[10] Bowler, C.; Slooten, L.; Vandenbranden, S.; De Rycke, R.; Botterman, J.; Sybesma, C.; Van Montagu, M. and Inze, D. (1991) Manganese superoxide dismutase can reduce cellular damage mediated by oxygen radicals in transgenic plants. *EMBO J* **10**:1723–32.

[11] Lohr, J. (1991) Oxygen radicals and neuropsychiatric illness. Some speculations. *Arch Gen Psychiatry* **48**:1097–106.

[12] Liochev, S. and Fridovich, I. (1991) Effects of overproduction of superoxide dismutase on the toxicity of paraquat toward *Escherichia coli*. *J Biol Chem* **266**:8747–50.

[13] Ceballos-Picot, I.; Nicole, A. and Sinet, P. (1992) Cellular clones and transgenic mice overexpressing copper-zinc superoxide dismutase: Models for the study of free radical metabolism and aging. In I. Emerit and B. Chance (Editors), *Free radicals and aging*, 89–98. Basel:Birkhauser Verlag, Switzerland.

[14] Costa, V.; Reis, E.; Quintanilha, A. and Moradas-Ferreira, P. (1993) Acquisition of ethanol tolerance in *Saccharomyces cerevisiae*: The key role of the mitochondrial superoxide dismutase. *Arch Biochem Biophys* **300**:608–614.

[15] Mao, G.; Thomas, P.; Lopaschuk, G. and Poznansky, M. (1993) Superoxide dismutase (SOD)-catalase conjugates. Role of hydrogen peroxide and the Fenton reaction in SOD toxicity. *J Biol Chem* **268**:416–20.

[16] de Haan JB; Cristiano, F.; Iannello, R.; Bladier, C.; Kelner, M. and Kola, I. (1996) Elevation in the ratio of Cu/Zn-superoxide dismutase to glutathione peroxidase activity induces features of cellular senescence and this effect is mediated by hydrogen peroxide. *Hum Mol Genet* **5**:283–92.

[17] Offer, T.; Russo, A. and Samuni, A. (2000) The pro-oxidative activity of SOD and nitroxide SOD mimics. *FASEB J* **14**:1215–23.

[18] Lee, M.; Hyun, D.; Jenner, P. and Halliwell, B. (2001) Effect of overexpression of wild-type and mutant Cu/Zn-superoxide dismutases on oxidative damage and antioxidant defences: Relevance to Down's syndrome and familial amyotrophic lateral sclerosis. *J Neurochem* **76**:957–65.

[19] Liochev, S. and Fridovich, I. (1994) The role of $O_2^{\bullet -}$ in the production of $HO^{\bullet}$: In vitro and in vivo. *Free Radic Biol Med* **16**:29–33.

[20] Teixeira, H.; Schumacher, R. and Meneghini, R. (1998) Lower intracellular hydrogen peroxide levels in cells overexpressing CuZn-superoxide dismutase. *Proc Natl Acad Sci U S A* **95**:7872–5.

[21] Gardner, R.; Salvador, A. and Moradas-Ferreira, P. (2002) Why does SOD overexpression sometimes enhance, sometimes decrease, hydrogen peroxide production? A minimalist explanation. *Free Radic Biol Med* **32**:1351–7.

[22] Seaver, L. and Imlay, J. (2001) Alkyl hydroperoxide reductase is the primary scavenger of endogenous hydrogen peroxide in *Escherichia coli*. *J Bacteriol* **183**:7173–81.

[23] Voit, E. (Editor) (2000) *Computational analysis of biochemical systems. A practical guide for biochemists and molecular biologists.* Cambridge University Press, Cambridge, UK.

[24] Chance, B.; Sies, H. and Boveris, A. (1979) Hydroperoxide metabolism in mammalian organs. *Physiol Rev* **59**:527–605.

[25] Aebi, H. (1983) Catalase. In H. Bergmeyer (Editor), *Methods of enzymatic analysis, Vol III*, 273–285. Weinheim: Verlag Chemie.

[26] Flohe, L. (1978) Glutathione peroxidase: Fact and fiction. *Ciba Found Symp* 95–122.

[27] Irvine, D. (1991) The method of controlled mathematical comparison. In E. Voit (Editor), *Canonical Nonlinear Modeling. S-system approach to understanding complexity.*, 90–109. Van Nostrand Reinhold, New York.

[28] Cairo, G.; Castrusini, E.; Minotti, G. and Bernelli-Zazzera, A. (1996) Superoxide and hydrogen peroxide-dependent inhibition of iron regulatory protein activity: A protective stratagem against oxidative injury. *FASEB J* **10**:1326–35.

[29] Chan, E. and Weiss, B. (1987) Endonuclease IV of *Escherichia coli* is induced by paraquat. *Proc Natl Acad Sci U S A* **84**:3189–93.

[30] Walkup, L. and Kogoma, T. (1989) *Escherichia coli* proteins inducible by oxidative stress mediated by the superoxide radical. *J Bacteriol* **171**:1476–84.

[31] Godon, C.; Lagniel, G.; Lee, J.; Buhler, J.; Kieffer, S.; Perrot, M.; Boucherie, H.; Toledano, M. and Labarre, J. (1998) The H_2O_2 stimulon in *Saccharomyces cerevisiae*. *J Biol Chem* **273**:22480–9.

[32] Storz, G.; Tartaglia, L. and Ames, B. (1990) The OxyR regulon. *Antonie Van Leeuwenhoek* **58**:157–61.

[33] Martins, E.; Robalinho, R. and Meneghini, R. (1995) Oxidative stress induces activation of a cytosolic protein responsible for control of iron uptake. *Arch Biochem Biophys* **316**:128–34.

[34] Pantopoulos, K. and Hentze, M. (1995) Rapid responses to oxidative stress mediated by iron regulatory protein. *EMBO J* **14**:2917–24.

[35] Pigeolet, E. and Remacle, J. (1991) Susceptibility of glutathione peroxidase to proteolysis after oxidative alteration by peroxides and hydroxyl radicals. *Free Radic Biol Med* **11**:191–5.

[36] Halliwell, B. and Gutteridge, M. (Editors) (1999) *Free Radicals in Biology and Medicine*. Oxford University Press, UK.

[37] Burk, R.; Nishiki, K.; Lawrence, R. and Chance, B. (1978) Peroxide removal by selenium-dependent and selenium-independent glutathione peroxidases in hemoglobin-free perfused rat liver. *J Biol Chem* **253**:43–6.

[38] Stults, F.; Forstrom, J.; Chiu, D. and Tappel, A. (1977) Rat liver glutathione peroxidase: Purification and study of multiple forms. *Arch Biochem Biophys* **183**:490–7.

[39] Forstrom, J.; Stults, F. and Tappel, A. (1979) Rat liver cytosolic glutathione peroxidase: Reactivity with linoleic acid hydroperoxide and cumene hydroperoxide. *Arch Biochem Biophys* **193**:51–5.

[40] Radi, R.; Turrens, J.; Chang, L.; Bush, K.; Crapo, J. and Freeman, B. (1991) Detection of catalase in rat heart mitochondria. *J Biol Chem* **266**:22028–22034.

[41] Bull, C.; McClune, G. and Fee, J. (1983) The mechanism of Fe-EDTA catalysed superoxide dismutation. *J. Am. Chem. Soc.* **105**:5290–5300.

[42] Rush, J. and Koppenol, W. (1990) Reactions of Fe(II)-ATP and Fe(II)-citrate complexes with t-butyl hydroperoxide and cumyl hydroperoxide. *FEBS Lett* **275**:114–6.

Chapter 5

Biphasic dose-response of lipid peroxidation to SOD in ischemia-reperfusion injury: A mathematical analysis.

Contents

Summary

The implication of reactive oxygen species (ROS) as mediators of cardiac ischemia-reperfusion injury has been well documented. Among the types of damage associated with ROS-mediated ischemia-reperfusion are the changes in the rate of lipid hydroperoxide formation. To ameliorate the toxicity caused by an increase in lipid peroxidation several therapeutical strategies have been devised that include the use of superoxide dismutase (SOD) to overscavenge superoxide radical ($O_2^{\bullet -}$). However, in addition to a growing body of evidence showing that SOD can become toxic at high activities, a bell-shaped dose-response of lipid peroxidation to SOD has also been reported. These studies suggest there is an optimal activity of SOD above which the protective effects are significantly lost, and raise serious concerns about the use of SOD or SOD mimics as therapeutical agents. In an effort to understand the mechanisms responsible for the biphasic response of lipid hydroperoxide production to changes in SOD activity observed in reperfused tissues we analyzed a mathematical model of lipid peroxidation. The results show that the effect of increasing SOD activity on $O_2^{\bullet -}$ depletion and H_2O_2 production does not produce a biphasic response of the rate of initiation of lipid peroxidation and consequently does not account for the bell-shaped dose response of lipid peroxidation to SOD. As the rate of lipid hydroperoxide formation is given by the product between the rate of initiation and the chain-length of peroxidation, we hypothesized that the biphasic response of lipid peroxidation can arise from the decrease in initiation at low doses of SOD and an increase in chain-length at higher SOD activities. We show that a decrease of $O_2^{\bullet -}$ concentration elicited by elevation of SOD activity may do both: decrease the rate of lipid peroxidation by lowering the rate of initiation by perhydroxyl radicals at low SOD activities, without a significant increase in chain-length; while at higher SOD activities depletion of $O_2^{\bullet -}$ may exacerbate the chain-length by assuming that $O_2^{\bullet -}$ can either inhibit metal-catalyzed chain-branching reactions, or induce the rate of termination or the rate of lipid hydroperoxide removal.

Abbreviations: SOD - superoxide dismutase; $O_2^{\bullet -}$ - superoxide; H_2O_2 - hydrogen peroxide; LH - ; LOOH; LOO; ; IRP - iron regulatory protein;

5.1 Introduction

The involvement of reactive oxygen species (ROS) in the pathogenesis of ischemia-reperfusion has been well established [1–5, and references therein]. One of the main sources of ROS is the superoxide radical ($O_2^{\bullet -}$), and its rate of formation is increased after oxygen reflow following ischemia [6]. One of the main antioxidant defenses against $O_2^{\bullet -}$ is the enzyme superoxide dismutase (E.C.: 1.15.1.1) (SOD) [7]. It is generally believed that increasing the activity of the enzyme will lead to higher protection to oxidative injury following ischemia. In fact, SOD mimetics are currently being tested as pharmaceutical candidates to treat conditions such as transplant-induced reperfusion injury [8]. However, serious concerns have been raised on the potential benefits of therapeuties using SOD or SOD mimetics due to the growing body of evidence showing that elevated levels of SOD activity can lead to deleterious effects [9–22]. Adding to this evidence, are reports of an anomalous bell-shaped dose-response to SOD observed in studies using isolated reperfused hearts [23–27]. In these studies, exogenous SOD was added to the perfusate after the organ was injured by a period of ischemia. Low doses of exogenous SOD provided improved recovery of function compared to controls. However, addition of SOD beyond a certain optimal level lead eventually to a dramatic decrease in recovery, with damage actually exceeding that of controls, i.e., without exogenous SOD added to the perfusate.

In an effort to understand the mechanisms responsible for the biphasic response to SOD a few potential explanations have been put forward over the years. Some have suggested that while SOD decreases superoxide levels, higher doses of SOD may cause an excessive increase in H_2O_2 formation that will exacerbate hydroxyl-mediated damage either through the Fenton reaction [20] or through the peroxidase activity of SOD [28]. Both these mechanisms require a significant increase in H_2O_2, which has not been measured yet. Furthermore, a dose-response curve was also observed with Mn-SOD [25], which lacks peroxidative activity [29], suggesting that this may not be the main mechanism leading to the biphasic behavior [25]. Others have suggested that as SOD activity rises, the drop in $O_2^{\bullet -}$ concentration leaves the oxidized form of SOD more available to react with the target molecules for which it was supposed to provide protection [22]. In other words, increasing SOD will favor the superoxide reductase (SOR) activity over the superoxide dismutase activity [30]. Another hypothesis is that superoxide may play opposite roles in cell physiology and an adequate amount of SOD should be required to maintain optimal levels of $O_2^{\bullet -}$ [27]. For example, increasing SOD may reduce nitric oxide scavenging by $O_2^{\bullet -}$ causing extravasation and edema observed in post-ischemic injury [25]. The dual role of superoxide as initiator and terminator of lipid peroxidation was also proposed as the mechanism responsible for the bell shape dose-response of lipid peroxidation to SOD [27]. However, it is highly

unlikely that superoxide may play a significant role as terminator of lipid peroxidation because of the presence of much more efficient chain-breaking antioxidants such as α-tocopherol and ubiquinol, whose concentrations are not significantly affected in membranes of reperfused myocardium [31]. Still, observations that the xanthine oxidase inhibitor allopurinol also produces a bell-shaped dose response in reperfusion injury [23] seem to implicate $O_2^{\bullet -}$ rather than H_2O_2 in mediating the biphasic behavior. Moreover, evidence that addition of catalase to reperfused medium with high SOD activities failed to diminish significantly the exacerbatory effects of SOD on the steady-state rate of lipid peroxidation [27], further supports this view.

To understand the mechanisms responsible for the biphasic dose-response to SOD, and in particular the response in terms of lipid peroxidation, we set up a mathematical model of lipid peroxidation and examined the effect of various doses of SOD activity on the steady-state rate of lipid peroxidation. Our results indicate that the effect of SOD on initiation alone *via* $O_2^{\bullet -}$ and H_2O_2 does not account for a biphasic response, and that the inverted bell-shape response of lipid peroxidation can arise when SOD-mediated decrease in $O_2^{\bullet -}$ increases the chain-length by increasing metal-catalyzed chain-branching reactions or decreasing either termination or lipid hydroperoxide removal from membranes.

5.2 The Model

5.2.1 Lipid Peroxidation

The minimal scheme proposed by Bolland [32] provides a sufficiently accurate description of lipid peroxidation that assumes a single polyunsaturated aggregated lipid species (LH) as substrate, which is oxidized into more than one molecule of lipid hydroperoxide (LOOH) per molecule of initiator. The mechanism consists of three basic conceptual modules:

1. Initiation

$$\text{LH (substrate)} + \text{Initiator} \xrightarrow{k_{\text{init}}} \text{L}^{\bullet} \text{or LOO}^{\bullet} \tag{5.1}$$

2. Propagation

$$\begin{aligned} \text{L}^{\bullet} + \text{O}_2 &\longrightarrow \text{LOO}^{\bullet} \\ \text{LH (substrate)} + \text{LOO}^{\bullet} &\xrightarrow{k_{\text{p}}} \text{L}^{\bullet} + \text{LOOH} \end{aligned} \tag{5.2}$$

3. Termination

$$\text{LOO}^{\bullet} + \text{LOO}^{\bullet} \xrightarrow{k_{\text{T}}} \text{non-radical products} \tag{5.3}$$

Initiation is defined as the introduction of radicals in the system. Two main pathways of initiation are considered: initiaton by perhydroxyl radicals (proportional to superoxide concentration) and by hydroxyl radicals (proportional to hydrogen peroxide concentration). Once a radical species ($L^\bullet$ or $LOO^\bullet$) is formed, the autocatalytic cycle represented by the propagation mechanism will keep on producing lipid hydroperoxides while maintaining the number of radicals constant in each cycle. Under physiological oxygen pressure, the reaction between carbon-centered lipid radicals ($L^\bullet$) and dioxygen is very fast compared with the subsequent reaction involving peroxyl radicals. In these conditions, the self-propagating cycle can be expressed simply by:

$$\text{LH (substrate)} \xrightarrow{k_p[LOO^\bullet]} \text{LOOH} \tag{5.4}$$

The autoxidation of unsaturated lipids progresses indefinitely unless the radicals are removed through the termination pathway.

5.2.2 Chain-Breaking Antioxidants

In vivo, highly effective chain-breaking antioxidants (TH) such as α-tocopherol (vitamin E) or ubiquinol exist that assure fast lipid radical removal. These antioxidants act by trapping the peroxyl radical and thereby "breaking" the autoxidation process [33]:

$$\begin{aligned} TH + LOO^\bullet &\xrightarrow{k_t} T^\bullet + LOOH \\ T^\bullet + LOO^\bullet &\longrightarrow \text{non-radical products} \end{aligned} \tag{5.5}$$

Termination by chain-breaking antioxidants is much more effective than through the reaction between two peroxyl radicals due to the much higher concentration of these antioxidants in the membrane. Ubiquinol, for example, can be up to five orders of magnitude more concentrated in the lipid bilayer than peroxyl radicals, while the second-order kinetic constant for ubiquinol is just two orders of magnitude lower than that for peroxyl radicals [34]. In our model, only the termination through chain-breaking antioxidants will be considered.

5.2.3 Lipid Hydroperoxide Decomposition and Removal

Lipid hydroperoxide accumulation in biological membranes is avoided or reduced by enzymes such phospholipid hydroperoxide glutathione peroxidase (E.C.:1.11.1.12) (PHGPX) that can repair directly the products of lipid peroxidation in the mem-

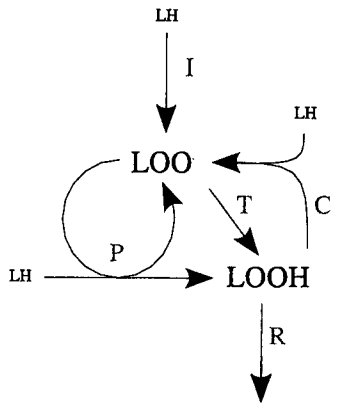

Figure 5.1: Basic Scheme of Lipid Peroxidation. (I) Initiation of lipid peroxidation by perhydroxyl and hydroxyl radicals, (P) propagation, (T) termination by chain-breaking antioxidants, (R) enzymatic removal of lipid hydroperoxides and (C) metal-catalyzed chain-branching reactions.

brane.

$$\begin{aligned} \mathrm{LOOH} + \mathrm{PHGPX}_{red} + \mathrm{H}^{+} &\xrightarrow{k_{\text{removal}}} \mathrm{PHGPX}_{ox} + \mathrm{LOH} \\ \mathrm{PHGPX}_{ox} + 2\mathrm{GSH} &\longrightarrow \mathrm{PHGPX}_{red} + \mathrm{GSSG} \end{aligned} \tag{5.6}$$

However, a small percentage of the lipid hydroperoxide pool may escape the removal pathway and re-enter the autoxidation cycle, forming a branch in the oxidation chain [35].

5.2.4 Chain-Branching Reactions

The chain-branching mechanism consists of a metal-catalyzed decomposition of LOOH to alkoxyl radicals ($LO^{\bullet}$). Subsequently, alkoxyl radicals may donate their unpaired electron to the unsaturated lipid moiety forming a carbon centered lipid radical ($L^{\bullet}$) that initiates another series of propagation cycles:

$$\begin{aligned} \mathrm{M}^{n} + \mathrm{LOOH} &\xrightarrow{k_{\text{chain}}} \mathrm{M}^{n+1} + \mathrm{LO}^{\bullet} + \mathrm{OH}^{-} \\ \mathrm{LH\ (substrate)} + \mathrm{LO}^{\bullet} &\longrightarrow \mathrm{L}^{\bullet} + \mathrm{LOH} \end{aligned} \tag{5.7}$$

As with peroxyl radicals, trapping of alkoxyl radicals by chain-breaking antioxidants should prevent the reaction with unsaturated lipid substrates. However, the kinetic advantage of the reaction between alkoxyl radicals and chain-breaking antioxidants is not large enough to be an efficient termination pathway [36]

The scheme of lipid peroxidation, summarized in Fig.5.1, can be described by: *initiation* (I), which is the initial input into the system; *propagation* (P) that keeps the

input switched on by generating directly LOOH; *termination* (T) that removes the autocatalyst and ending the propagation cycle; the output or *removal* (R) of lipid peroxidation damage by peroxidases; and finally, the *chain-branching reactions* (C) that can be regarded as a positive feedback loop feeding itself by regenerating $LOO^{\bullet}$. From this scheme we can derive the mathematical equations and the effects of SOD on the rate of lipid peroxidation can be interpreted of on the basis of these five modules.

5.2.5 Mathematical Equations

In our model, we consider both $O_2^{\bullet -}$ and H_2O_2 as the main initiators of lipid peroxidation. The overall rate of initiation is defined as the sum of the rates of initiation by both these species. Both rates, calculated at steady-state, are proportional to the amount of unsaturated phopholipids in the membrane and initiator steady-state concentrations:

$$v_{\text{init}} = v_{\text{init},1} + v_{\text{init},2} = k_{\text{init},1}[\text{LH}][O_2^{\bullet -}]_{\text{ss}} + k_{\text{init},2}[\text{LH}][H_2O_2]_{\text{ss}} \tag{5.8}$$

The oxidizable lipid substrate (LH) is much more concentrated (~0.5 M [34]) than any of the other chemical species involved in the reactions and can be considered constant. Superoxide may be consumed through three different pathways ([37], or Chapter 3): a) the dismutation pathway (rate law: $k_1[\text{SOD}] \cdot [O_2^{\bullet -}]$), b) the reductive pathway that includes the initiation reaction with LH (rate law: $k_2[O_2^{\bullet -}]$), and c) the non H_2O_2-producing pathway (rate law: $k_3[O_2^{\bullet -}]$). Assuming a constant rate of formation, v_f, the steady-state concentration of superoxide is given by:

$$[O_2^{\bullet -}]_{\text{ss}} = \frac{v_f}{k_1[\text{SOD}] + k_2 + k_3} \tag{5.9}$$

Hydrogen peroxide is produced mainly by dismutation and the reductive pathway, and consumed by two pathways that include detoxification by peroxidases such as GPX, and initiation of lipid peroxidation. The steady-state concentration of H_2O_2 is thus given by the following expression:

$$[H_2O_2]_{\text{ss}} = \frac{\frac{1}{2}k_1[\text{SOD}][O_2^{\bullet -}]_{\text{ss}} + k_2[O_2^{\bullet -}]_{\text{ss}}}{k_{\text{detox}} + k_{\text{init},2}[\text{LH}]} \tag{5.10}$$

where k_{detox} is a pseudo first-order kinetic constant that takes into account the concentration of catalase, GPX and/or other peroxidases depending on the system being studied. The resulting expression for the rate of initiation will be:

$$v_{\text{init}} = \frac{v_f[\text{LH}]}{k_1[\text{SOD}] + k_2 + k_3}\left(k_{\text{init},1} + k_{\text{init},2}\frac{\frac{1}{2}k_1[\text{SOD}] + k_2}{k_{\text{detox}} + k_{\text{init},2}[\text{LH}]}\right) \tag{5.11}$$

According to the basic scheme of lipid peroxidation shown in Fig. 5.1, peroxyl radicals are produced by initiation (v_{init}) and by the fraction of LOOH being produced that escapes removal, i.e., $\frac{k_{chain}[M^n]}{k_{chain}[M^n]+k_{removal}[Px]}(v_p + v_t)$, where [Px] is the concentration of peroxidases that decompose lipid hydroperoxides. At steady-state the flux of $LOO^\bullet$ production is equal to its flux of consumption ($v_t = k_t[TH][LOO^\bullet]$), which results in the following steady-state relation:

$$[LOO^\bullet]_{ss} = \frac{v_{init}}{k_t[TH] - \frac{k_{chain}[M^n]}{k_{chain}[M^n]+k_{removal}[Px]}(k_p[LH] + k_t[TH])} \tag{5.12}$$

As for lipid hydroperoxides (LOOH), they are generated by each propagation event and by chain-breaking antioxidants (v_p+v_t), and consumed by peroxidase-catalyzed removal ($v_{removal} = k_{removal}[Px][LOOH]$). Consumption of LOOH, on the other hand, is through chain-branching reactions that generate peroxyl radicals ($v_{chain} = k_{chain}[M^n][LOOH]$). The following expression for the steady-state concentration of LOOH is obtained:

$$[LOOH]_{ss} = \frac{(k_p[LH] + k_t[TH])[LOO^\bullet]_{ss}}{k_{chain}[M^n] + k_{removal}[Px]} \tag{5.13}$$

The overall rate of lipid oxidation at steady-state is defined as the rate of lipid hydroperoxide production:

$$v_{LP} = v_p + v_t = (k_p[LH] + k_t[TH])[LOO^\bullet]_{ss} \tag{5.14}$$

One of the main properties of lipid peroxidation is that for every initiation event, more than one lipid hydroperoxide is formed. This amplification, also known as the kinetic chain-length, is defined as the ratio between the overall rate of lipid peroxidation and the rate of initiation:

$$\begin{aligned} \text{chain-length} = \frac{v_{LP}}{v_{init}} &= \frac{(k_p[LH] + k_t[TH])[LOO^\bullet]_{ss}}{v_{init}} \\ &= \frac{(k_p[LH] + k_t[TH])(k_{chain}[M^n] + k_{removal}[Px])}{k_t[TH]k_{removal}[Px] - k_{chain}[M^n]k_p[LH]} \end{aligned} \tag{5.15}$$

Evidently, from the previous definitions that the rate of lipid peroxidation can be expressed simply by $v_{init} \times$ chain-length.

5.3 Results

5.3.1 Effect of SOD on initiation

It has been suggested that the dose response to SOD is due to increased production of H_2O_2 [20, 23]. In other words, the direct opposite effects of SOD on $O_2^{\bullet-}$

depletion and H_2O_2 formation could be responsible for the biphasic response of lipid peroxidation. Given that both $O_2^{\bullet -}$ and H_2O_2 are initiators *via* perhydroxyl and hydroxyl radicals, respectively, the decrease in initiation due to $O_2^{\bullet -}$ depletion could be surpassed by an increased initiation due to H_2O_2 at higher concentrations of SOD. Assuming conditions in which increasing SOD activity leads to an increase in H_2O_2 we analyzed the effect of changing the levels of SOD activity on the initiation rate of lipid peroxidation.

The overall initiation rate is given by the sum of initiation by $O_2^{\bullet -}$ and H_2O_2 (expression 5.8). We know from expression 5.10 that the steady-state concentration of H_2O_2 (and therefore the rate of initiation through H_2O_2) is proportional to $[O_2^{\bullet -}]_{ss}$, which is a monotonously decreasing function of SOD. The overall rate of initiation is then $[O_2^{\bullet -}]_{ss}$ multiplied by a linear function of SOD that also results in a monotonous function of SOD (equation 5.11). However, depending on the magnitude of the initial slope of $v_{init,1}$, the overall initiation rate can either be an increasing or decreasing function. This result can also be confirmed by finding the zero solution of the derivative relative to SOD. If increasing SOD activity can produce a biphasic curve on initiation, then there is a point where v_{init} will be minimum and its slope will be zero. However, as seen by the following expression, there is no minimum as the derivative is never zero for any value of SOD.

$$\frac{dv_{init}}{d[SOD]} = \frac{v_f k_1 [LH]}{2(k_{detox} + k_{init,2})} \cdot \frac{(k_{init,2} k_3 - 2k_{init,1}(k_{detox} + k_{init,2}))}{(k_3 + k_1[SOD])^2}$$

What this result implies is that increasing SOD activity does not produce a biphasic response of the initiation rate of lipid peroxidation, and thus changes in the rate of initiation alone cannot be responsible for the bell-shaped response of lipid peroxidation to SOD.

5.3.2 Effect of SOD on chain-length

Analysis of the steady-state expressions of $LOO^{\bullet}$ and LOOH shows that when the rate of peroxyl radical formation by chain-branching reactions exceeds the rate of termination the system can no longer reach a stable steady-state. This happens where the amount of peroxyl radicals fed in by chain-branching reactions exceeds the capacity of chain-breaking antioxidants to remove these radicals. The actual point where this capacity is exceed is when:

$$k_t[TH]k_{removal}[Px] = k_{chain}[M^n]k_p[LH] \tag{5.16}$$

Notice that this expression is independent of the initiation rate. If increasing SOD activity has the effect of increasing the rate of termination or damage removal the rate of lipid peroxidation will begin to increase dramatically close to this

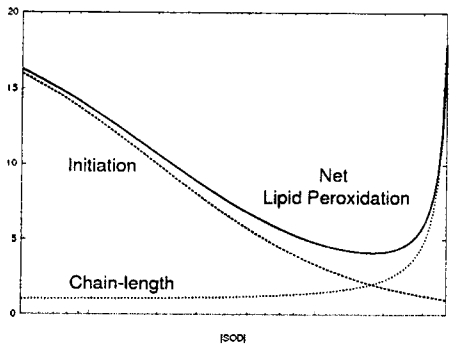

Figure 5.2: Effect of chain-length on the rate of lipid peroxidation ($v_{LP} = v_{init} \times$ chain-length). If chain-length is constant (independent of [SOD]), net changes in the rate of lipid peroxidation follow the changes in rate of initiation. Yet, if [SOD] can influence the chain-length the net rate of lipid peroxidation, a biphasic curve such as the one depicted here may be observed.

point. The same is observed if higher SOD activites decrease the rate of propagation or the rate of chain-branching reactions. This may also be seen from expression 5.15, where amplification grows to infinity if $k_{chain}[M^n]k_p[LH]$ approaches $k_t[TH]k_{removal}[Px]$.

A biphasic curve in response to SOD activity can then be expected as long as i) the decrease in the rate of initiation is greater than the increase of chain-length at low SOD activities and ii) as the levels of SOD activity become higher the system may approach rapidly the point where the increase in chain-length vastly exceeds the decrease in the steady-state rate of initiation (expression 5.16)(Fig. 5.2).

We can then hypothesize that if SOD can affect either one of the four processes - propagation (P), termination (T), LOOH removal (R) or chain-branching reactions (C) - directly or indirectly through $O_2^{\bullet -}$ or H_2O_2, then in conditions where the two criteria mentioned above are met a biphasic dose-response of lipid peroxidation to SOD activity should be observed. To assess this hypothesis we analysed three possible scenarios: the stimulation of lipid hydroperoxide removal (R) or of termination (T) by $O_2^{\bullet -}$ and the inhibition of chain-branching reactions (C) by $O_2^{\bullet -}$. As the propagation reaction is not enzyme-catalysed it is unlikely that SOD may affect the rate of this reaction through mechanisms other than by initiation.

For now, the interactions are defined generically. Their physiological relevance will be discussed in the final section.

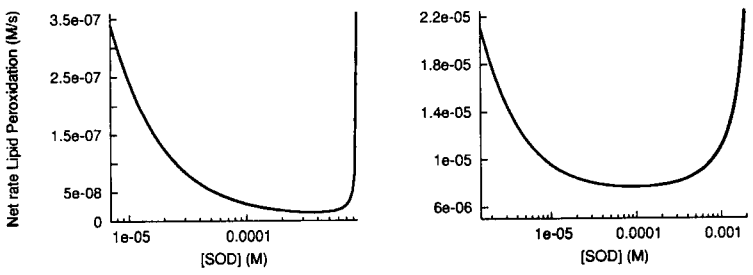

(a) (b)

Figure 5.3: Biphasic response of lipid peroxidation when $O_2^{\bullet -}$ induces rate of (a) lipid hydroperoxide removal ($h = 1$; $k = 10^3$ M; $V = 10^{10}$ Ms^{-1}) and (b) termination ($h = 1$; $k = 10^{-9}$ M; $V = 1$ Ms^{-1}). Remaining parameters are presented in Table 5.1.

5.3.2.1 $O_2^{\bullet -}$ induction of the rate of damage removal and the rate of termination

A positive interaction of $O_2^{\bullet -}$ on the rate of damage removal by peroxidases (R) can be represented generically by Hill kinetics with Hill number h:

$$f(O_2^{\bullet -}) = \frac{V \cdot [O_2^{\bullet -}]^h}{k^h + [O_2^{\bullet -}]^h} \tag{5.17}$$

This function is introduced in the rate expression of the damage removal reactions that become a function of SOD activity. It modifies the chain-length without affecting the rate of initiation:

$$\text{chain-length} = \frac{(k_p[\text{LH}] + k_t[\text{TH}]) \cdot (k_{\text{chain}}[\text{M}^n] + f(O_2^{\bullet -}))}{f(O_2^{\bullet -})k_t[\text{TH}] - k_{\text{chain}}[\text{M}^n]k_p[\text{LH}]} \tag{5.18}$$

The rate of lipid peroxidation is now given by the product between the rate of initiation and the new chain-length. Fig. 5.3(a) shows a bell-shaped dose response of the steady-state rate of lipid peroxidation to changes in SOD activity with $O_2^{\bullet -}$ acting as inducer of the rate of lipid hydroperoxide removal. The parameters used to produce the biphasic curve are presented in Table 5.1.

As SOD activity increases, the rate of initiation decreases due essentially to a higher $O_2^{\bullet -}$-removal rate. The decreased $O_2^{\bullet -}$ availability reduces the rate of damage removal, leading to accumulation of lipid hydroperoxides. Subsequently, the rate of chain-branching increases, and as it approaches the rate of termination the chain-length becomes exceedingly high, exacerbating lipid peroxidation. The same behavior was observed when considering stimulation of termination by $O_2^{\bullet -}$ (Fig.

Table 5.1: Parameter values used to model biphasic response.

Parameter	Value	Description	Refer.
v_f	1.6×10^{-5} M.s^{-1}	Rate of $O_2^{\bullet -}$ production.	[34]
k_1	4.7×10^{9} M^{-1}s^{-1}	Second order kinetic constant of SOD-catalyzed dismutation.	[38]
k_2	0.6×10^{3} s^{-1}	Pseudo first-order kinetic constant of the reductive pathway of $O_2^{\bullet -}$ consumption. Chosen to be at least higher than the rate of initiation through $O_2^{\bullet -}$.	–
k_3	0.6×10^{3} s^{-1}	Pseudo first-order kinetic constant of the non H_2O_2-producing pathway of $O_2^{\bullet -}$ consumption. Chosen to be equal to k_2.	–
k_{detox}	2.1×10^{2} s^{-1}	Pseudo first-order rate constant of H_2O_2 reduction to water. Chosen to obtain $[H_2O_2]_{ss} = 3.8 \times 10^{-8}$M as in [34].	–
$k_{\text{init},1}$	0.6×10^{3} M^{-1}s^{-1}	Second order kinetic constant of initiation through $O_2^{\bullet -}$/$HO_2^{\bullet}$. Adjusted to obtain a rate of 9.3×10^{-8}M.s^{-1} as in [34].	–
$k_{\text{init},2}$	3.4×10^{-4} M^{-1}s^{-1}	Second order kinetic constant of initiation through H_2O_2/$HO^{\bullet}$. Adjusted to obtain a rate of 6.5×10^{-12}M.s^{-1} as in [34].	–
k_{p}	26 M^{-1}s^{-1}	Second order kinetic constant of hydrogen abstraction by peroxyl radicals.	[34]
k_{t}	4.7×10^{4} M^{-1}s^{-1}	Second order kinetic constant of termination by α-tocopherol.	[39]
k_{removal}	$\sim 1 \times 10^{7}$ M^{-1}s^{-1}	Second order kinetic constant of the reaction between PHGPX and LOOH.	[34]
k_{chain}	3.2×10^{2} M^{-1}s^{-1}	Second order kinetic constant of the reaction between "free iron" and LOOH.	[34]
[LH]	0.5 M	Total phospholipid concentration.	[34]
[TH]	2.0×10^{-4} M	Concentration of chain-breaking antioxidants. Only α-tocopherol is considered.	[34]
[Px]	3.8×10^{-8} M	Concentration of peroxidases capable of removing lipid hydroperoxides. Only PHGPX is considered.	[34]
[Fe^{2+}]	$\sim 10^{-7}$ M	Concentration of labile "free-iron" in liver mitochondria.	[34]

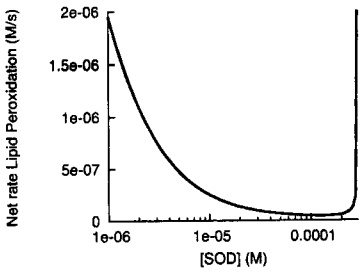

Figure 5.4: Biphasic response of lipid peroxidation when $O_2^{\bullet -}$ inhibits rate of metal-catalyzed chain-branching reactions ($h = 1$; $k = 10^{-13}$ M; $V = 30$ Ms^{-1}). Remaining parameters are presented in Table 5.1.

5.3(b)). Using the same Hill function, the chain-length is modified to:

$$\text{chain-length} = \frac{(k_p[\text{LH}] + f(O_2^{\bullet -})) \cdot (k_{\text{chain}}[M^n] + k_{\text{removal}}[\text{Px}])}{k_{\text{removal}}[\text{Px}] f(O_2^{\bullet -}) - k_{\text{chain}}[M^n] k_p[\text{LH}]} \tag{5.19}$$

As $O_2^{\bullet -}$ is depleted by SOD, the rate of termination decreases and approaches the rate of chain-branching reactions. The dramatic increase in chain-length and consequently on the rate of lipid peroxidation is seen as SOD approaches this point.

5.3.2.2 $O_2^{\bullet -}$ inhibition of metal-catalyzed chain-branching reactions

The possibility of SOD affecting the rate of damage removal through an inhibitory effect by $O_2^{\bullet -}$ was also explored. The negative interaction can be expressed generically by a declining Hill function, as follows:

$$f'(O_2^{\bullet -}) = V \cdot \left(1 - \frac{[O_2^{\bullet -}]^h}{k^h + [O_2^{\bullet -}]^h}\right) = \frac{V \cdot k^h}{k^h + [O_2^{\bullet -}]^h} \tag{5.20}$$

This interaction has also no effect on the rate of initiation, and is only included in the chain-length expression:

$$\text{chain-length} = \frac{(k_p[\text{LH}] + k_t[\text{TH}]) \cdot (f'(O_2^{\bullet -}) + k_{\text{removal}}[\text{Px}])}{k_{\text{removal}}[\text{Px}] k_t[\text{TH}] - f'(O_2^{\bullet -}) k_p[\text{LH}]} \tag{5.21}$$

Using the parameter values in Table 5.1, a biphasic response of lipid peroxidation is also observed when SOD activity is increased (Fig. 5.4). As levels of $O_2^{\bullet -}$ are reduced the inhibitory effect is lifted and the rate of chain-branching reactions is increased slowly until it reaches close to the rate of termination, leading to an excessive increase in chain-length and consequently on the net rate of lipid peroxidation.

5.4 Discussion

Though it has been suggested that the toxicity of high doses of SOD may due to an increase in H_2O_2 steady-state concentration, we did not consider the effects of H_2O_2 on the chain-length. Even in conditions where H_2O_2 is increased with SOD ($k_2 > k_3$), progressively high SOD concentrations will lead to progressively smaller increases in H_2O_2 concentration. This is the opposite of what would be necessary for H_2O_2 to mediate the exacerbation of damage at high levels of SOD activity. In fact, increasing k_{detox} in our model by two orders of magnitude did not change significantly the biphasic response (not shown). This is in agreement with the the dose-response study carried out by Omar and coworkers [25] where relatively high amounts of catalase added together with the highest dose of SOD used in the experiments did not significantly counteract the exacerbation of damage.

In the parameter set we used to produce the biphasic curves (Table 5.1) H_2O_2 was considered to remain relatively constant at any value of SOD. This was done by choosing $k_3 = k_2$, as these parameters are unknown, though k_2 has a lower limit set by the reactions between $O_2^{\bullet -}$ and the lipid substrate LH that generates H_2O_2. A larger k_3 would lead to an increase in the steady-state concentration of H_2O_2 with the concentration of SOD, at low doses of the latter. Under these circumstances, H_2O_2 might attenuate the decrease in initiation of lipid peroxidation with SOD activity, or even increase initiation. However, an increase of k_3 in our model does not produce significant changes in the biphasic behavior (not shown). This happens because the parameters we used consider a rather low contribution of $HO^{\bullet}$ radicals to the rate of initiation, as indicated by the results in [34]. This is also in aggreement with evidence that $HO^{\bullet}$ does not seem to play a direct role in early reperfusion injury following ischemia [40, 41].

We also tried changing the parameters in search of conditions that might produce a biphasic curve mediated by the effects of H_2O_2 (rather than $O_2^{\bullet -}$), on the rates of termination, hydroperoxide removal and chain-branching reactions (not shown). This was done in conditions where H_2O_2 increases with SOD ($k_3 > k_2$). Even with higher Hill coefficients (more cooperative kinetics) we could not generate a biphasic curve with a significant decrease in initiation that would be detected experimentally. In these cases, the steady-state rate of initiation remains relatively constant at lower levels of SOD since it cannot compete with the rates of non-H_2O_2 producing processes that also consume $O_2^{\bullet -}$. At higher SOD activities, when the steady-state rate of initiation starts to decrease, the effect of SOD on chain length is already significant and only a negligible drop in the rate of lipid peroxidation is observed. Still, though we explored extensively the space of parameters, we cannot formally discard the hypothesis that H_2O_2 may play a role on the biphasic response of lipid peroxidation. However, if the hypothesis is correct that the biphasic response is produced by the concerted decrease in initiation at low lev-

els of SOD and increase in chain-length at high SOD activities then superoxide is most likely the mediator of both effects. The involvement of superoxide rather than H_2O_2 in ischemia-reperfusion injury is further supported by evidence that both SOD and the xanthine oxidase inhibitor allopurinol produce an inverted bell-shape dose-response of arrhytmic and contractile indexes in postischemic rat heart, while catalase produces a linear dose-response [23].

In what ways can superoxide influence the chain-length? The results presented in the previous section suggest three modes of action of $O_2^{\bullet -}$ that might lead to increased chain-length at high SOD activities. Namely: (i) a stimulation of chain-termination reactions; (ii) a stimulation of the removal of phospholipid hydroperoxides from the membrane; and (iii) the inhibition of metal-catalyzed chain-branching reactions.

The latter seems the most likely mechanism for mediating the SOD-dependent increase in chain-length that may occur in conditions in which the biphasic response of lipid peroxidation to SOD activity was observed. Iron is increased in tissues following ischemia-reperfusion [42] and seems to play a major role in oxidative injury demonstrated by evidence that iron chelators, such as desferrioxamine, improve tissue functional and metabolic recovery after ischemia-reperfusion [43]. It was recently reported that non-transferrin-bound iron can be imported into the cell by a superoxide-dependent ferri-reductase activity [44]. The iron transported into the cell can then be efficiently sequestred by ferritin, which could constitue a simple stratagem of cells to remove catalytically active iron from the extracellular space. The involvement of superoxide in the import of iron was further evidenced by the remarkable inhibition of iron uptake by addition of extracellular SOD [44]. This pathway could also constitute a mechanisms by which addition of extracellular SOD might lead to an increase in metal-catalyzed chain-branching reactions. The cytosolic iron regulatory proteins (IRP) may also be a candidate for $O_2^{\bullet -}$-mediated inhibition of chain-branching reactions. It has been reported that superoxide inhibits the mRNA binding activity of IRP, leading to a concerted increase in ferritin synthesis and decrease in translation of tranferrin-receptor mRNA [45]. Decreasing superoxide would lead to increased levels of intracellular iron and increased lipid peroxidation through metal-catalyzed decomposition of lipid hydroperoxides. However one would have to assume that extracellular levels of SOD can influence the intracellular levels of superoxide. On the other hand, nitric oxide (NO), which diffuses well through biological membranes could be the biological mediator by exherting a negative effect on the rate of chain-branching reactions. Overscavenging of superoxide would decrease the rate of reaction between superoxide and NO that forms peroxynitrite, and increase NO availability. NO has also has been shown to induce the mRNA binding activity of IRP and consequently increasing the labile intracellular iron pool. Reducing the competition for superoxide by increasing SOD would increase the amount of NO able to react with cytosolic IRP. However,

it has been reported that the induction of IRP activity by NO is rather slow (~15h) and would not apply to the reported cases of the biphasic response given the much shorter times since addition of SOD in the blood/reperfusate to the end of the reperfusion period (<3h in [24, 25, 27]).

Besides iron, copper is also a good target for superoxide-mediated increase in metal-catalyzed chain-branching reactions. Copper chelators such as bathocuproin can reduce oxidative damage in reperfused myocardium [43], indicating the involvement of copper in reperfusion injury. However, further studies are needed to assess the role of both copper and iron in the biphasic response of lipid peroxidation to SOD in postischemic tissues.

An increase in chain-length at high SOD activities might also result from termination reactions being stimulated by $O_2^{\bullet -}$. It was proposed that $O_2^{\bullet -}$ may itself serve as terminator of lipid peroxidation [27]. However, even with incresed levels of $O_2^{\bullet -}$ generation it is highly unlikely that it would be able to compete with other chain-breaking antioxidants such as α-tocopherol or ubiquinol, or even with $LOO^{\bullet}$ itself. Ubiquinol and α-tocopherol do not seem to be significantly changed in reperfused myocardium [31]. Therefore, to increase chain-length at high SOD activities superoxide would have to somehow decrease the levels of ubiquinol and α-tocopherol significantly. Alternatively, an increase in chain length at high SOD doses could also be achieved by $O_2^{\bullet -}$-dependent induction of PHGPX, or other enzymes and cofactors involved in the enzyme-catalyzed removal of lipid hydroperoxides.

Though we considered the effect of SOD on iron at the level of the metal-catalyzed chain-branching reactions we did not analyse this effect on the rate of initiation through the Fenton reaction. In principle, the increase in iron or other reduced transition metals with increasing SOD activities can produce a biphasic response in the rate of initiation and consequently on the rate of lipid peroxidation. However, this effect of iron or other transition metals on the rate of initiation is unlikely to contribute more to the rate of lipid peroxidation than the effect on chain-length that is mediated by increased chain-branching reactions. The latter effect is specially important in conditions where the rate of chain-branching reactions approaches the rate of termination ($v_{chain} = v_t$), as here the chain-length increases dramatically with the rate of the chain-branching reactions. In contrast, the rate of lipid peroxidation increases linearly with the rate of primary initiation by hydroxyl or perhydroxyl radicals.

Increasing iron concentration even further can switch lipid peroxidation from a self-propagated process (steady-state with fixed amplification) to a chain-reaction (no steady-state, lipid hydroperoxides accumulate). Still, even without considering this situation, the rate of $HO^{\bullet}$-mediated initiation is considerably lower than the rate of $LOO^{\bullet}$ formation through chain-branching reactions, and should not have pronounced effects.

The sources of the radical species involved in postischemic reperfusion injury, their location and modes of action are still not well understood. One of the issues that remains to be resolved is whether the experimentally observed variations in the rate of lipid peroxidation at different SOD activities occur in the cellular, mitochondrial or other subcellular membranes. This would help significantly the analysis and interpretation of the results. Still, our model points to directions that can aid experimental design in order to narrow down the possible mechanisms involved in the exacerbation of ischemia-reperfusion damage at high SOD doses.

References

[1] Arroyo, C.; Kramer, J.; Dickens, B. and Weglicki, W. (1987) Identification of free radicals in myocardial ischemia/reperfusion by spin trapping with nitrone DMPO. *FEBS Lett* **221**:101–4.

[2] Garlick, P.; Davies, M.; Hearse, D. and Slater, T. (1987) Direct detection of free radicals in the reperfused rat heart using electron spin resonance spectroscopy. *Circ Res* **61**:757–60.

[3] Vandeplassche, G.; Hermans, C.; Thone, F. and Borgers, M. (1989) Mitochondrial hydrogen peroxide generation by NADH-oxidase activity following regional myocardial ischemia in the dog. *J Mol Cell Cardiol* **21**:383–92.

[4] Zweier, J.; Flaherty, J. and Weisfeldt, M. (1987) Direct measurement of free radical generation following reperfusion of ischemic myocardium. *Proc Natl Acad Sci U S A* **84**:1404–7.

[5] Bolli, R. (1998) Causative role of oxyradicals in myocardial stunning: A proven hypothesis. A brief review of the evidence demonstrating a major role of reactive oxygen species in several forms of postischemic dysfunction. *Basic Res Cardiol* **93**:156–62.

[6] Zweier, J. (1988) Measurement of superoxide-derived free radicals in the reperfused heart. Evidence for a free radical mechanism of reperfusion injury. *J Biol Chem* **263**:1353–7.

[7] Fridovich, I. (1997) Superoxide anion radical ($O_2^{\bullet -}$), superoxide dismutases, and related matters. *J Biol Chem* **272**:18515–7.

[8] Salvemini, D. and Cuzzocrea, S. (2003) Therapeutic potential of superoxide dismutase mimetics as therapeutic agents in critical care medicine. *Crit Care Med* **31**:S29–38.

[9] Bloch, C. and Ausubel, F. (1986) Paraquat-mediated selection for mutations in the manganese-superoxide dismutase gene *sodA*. *J Bacteriol* **168**:795–8.

[10] Elroy-Stein, O.; Bernstein, Y. and Groner, Y. (1986) Overproduction of human Cu/Zn-superoxide dismutase in transfected cells: Extenuation of paraquat-mediated cytotoxicity and enhancement of lipid peroxidation. *EMBO J* **5**:615–622.

[11] Scott, M.; Meshnick, S. and Eaton, J. (1987) Superoxide dismutase-rich bacteria. Paradoxical increase in oxidant toxicity. *J Biol Chem* **262**:3640–5.

[12] Elroy-Stein, O. and Groner, Y. (1988) Impaired neurotransmitter uptake in PC12 cells overexpressing human Cu/Zn-superoxide dismutase–implication for gene dosage effects in down syndrome. *Cell* **52**:259–67.

[13] Kedziora, J. and Bartosz, G. (1988) Down's syndrome: A pathology involving the lack of balance of reactive oxygen species. *Free Radic Biol Med* **4**:317–30.

[14] Scott, M.; Meshnick, S. and Eaton, J. (1989) Superoxide dismutase amplifies organismal sensitivity to ionizing radiation. *J Biol Chem* **264**:2498–501.

[15] Amstad, P.; Peskin, A.; Shah, G.; Mirault, M.; Moret, R.; Zbinden, I. and Cerutti, P. (1991) The balance between Cu,Zn-superoxide dismutase and catalase affects the sensitivity of mouse epidermal cells to oxidative stress. *Biochemistry* **30**:9305–13.

[16] Bowler, C.; Slooten, L.; Vandenbranden, S.; De Rycke, R.; Botterman, J.; Sybesma, C.; Van Montagu, M. and Inze, D. (1991) Manganese superoxide dismutase can reduce cellular damage mediated by oxygen radicals in transgenic plants. *EMBO J* **10**:1723–32.

[17] Lohr, J. (1991) Oxygen radicals and neuropsychiatric illness. Some speculations. *Arch Gen Psychiatry* **48**:1097–106.

[18] Ceballos-Picot, I.; Nicole, A. and Sinet, P. (1992) Cellular clones and transgenic mice overexpressing copper-zinc superoxide dismutase: Models for the study of free radical metabolism and aging. In I. Emerit and B. Chance (Editors), *Free radicals and aging*, 89–98. Basel:Birkhauser Verlag, Switzerland.

[19] Costa, V.; Reis, E.; Quintanilha, A. and Moradas-Ferreira, P. (1993) Acquisition of ethanol tolerance in *Saccharomyces cerevisiae*: The key role of the mitochondrial superoxide dismutase. *Arch Biochem Biophys* **300**:608–614.

[20] Mao, G.; Thomas, P.; Lopaschuk, G. and Poznansky, M. (1993) Superoxide dismutase (SOD)-catalase conjugates. Role of hydrogen peroxide and the Fenton reaction in SOD toxicity. *J Biol Chem* **268**:416–20.

[21] de Haan JB; Cristiano, F.; Iannello, R.; Bladier, C.; Kelner, M. and Kola, I. (1996) Elevation in the ratio of Cu/Zn-superoxide dismutase to glutathione peroxidase activity induces features of cellular senescence and this effect is mediated by hydrogen peroxide. *Hum Mol Genet* **5**:283–92.

[22] Offer, T.; Russo, A. and Samuni, A. (2000) The pro-oxidative activity of SOD and nitroxide SOD mimics. *FASEB J* **14**:1215–23.

[23] Bernier, M.; Manning, A. and Hearse, D. (1989) Reperfusion arrhythmias: Dose-related protection by anti-free radical interventions. *Am J Physiol* **256**:H1344–52.

[24] Omar, B.; Gad, N.; Jordan, M.; Striplin, S.; Russell, W.; Downey, J. and McCord, J. (1990) Cardioprotection by Cu,Zn-superoxide dismutase is lost at high doses in the reoxygenated heart. *Free Radic Biol Med* **9**:465–71.

[25] Omar, B. and McCord, J. (1990) The cardioprotective effect of Mn-superoxide dismutase is lost at high doses in the postischemic isolated rabbit heart. *Free Radic Biol Med* **9**:473–8.

[26] Galinanes, M.; Ferrari, R.; Qiu, Y.; Cargnoni, A.; Ezrin, A. and Hearse, D. (1992) PEG-SOD and myocardial antioxidant status during ischaemia and reperfusion: dose-response studies in the isolated blood perfused rabbit heart. *J Mol Cell Cardiol* **24**:1021–30.

[27] Nelson, S.; Bose, S. and McCord, J. (1994) The toxicity of high-dose superoxide dismutase suggests that superoxide can both initiate and terminate lipid peroxidation in the reperfused heart. *Free Radic Biol Med* **16**:195–200.

[28] Yim, M.; Chock, P. and Stadtman, E. (1990) Copper, zinc superoxide dismutase catalyzes hydroxyl radical production from hydrogen peroxide. *Proc Natl Acad Sci U S A* **87**:5006–10.

[29] Hodgson, E. and Fridovich, I. (1975) The interaction of bovine erythrocyte superoxide dismutase with hydrogen peroxide: Chemiluminescence and peroxidation. *Biochemistry* **14**:5299–303.

[30] Liochev, S. and Fridovich, I. (2000) Copper- and zinc-containing superoxide dismutase can act as a superoxide reductase and a superoxide oxidase. *J Biol Chem* **275**:38482–5.

[31] Haramaki, N.; Stewart, D.; Aggarwal, S.; Ikeda, H.; Reznick, A. and Packer, L. (1998) Networking antioxidants in the isolated rat heart are selectively depleted by ischemia-reperfusion. *Free Radic Biol Med* **25**:329–39.

[32] Bolland, J. L. (1949) Kinetics of olefin oxidation. *Quart. Rev.* **3**:1–21.

[33] Ingold, K. U. (1961) Inhibition of the autoxidation of organic substances in the liquid phase. *Chem. Rev.* **61**:563–589.

[34] Antunes, F.; Salvador, A.; Marinho, H.; Alves, R. and Pinto, R. (1996) Lipid peroxidation in mitochondrial inner membranes. I. An integrative kinetic model. *Free Radic Biol Med* **21**:917–43.

[35] Antunes, F. (2001) Lipid peroxidation in mitochondrial inner membranes. In M. Ebadi; J. Marwah and R. Chopra (Editors), *Mitochondrial Ubiquinone (Coenzyme Q10): Biochemical, Functional, Medical, and Therapeutic aspects in human health and disease*, 399–424. Prominent Press, Scottsdale.

[36] Evans, C.; Scaiano, J. C. and Ingold, K. U. (1992) Absolute kinetics of hydrogen abstraction from α-tocopherol by several reactive species including alkyl radical. *J. Am. Chem. Soc.* **114**:4589–4593.

[37] Gardner, R.; Salvador, A. and Moradas-Ferreira, P. (2002) Why does SOD overexpression sometimes enhance, sometimes decrease, hydrogen peroxide production? A minimalist explanation. *Free Radic Biol Med* **32**:1351–7.

[38] Forman, H. and Fridovich, I. (1973) Superoxide dismutase: A comparison of rate constants. *Arch Biochem Biophys* **158**:396–400.

[39] Barclay, L.; Vinqvist, M.; Antunes, F. and Pinto, R. (1997) Antioxidant activity of vitamin E determined in a phospholipid membrane by product studies: Avoiding chain transfer reactions by vitamin E radicals. *J. Am. Chem. Soc.* **119**:5764–5765.

[40] Chen, Y.; Ho, K.; Xia, Q. and Qian, Z. (2002) Hydrogen peroxide enhances iron-induced injury in isolated heart and ventricular cardiomyocyte in rats. *Mol Cell Biochem* **231**:61–8.

[41] Takemura, G.; Onodera, T. and Ashraf, M. (1992) Quantification of hydroxyl radical and its lack of relevance to myocardial injury during early reperfusion after graded ischemia in rat hearts. *Circ Res* **71**:96–105.

[42] Halliwell, B. and Gutteridge, M. (Editors) (1999) *Free Radicals in Biology and Medicine*. Oxford University Press, UK.

[43] Spencer, K.; Lindower, P.; Buettner, G. and Kerber, R. (1998) Transition metal chelators reduce directly measured myocardial free radical production during reperfusion. *J Cardiovasc Pharmacol* **32**:343–8.

[44] Ghio, A.; Nozik-Grayck, E.; Turi, J.; Jaspers, I.; Mercatante, D.; Kole, R. and Piantadosi, C. (2003) Superoxide-dependent iron uptake: a new role for anion exchange protein 2. *Am J Respir Cell Mol Biol* **29**:653–60.

[45] Cairo, G.; Castrusini, E.; Minotti, G. and Bernelli-Zazzera, A. (1996) Superoxide and hydrogen peroxide-dependent inhibition of iron regulatory protein activity: A protective stratagem against oxidative injury. *FASEB J* **10**:1326–35.

Part III

General Discussion

Chapter 6

General Discussion and Perspectives

Over the last years, it has become increasingly evident that all aerobic organisms generate ROS. The general belief is that these species are by-products of cellular respiration and metabolism, which exert toxic effects and thus must be eliminated from the cell. Yet, recent evidences have demonstrated that ROS are produced in a controlled fashion and are likely to play a critical role in cellular function and response to external environment [reviewed in 1]. It is conceivable that in the course of evolution, while organisms adapted to increasing concentrations of oxygen they took advantage of the by-products of oxygen reduction and explored their redox capabilities to sense changes in environments or to promote cellular proliferation. In fact, environmental changes may dictate the best time to proliferate, to halt growth or commit suicide (apoptosis), which are all processes that involve ROS. Even simple organisms such as bacteria use ROS to their advantage. This is evidenced by the capability of $O_2^{\bullet -}$ and H_2O_2 to modulate the *E. coli* SoxRS and OxyR regulons, which induce expression of the so-called antioxidant defenses that play a crucial role in controlling the intracellular steady-state levels of ROS. One of the key elements in the regulation of ROS is the SOD enzyme. The importance of maintaining the right balance of intracellular SOD activity [2–5], is evidenced by the adverse effects observed in mutants lacking [6–10] or overexpressing SOD [11–14, 3, 4, 15–19], by the control of expression of the SOD genes in aerobic organisms from bacteria to higher eukaryotes [20, 21], and the narrow distribution of SOD activity levels found in the human population [2].

Yet, despite the evidence of the adverse effects observed in cells overexpressing SOD, the causes for these effects are still unclear and the question remains: What are the prooxidative effects of high SOD activities?

The results presented in this work do not provide an answer to the actual mechanisms contributing to the negative effects of high SOD activities. However, the results show that there is no unique answer to this question, as the deleterious effects exhibited at high SOD activities can involve either inhibition of the beneficial $O_2^{\bullet -}$-dependent processes by excessive $O_2^{\bullet -}$ depletion, or changes in H_2O_2 concentration. The latter mechanism can involve either an increase in H_2O_2 and consequently in H_2O_2-mediated damage, or a decrease in H_2O_2, which may inhibit

beneficial H_2O_2-dependent processes. The involvement of either $O_2^{\bullet-}$ or H_2O_2 in the deleterious effects of high SOD activities is dependent on the physiological conditions, as seen for instance, from the results in Chapters 3 and 4. For this reason, the actual mechanisms responsible for the deleterious effects of high SOD activities have to be assessed for each particular system. This was done, for example, in the particular model of ischemia-reperfusion injury presented in Chapter 5 where it is shown that the exacerbation of oxidative stress damage at high SOD activities is most likely due to excessive $O_2^{\bullet-}$ depletion, and the bell-shaped response of damage to increasing levels of SOD activity may be related to the dual role of $O_2^{\bullet-}$ as a toxic product and a physiological intermediate in cellular protection.

Still, an important contribution would be to identify the conditions in which either type of mechanism (whether involving $O_2^{\bullet-}$ or H_2O_2) is predicted to be responsible for the prooxidative effects of SOD, and this is possible based on the results presented here.

What happens then with $O_2^{\bullet-}$ and H_2O_2 when SOD activity is increased? Assuming all enzymatic activities constant, one inevitable consequence of increasing SOD activity is that the steady-state concentration of $O_2^{\bullet-}$ will decrease. But the magnitude of this decrease will depend on the ability of other pathways of $O_2^{\bullet-}$ consumption to compete with the SOD-catalysed dismutation. One possible misconception often presented in the literature is that SOD is by far the main scavenger of $O_2^{\bullet-}$. It is also shown in Chapter 3 that there are several other pathways that may possibly consume $O_2^{\bullet-}$ at rates close to, or higher than through dismutation, and therefore influence the outcome. These include $O_2^{\bullet-}$ reduction by GSH or by reaction with the [4Fe-4S] clusters of dehydratases. Although the second-order rate constants for these reactions may be lower than that of dismutation, the actual rate of the reaction is determined by the availability of the reactants, which in the case of GSH, for example, can be in the range 1-10mM [22], i.e., three orders of magnitude greater than SOD [23, 24]. Another process that may also compete with SOD is the backward reaction of $O_2^{\bullet-}$ production (see discussion below). Nevertheless, the contribution of these processes to the consumption of $O_2^{\bullet-}$ *in vivo* remains to be assessed. Moreover, as the values of the rates depend on the intracellular concentrations of the metabolites involved in these reactions, their ability to compete with SOD may vary according to metabolic conditions. In this context, it is not surprising that the apparent contradictory results regarding the effects of increasing the activity of SOD may be a result of measuring the effects under different conditions. Thus, results observed in a particular biological system should not be extrapolated to others.

As for the influence of SOD on H_2O_2, before the present work there was still a controversy regarding whether increasing SOD activity would produce an increase or decrease in H_2O_2 production. Despite all the evidence, one of the difficulties in assessing this problem stems from the lack of a systematic approach to evaluate

the physiological conditions in which each result was obtained, which prevents the comparison between different observations in various studies. This may be due in part to the almost exclusive use of a reductionist approach that characterizes the field of free radical research. Though the reductionist approach is undoubtedly of extreme value in scientific discovery, one of its weaknesses is that it can create misconceptions as the approach does not take into account the interactions between different parts of the same biological system. One must be aware that this kind of approach brings important information about the structure of a system but not too much about its function, and how the different parts of the system interact with each other. This latter aspect is usually an extrapolation based on our knowledge of a collection of evidences usually captured also through a reductionist approach. As mentioned in Chapter 2, one of the advantages of mathematical modeling is that it provides the ability to analyze many key ideas, concepts and data together, allowing a more integrative and correct perspective of the biological system under study.

With this in mind, in order to assess the influence of SOD activity on H_2O_2 production, a minimal model of $O_2^{\bullet -}$ metabolism was analyzed (Chapter 3). This model is a general representation of all the possible pathways that consume $O_2^{\bullet -}$ in any biological system that generates this radical and where SOD is present. The fundamental question of whether increasing SOD can increase or decrease H_2O_2 production could then be answered, and constitutes one of the main contributions of this work. The results in Chapter 3 show that increasing SOD activity can exacerbate, diminish or have no effect on the rate of H_2O_2 production, and the conditions in which each different outcome can be observed are clearly described. Interestingly, though all the different outcomes had been suggested previously in the published literature [25–29], the confusion remained since a clear theoretical assessment was lacking, highlighting the importance of developing quantitative and analytical mathematical models even for simple conceptual models such as the present one. Still, given the complexity of biological systems and consequently of ROS metabolism, the *minimal* model presented in Chapter 3 should be regarded as a local representation of how the rate of H_2O_2 can be directly influenced by SOD. There are many processes that can potentially influence the rate of H_2O_2 production indirectly when SOD activity is increased, and the effects of some of these interactions are described in Chapter 4.

Thus, from the results of Chapter 3 and 4, the prediction of whether $O_2^{\bullet -}$ or H_2O_2 are involved in the prooxidative mechanisms of SOD is highly dependent on the metabolic conditions and redox status that dictate the balance between the fluxes of the three possible pathways of $O_2^{\bullet -}$ consumption presented both in the minimal model and those presented in Chapter 4. The discussion can thus be based in terms of flux ratios of these three pathways (see Table 6.1).

Table 6.1: Potential involvement of $O_2^{\bullet-}$ and H_2O_2 in the adverse effects of high SOD activities in different conditions.

			Involved Species[a]	
cases	$L(v_H, [SOD])$	$L([O_2^{\bullet-}], [SOD])$	H_2O_2	$O_2^{\bullet-}$
1	0	−1		x
2	1/2	−1/2	x	x
3	1	0	x	
4	−1/6	−1/2	?	x
5	0	−1/3		x
6	1/3	0	x	
7	0	0		
8	0	0		
9	0	0		

[a] (x) indicates that $O_2^{\bullet-}$ or H_2O_2 may be involved in the mechanisms leading to the deleterious effects elicited by high SOD activities.

In a biological system where most of the flux of H_2O_2 formation is through the reductive pathway (*cases* 7-9), neither the concentration of $O_2^{\bullet-}$ nor the rate of H_2O_2 will change significantly when SOD activity is increased. In such a system, no significant prooxidative effects are expected. Furthermore, the analysis in Chapter 3 shows that, given the expected pseudo first-order rate constants, this scenario is not physiologically plausible. However, it could occur under anomalous conditions, such as in pathological states or due to experimental handling.

When the rate of $O_2^{\bullet-}$ consumption through dismutation is equal to that through the reductive pathway, i.e., the rate of H_2O_2 production through dismutation is one half of that through the reductive pathway (*cases* 4-6), an increase in SOD activity will decrease, increase or have no effect on the rate of H_2O_2 generation. The outcome depends on the relative contribution of the non-H_2O_2-producing reactions on the overall rate of $O_2^{\bullet-}$ consumption. For example, when most of the flux of $O_2^{\bullet-}$ consumption is through the non-H_2O_2-producing pathway (*case* 6), H_2O_2 production is increased and therefore, in principle, could be responsible for the adverse effects observed at high SOD activities. Still, according to results in Chapter 4, the potential increase in oxidative damage will always be sublinear relative to the increase in SOD activity. In this *case* also, when SOD is increased changes in $O_2^{\bullet-}$ concentration are negligible. In these conditions, $O_2^{\bullet-}$ is not expected to exert any effect. However, if the flux of $O_2^{\bullet-}$ consumption is equally distributed through the three possible pathways (*case* 5) then H_2O_2 production will remain constant as SOD activity is increased. In contrast, a decrease in $O_2^{\bullet-}$ when SOD activity is augmented may be significant, a decrease in $O_2^{\bullet-}$ concentration will be observed at high SOD activities, which could lead to deleterious effects. When the rate of

non-H_2O_2-producing reactions is negligible (*case* 4), both $O_2^{\bullet-}$ concentration and H_2O_2 production decrease with increasing SOD activity. From the analysis of the minimal model, it seems unlikely that a decrease in H_2O_2 may be responsible for the adverse effects observed when increasing SOD activity. In conditions where a decrease in H_2O_2 could be maximal ($v_1 = v_2 \gg v_3$), and considering the values presented in chapter 3 for the respective pseudo first-order kinetic constants ($k_1 = k_2 = 10^4 s^{-1}$; $k_3 = 10^2 s^{-1}$, a ten-fold increase in SOD activity would decrease the rate from 75% of the maximum rate of $O_2^{\bullet-}$ production to 55% (where a value of 50% would indicate that all of the H_2O_2 is produced by dismutation). This corresponds to a ~27% decrease in the rate of H_2O_2 at normal levels of SOD. Considering there are other cellular sources of H_2O_2 that do not involve $O_2^{\bullet-}$ and that H_2O_2 diffuses easily across cellular compartments [30], it seems unlikely that cells would not be able to cope with a decrease of this magnitude. Nevertheless, a recent study demonstrated that smooth muscle cells overexpressing catalase have decreased rates of DNA synthesis and cell proliferation, and higher rates of apoptosis [31]. Thus, it may be possible that a significant decrease in H_2O_2 production induced by high SOD activities may have adverse effects. Regarding the effect of $O_2^{\bullet-}$ depletion, as seen in Table 6.1, it may contribute also in these conditions to the toxicity of high SOD activities, though again, it is expected that oxidative damage will increase at most linearly with SOD activity.

In cells or cellular compartments where the flux of H_2O_2 is mostly through dismutation (*cases* 1-3), the relative changes in H_2O_2 production and in the steady-state concentration of $O_2^{\bullet-}$ when SOD activity is increased will depend only on the balance between the rates of dismutation and the non-H_2O_2-producing reactions. When most of $O_2^{\bullet-}$ is consumed through the non-H_2O_2-producing reactions (*case* 3) the decrease in $O_2^{\bullet-}$ due to increased SOD activity should be negligible. However, most of the increase in SOD activity is "compensated" by a transfer of flux from the non-H_2O_2-producing reactions to the SOD-catalysed dismutation reaction, and therefore increasing H_2O_2 almost linearly with SOD ($L(v_H, [SOD]) \simeq 1$). In these conditions, it is likely that any adverse effect caused by increasing SOD activity may involve changes in H_2O_2 production. When the flux of $O_2^{\bullet-}$ consumption is equally distributed through dismutation and the non-H_2O_2-producing pathway (*case* 2), the decrease of $O_2^{\bullet-}$ concentration when SOD activity is increased is equally likely to contribute to the adverse effects than the increase in H_2O_2 production, according to the minimal model. Yet, results in chapter 4 show that $O_2^{\bullet-}$ depletion may cause greater oxidative damage when considering these flux ratios. However, the models presented in Chapter 4 did not consider direct damage of $O_2^{\bullet-}$ on the [4Fe-4S] clusters of dehydratases (see below), which releases reduced iron (Fe^{2+}) [32]. Consequently, by decreasing $O_2^{\bullet-}$ at increasing levels of SOD activity, less reduced iron will be available for the Fenton reaction and it may be possible that there might not be amplification of H_2O_2-mediated oxidative damage in some

situations predicted by the models in Chapter 4. When most of the flux of $O_2^{\bullet-}$ consumption is through dismutation, no changes in the rate of H_2O_2 production are expected. In contrast, $O_2^{\bullet-}$ will decrease linearly in magnitude with SOD activity. It is most likely that potential toxic effects of increasing SOD activity under these conditions may be due to excessive depletion of $O_2^{\bullet-}$, rather than through changes in H_2O_2 production.

One further advantage of the type of analysis presented in this work, is that it provides a theoretical framework based on which it is possible to design experiments to assess the influence of SOD on both $O_2^{\bullet-}$ and H_2O_2.

For instance, as mentioned before, there are many processes that can potentially influence the rate of H_2O_2 production indirectly when SOD activity is increased. This presents a challenge when trying to assess the question experimentally, since measuring changes in the concentration of H_2O_2 or in the rate of H_2O_2 production when SOD activity is increased may not be indicative of the direct influence that changes in SOD activity can exert on the rate of H_2O_2 production. So, when faced with an experimental system, the question of whether increasing SOD activity will raise or lower the rate of H_2O_2 production still remains. The way the minimal model was setup and analyzed provides clues on how to answer this question. The minimal model predicts that the rate of H_2O_2 production increases when the ratio between the rates of the non-H_2O_2-producing reactions and the rates of $O_2^{\bullet-}$ reduction at normal levels of SOD is greater than 1 ($v_3/v_2 > 1$, according to the notation used in Chapter 3), will not change if the ratio is equal to 1, and decrease otherwise. As the rates are proportional to the steady-state concentration of $O_2^{\bullet-}$, the ratio between rates is equivalent to the ratio between the respective pseudo first-order rate constants (k_3/k_2). The rate constants k_3 and k_2 are the sums of the individual rate constants of each process contributing to the non-H_2O_2-producing reactions and $O_2^{\bullet-}$ reduction, respectively:

$$k_3 = \sum_i k_{3i} = \sum_i k'_{3i}[\mathrm{M}_i] \tag{6.1}$$

and

$$k_2 = \sum_j k_{2j} = \sum_j k'_{2j}[\mathrm{M}_j] \tag{6.2}$$

where $[\mathrm{M}_i]$ and $[\mathrm{M}_j]$ are the concentrations of the different metabolites of the ith and jth processes contributing to v_3 and v_2, whereas k'_{3i} and k'_{2j} are the respective second order rate constants. In other words, rather than measuring the rate of H_2O_2 production, one can identify the most relevant reactions consuming $O_2^{\bullet-}$ by measuring the steady-state concentrations of the strongest potential *candidate* metabolites that may compete between each other for $O_2^{\bullet-}$, such as the [4Fe-4S] clusters of dehydratases, GSH, ascorbate, cytochrome *c*, ferritin, and others. As-

suming that their respective second-order rate constants are known (which is the case for many examples [33]), in principle only their concentrations are needed to be measured to assess how the rate of H_2O_2 will change when SOD is increased.

Still, there are second order kinetic constants for some reactions that have not been measured under physiological conditions and therefore even measuring the concentrations of the respective metabolites allows only a very rough estimate of what the rate of the reaction with $O_2^{\bullet-}$ should be. One of these examples was mentioned in Chapter 3: Possibly all biological systems produce $O_2^{\bullet-}$ through a reversible reaction and the backward reaction of $O_2^{\bullet-}$ production may play an important contribution to the non-H_2O_2-producing processes. For instance, one of the main generators of $O_2^{\bullet-}$ in mitochondria is the bc_1-complex of the respiratory chain, also known as complex III [34, 35]. Formation of $O_2^{\bullet-}$ occurs through a univalent reduction of O_2 by the ubisemiquinone radical ($UQ^{\bullet-}$) at a specific active site (Q_o) where ubiquinol is oxidized to ubiquinone in a two step process ($UQH_2 \rightarrow UQ^{\bullet-} \rightarrow UQ$) [35]. The reaction of $O_2^{\bullet-}$ formation is reversible [25], as $O_2^{\bullet-}$ can react with ubiquinone to yield O_2 and ubisemiquinone radical. This backward reaction of $O_2^{\bullet-}$ generation is actually thermodynamically more favorable than the forward reaction, though enzymes such as SOD are able to "pull" the reaction in the direction of $O_2^{\bullet-}$ production [25]. Again, in principle, knowing the concentration of the oxidized ubiquinone and the second-order rate constant of the reaction between $O_2^{\bullet-}$ and ubiquinone would be sufficient to evaluate the importance of the backward reaction in the non-H_2O_2-producing pathway. However, the second-order rate constant for this reaction was only measured in aqueous solution [36], which may be far from the physiological value since it occurs in the active site of an enzymatic complex embedded in the inner mitochondrial membrane. According to the estimates presented in Chapter 3, the value of the pseudo first-order rate constant for the backward reaction of $O_2^{\bullet-}$ production could lay between $\sim 10^2 - 10^5\ s^{-1}$, which is still a wide range. However, it may be possible to determine experimentally the pseudo first-order rate constant of the backward reaction of $O_2^{\bullet-}$ production from complex III. Using complex III isolated from the mitochondrial membrane [35] and an extra source of $O_2^{\bullet-}$, it is possible to follow H_2O_2 production for different values of SOD (Fig. 6.1). Assuming that in this isolated system the processes of $O_2^{\bullet-}$ consumption contributing to the production of H_2O_2 at higher yields (v_2) are negligible, expression 3.6 is simplified to:

$$v_H = \frac{1}{2}\frac{k_1[SOD]}{k_1[SOD] + k_3} \tag{6.3}$$

and can be used to fit the experimental values and determine k_3 (note that the expression was normalized, i.e., divided by the rate of total $O_2^{\bullet-}$ production). However, this pseudo first-order rate constant may still be taking into account other processes that also contribute to the non-H_2O_2-producing reactions. In the pres-

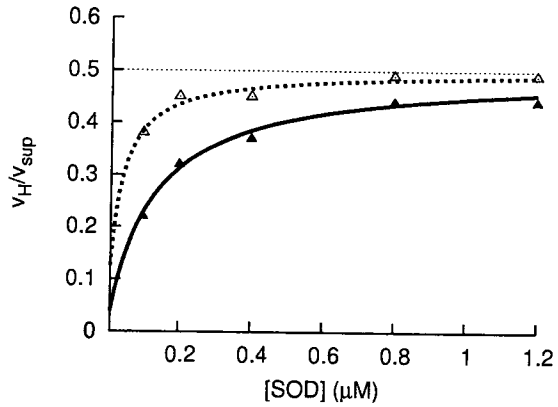

Figure 6.1: Determining the pseudo first-order rate constant of the backward reaction of $O_2^{\bullet-}$ production. The rate of H_2O_2 production can be determined for several concentrations of SOD in isolated complex III in the absence (▲) and in the presence of inhibitor (△). Lines would be the fitted curves using expression (6.3). The plots are normalized, i.e., divided by the total production of $O_2^{\bullet-}$ (v_{sup}), which is double the rate of H_2O_2 at full saturation. This way, the differences in both curves are given only by the absence of the backward reaction of $O_2^{\bullet-}$ production.

ence of a Q_o-site inhibitor, such as myxothiazol, there should be no $O_2^{\bullet-}$ production at this site [37]. Measuring H_2O_2 production for different SOD activities in the presence of an inhibitor (Fig. 6.1), a second pseudo first-order rate constant can be obtained ki_3 that takes into account every process contributing to the non-H_2O_2-producing reactions except the backward reaction of $O_2^{\bullet-}$ generation at complex III. By subtracting k_3 by ki_3 it should be possible to obtain an estimate of the pseudo first-order rate constant of the backward reaction of $O_2^{\bullet-}$ production at the bc_1-complex. By measuring the concentration of oxidized ubiquinone in the isolated system that is contributing to this reaction, a second-order rate constant could be determined.

Another interesting point that was not emphasized in Chapter 3 is that if the rates of both the $O_2^{\bullet-}$ reduction processes and the non-H_2O_2-producing reactions are equal, even if an increase in SOD can still increase significantly the flux of H_2O_2 production through dismutation, the overall rate of H_2O_2 production will not change as it is "compensated" by the decrease in the rate of H_2O_2 production through the reductive pathway. This is a consequence of the differences in stoichiometries regarding both processes of H_2O_2 production. The result of the mathematical analysis of the minimal model (see Table 3.1 in Chapter 3) considered that dismutation produces exactly half of the H_2O_2 than through the reductive pathway. However, $O_2^{\bullet-}$ can undergo chain reactions, e.g. involving GSH [38], where more than 1 molecule of H_2O_2 is produced per molecule of $O_2^{\bullet-}$ consumed . Assuming that $O_2^{\bullet-}$ reduction produces n molecules of H_2O_2 per molecule of $O_2^{\bullet-}$, the result

would be adjusted in the following way (compare with expression 3.5):

$$v_H = {}^1/_2 v_1 + n \cdot v_2, \qquad n > 1 \tag{6.4}$$

The resulting log gain will be (compare also with expression 3.7):

$$L(v_H, [SOD]) = \frac{k_1[SOD](k_3 - (2n-1)k_2)}{(k_1[SOD] + k_2 + k_3)(k_1[SOD] + n \cdot 2k_2)} \tag{6.5}$$

Therefore, for no changes in H_2O_2 production to be observed when increasing SOD activity, the overall rate of non H_2O_2-producing processes would have to be approximately $(2n-1)$ times the rate through the $O_2^{\bullet -}$ reducing pathway. An increase in the overall rate of H_2O_2 production would only be observed for values of k_3 higher than $(2n-1)\ k_2$. Still, to consider these reactions with higher H_2O_2 yield, they must be able to compete with other reactions contributing to the reductive pathway, such as the univalent oxidation of the [4Fe-4S] clusters of dehydratases by $O_2^{\bullet -}$.

The advantages of mathematical models in helping rationalize future experiments are again evidenced in Chapter 5. The analysis of the model allows the identification of three possible $O_2^{\bullet -}$-dependent mechanisms by which an increase in SOD activity may produce a biphasic response of lipid peroxidation. Assuming that $O_2^{\bullet -}$ is able to either serve as a terminator of lipid peroxidation, induce lipid hydroperoxide removal, or inhibit chain-branching reactions, excessive depletion of $O_2^{\bullet -}$ by increasing SOD could lead to a dramatic increase in chain-length and revert the beneficial effect of diminishing $O_2^{\bullet -}$-dependent initiation of lipid peroxidation. In principle, it could be possible to evaluate experimentally the importance of these processes on the biphasic response. However, before that, it would be important to assess whether the lipid damage that follows a biphasic response is occurring in the mitochondrial or cytoplasmic membranes. It would then be possible to target specifically those membranes and measure oxidant status in the respective compartments at different SOD activities. For instance, if at different values of SOD activities α-tocopherol levels remain relatively constant, it would be highly unlikely that the biphasic response would be the result of the decrease in the rate of termination by $O_2^{\bullet -}$. The activity of PHGPX could also be monitored at different levels of SOD activity to assess the importance of this process on the biphasic response. The processes involving chain-branching reactions can be more complicated to evaluate since the mechanisms involving the action of transition metals such as iron and copper in ischemia-reperfusion injury are still unclear. However, specific hypothesis as those presented in Chapter 5 could be tested. For example, the involvement of IRP-1 could be assessed by measuring its mRNA-binding activity at different levels of SOD activity, together with mRNA and protein levels of ferritin. The possibility of a $O_2^{\bullet -}$-dependent uptake of catalytically active iron being inhibited by SOD could be tested, for instance, by inhibiting the anion exchange

protein 2 (AE2) with stilbene AE inhibitors. This would prevent $O_2^{\bullet -}$ from being transported extracellularly and SOD should have no effect on the rate of external lipid peroxidation.

References

[1] Halliwell, B. and Gutteridge, M. (Editors) (1999) *Free Radicals in Biology and Medicine*. Oxford University Press, UK.

[2] Michelson, A.; Puget, K. and Durosay, P. (1977) Clinical aspects of the dosage of erythrocuprein. In A. M. Michelson; J. M. McCord and I. Fridovich (Editors), *Superoxide and superoxide dismutases*, 467–499. Academic Press, London.

[3] Scott, M.; Meshnick, S. and Eaton, J. (1989) Superoxide dismutase amplifies organismal sensitivity to ionizing radiation. *J Biol Chem* **264**:2498–501.

[4] Liochev, S. and Fridovich, I. (1991) Effects of overproduction of superoxide dismutase on the toxicity of paraquat toward *Escherichia coli*. *J Biol Chem* **266**:8747–50.

[5] McCord, J. (2002) Superoxide dismutase in aging and disease: an overview. *Methods Enzymol* **349**:331–41.

[6] Carlioz, A. and Touati, D. (1986) Isolation of superoxide dismutase mutants in *Escherichia coli*: is superoxide dismutase necessary for aerobic life? *EMBO J* **5**:623–30.

[7] Carlsson, L.; Jonsson, J.; Edlund, T. and Marklund, S. (1995) Mice lacking extracellular superoxide dismutase are more sensitive to hyperoxia. *Proc Natl Acad Sci U S A* **92**:6264–8.

[8] Li, Y.; Huang, T.; Carlson, E.; Melov, S.; Ursell, P.; Olson, J.; Noble, L.; Yoshimura, M.; Berger, C.; Chan, P. and et al. (1995) Dilated cardiomyopathy and neonatal lethality in mutant mice lacking manganese superoxide dismutase. *Nat Genet* **11**:376–81.

[9] Reaume, A.; Elliott, J.; Hoffman, E.; Kowall, N.; Ferrante, R.; Siwek, D.; Wilcox, H.; Flood, D.; Beal, M.; Brown, R., Jr; Scott, R. and Snider, W. (1996) Motor neurons in Cu/Zn superoxide dismutase-deficient mice develop normally but exhibit enhanced cell death after axonal injury. *Nat Genet* **13**:43–7.

[10] Melov, S.; Coskun, P.; Patel, M.; Tuinstra, R.; Cottrell, B.; Jun, A.; Zastawny, T.; Dizdaroglu, M.; Goodman, S.; Huang, T.; Miziorko, H.; Epstein, C. and Wallace, D. (1999) Mitochondrial disease in superoxide dismutase 2 mutant mice. *Proc Natl Acad Sci U S A* **96**:846–51.

[11] Bloch, C. and Ausubel, F. (1986) Paraquat-mediated selection for mutations in the manganese-superoxide dismutase gene *sodA*. *J Bacteriol* **168**:795–8.

[12] Elroy-Stein, O.; Bernstein, Y. and Groner, Y. (1986) Overproduction of human Cu/Zn-superoxide dismutase in transfected cells: Extenuation of paraquat-mediated cytotoxicity and enhancement of lipid peroxidation. *EMBO J* **5**:615–622.

[13] Scott, M.; Meshnick, S. and Eaton, J. (1987) Superoxide dismutase-rich bacteria. Paradoxical increase in oxidant toxicity. *J Biol Chem* **262**:3640–5.

[14] Elroy-Stein, O. and Groner, Y. (1988) Impaired neurotransmitter uptake in PC12 cells overexpressing human Cu/Zn-superoxide dismutase–implication for gene dosage effects in down syndrome. *Cell* **52**:259–67.

[15] Bowler, C.; Slooten, L.; Vandenbranden, S.; De Rycke, R.; Botterman, J.; Sybesma, C.; Van Montagu, M. and Inze, D. (1991) Manganese superoxide dismutase can reduce cellular damage mediated by oxygen radicals in transgenic plants. *EMBO J* **10**:1723–32.

[16] Amstad, P.; Peskin, A.; Shah, G.; Mirault, M.; Moret, R.; Zbinden, I. and Cerutti, P. (1991) The balance between Cu,Zn-superoxide dismutase and catalase affects the sensitivity of mouse epidermal cells to oxidative stress. *Biochemistry* **30**:9305–13.

[17] Ceballos-Picot, I.; Nicole, A. and Sinet, P. (1992) Cellular clones and transgenic mice overexpressing copper-zinc superoxide dismutase: Models for the study of free radical metabolism and aging. In I. Emerit and B. Chance (Editors), *Free radicals and aging*, 89–98. Basel:Birkhauser Verlag, Switzerland.

[18] Costa, V.; Reis, E.; Quintanilha, A. and Moradas-Ferreira, P. (1993) Acquisition of ethanol tolerance in *Saccharomyces cerevisiae*: The key role of the mitochondrial superoxide dismutase. *Arch Biochem Biophys* **300**:608–614.

[19] Lee, M.; Hyun, D.; Jenner, P. and Halliwell, B. (2001) Effect of overexpression of wild-type and mutant Cu/Zn-superoxide dismutases on oxidative damage and antioxidant defences: Relevance to Down's syndrome and familial amyotrophic lateral sclerosis. *J Neurochem* **76**:957–65.

[20] Gonzalez-Flecha, B. and Demple, B. (2000) Genetic responses to free radicals. Homeostasis and gene control. *Ann N Y Acad Sci* **899**:69–87.

[21] Griendling, K.; Sorescu, D.; Lassegue, B. and Ushio-Fukai, M. (2000) Modulation of protein kinase activity and gene expression by reactive oxygen species and their role in vascular physiology and pathophysiology. *Arterioscler Thromb Vasc Biol* **20**:2175–83.

[22] Forman, H. and Liu, R.-M. (1997) Glutathione cycling in oxidative stress. In L. Clerch and D. Massaro (Editors), *Oxygen, gene expression, and cellular function*, 99–121. Marcel Dekker, New York.

[23] Hartz, J.; Funakoshi, S. and Deutsch, H. (1973) The levels of superoxide dismutase and catalase in human tissues as determined immunochemically. *Clin Chim Acta* **46**:125–32.

[24] Tyler, D. (1975) Polarographic assay and intracellular distribution of superoxide dismutase in rat liver. *Biochem J* **147**:493–504.

[25] Winterbourn, C.; French, J. and Claridge, R. (1978) Superoxide dismutase as an inhibitor of reactions of semiquinone radicals. *FEBS Lett* **94**:269–272.

[26] Forman, H. and Boveris, A. (1982) Superoxide radical and hydrogen peroxide in mitochondria. In W. Pryor (Editor), *Free radicals in Biology*, 65–90. Academic Press, New York.

[27] Liochev, S. and Fridovich, I. (1994) The role of $O_2^{\bullet -}$ in the production of $HO^{\bullet}$: In vitro and in vivo. *Free Radic Biol Med* **16**:29–33.

[28] Omar, B. and McCord, J. (1990) The cardioprotective effect of Mn-superoxide dismutase is lost at high doses in the postischemic isolated rabbit heart. *Free Radic Biol Med* **9**:473–8.

[29] Rodriguez, A.; Carrico, P.; Mazurkiewicz, J. and Melendez, J. (2000) Mitochondrial or cytosolic catalase reverses the MnSOD-dependent inhibition of proliferation by enhancing respiratory chain activity, net ATP production, and decreasing the steady state levels of H_2O_2. *Free Radic Biol Med* **29**:801–13.

[30] Chance, B.; Sies, H. and Boveris, A. (1979) Hydroperoxide metabolism in mammalian organs. *Physiol Rev* **59**:527–605.

[31] Brown, M.; Miller, F., Jr; Li, W.; Ellingson, A.; Mozena, J.; Chatterjee, P.; Engelhardt, J.; Zwacka, R.; Oberley, L.; Fang, X.; Spector, A. and Weintraub, N. (1999) Overexpression of human catalase inhibits proliferation and promotes apoptosis in vascular smooth muscle cells. *Circ Res* **85**:524–33.

[32] Gardner, P. (1997) Superoxide-driven aconitase Fe-S center cycling. *Biosci Rep* **17**:33–42.

[33] Ross, A.; Mallard, W.; Helman, W.; Buxton, G.; Huie, R. and Neta, P. (1998) NDRL-NIST Solution Kinetics Database - Ver. 3. Tech. rep., Notre Dame Radiation Laboratory, Notre Dame, IN and NIST Standard Reference Data, Gaithersburg, MD.

[34] Boveris, A.; Cadenas, E. and Stoppani, A. (1976) Role of ubiquinone in the mitochondrial generation of hydrogen peroxide. *Biochem J* **156**:435–444.

[35] Cadenas, E.; Boveris, A.; Ragan, C. and Stoppani, A. (1977) Production of superoxide radicals and hydrogen peroxide by NADH-ubiquinone reductase and ubiquinol-cytochrome *c* reductase from beef-heart mitochondria. *Arch Biochem Biophys* **180**:248–257.

[36] Willson, R. (1971) Pulse radiolysis studies of electron transfer in aqueous quinone solutions. *Trans Faraday Soc* **67**:3020–3029.

[37] Turrens, J.; Alexandre, A. and Lehninger, A. (1985) Ubisemiquinone is the electron donor for superoxide formation by complex iii of heart mitochondria. *Arch Biochem Biophys* **237**:408–414.

[38] Winterbourn, C. (1993) Superoxide as an intracellular radical sink. *Free Radic Biol Med* **14**:85–90.

List of Figures

List of Tables